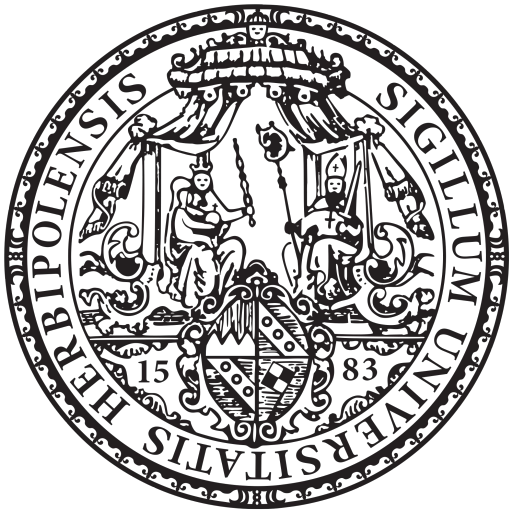

OxPAPC as an endogenous agonist of TRPA1 channels on nociceptors

OxPAPC als endogener Agonist von TRPA1 Kanälen auf Nozizeptoren

Doctoral thesis for a medical doctoral degree
at the Graduate School of Life Sciences,
Julius-Maximilians-Universität Würzburg,
Section Neuroscience

submitted by

Rafaela Mayer

from

Eigeltingen

Würzburg **2018**

Submitted on: ……

Office stamp

Members of the Promotionskomitee:

Chairperson: Prof. Dr. med. Klaus Peter Lesch

Primary Supervisor: Prof. Dr. med. Heike Rittner

Supervisor (Second): Dr. med. Beatrice Oehler

Supervisor (Third): PD Dr. rer. nat. Robert Blum

Date of Public Defence: ……

Date of Receipt of Certificates: ……..……

Table of contents

1 Introduction

1.1 Current state of research

1.1.1 Principles of the genesis of nociceptive pain

The *International Association for the Study of Pain* defines nociceptive pain as "pain that arises from actual or threatened damage to non-neural tissue and is due to the activation of nociceptors". Nociception is referred to as "the neural process of encoding noxious stimuli". Possible stimuli can be hot temperatures, change in pH and exogenous as well as endogenous irritants. Primary sensory neurons detecting pain-provoking stimuli are mostly slowly conducting, unmyelinated C fibers and more rapidly conducting, myelinated Aδ fibers. Nociceptive primary afferent neurons transmit electric potentials via Aδ and C fibers to the posterior horn of the spinal cord. Their cell bodies reside in dorsal root ganglia (DRG), trigeminal ganglia and nodose ganglia. DRG synapses project within the spinal cord dorsal horn to fibers of the spinothalamic tract (Caterina and Julius, 2001). Before ascending to the thalamus, the tracts cross over to the contralateral side of the spinal cord, from there to the limbic system and the cortex, where the sensation of pain is coming into conscience (Silbernagl S. , 2012).

Glutamate is a major mediator of synaptic transmission from peripheral nociceptors to spinal neurons. Mediators of inflammation are bradykinin, histamine, prostaglandins, protons, ATP, and nerve growth factor (NGF). Calcitonin gene-related peptide (CGRP), substance P, the brain-derived neurotrophic factor (BDNF), serotonin, histamine, and leukotriene exercise modulatory effects as co-transmitters (Gangadharan and Kuner, 2013). These mediators make up an 'inflammatory soup', which excites nociceptor terminals and causes neurogenic inflammation. The release of substance P and GCRP from synaptic vesicles induces neurogenic inflammation by provoking

vasodilatation, plasma extravasation and activation of immune cells, like neutrophil granulocytes or mast cells (Julius and Basbaum, 2001).

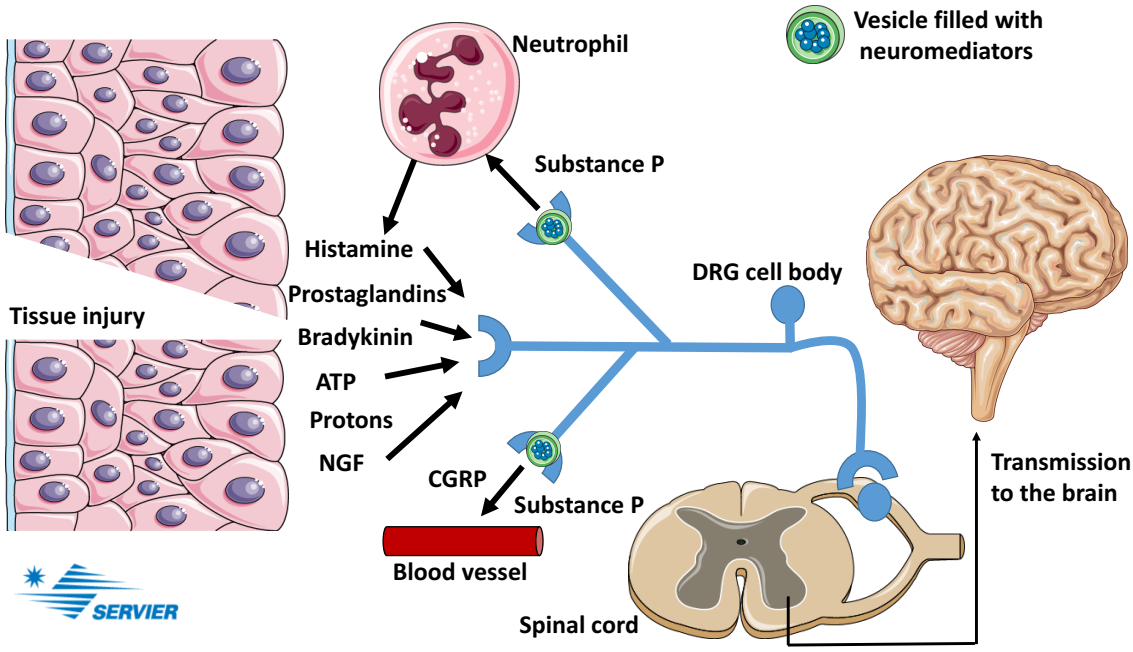

Figure 1: Inflammatory mediators for pain transmission in nociceptor terminals

Tissue injury triggers the release of inflammatory mediators, which activate nociceptor terminals. Afferent fibers transmit a painful stimulus to the dorsal horn of the spinal cord. Nociceptors also have efferent functions, which are responsible for the release of substance P and CGRP, causing neurogenic inflammation. Image modified from (Julius and Basbaum, 2001).

1.1.2 Limitations of pain management with non-steroidal antiphlogistic drugs

Non-steroidal antiinflammatory or antiphlogistic drugs (NSAIDs) are among the worldwide most commonly used drugs. They make up about 5-10 % of all prescribed medication (Wongrakpanich et al., 2018). They have analgesic, antipyretic, antiinflammatory, antitumoral and platelet aggregation-inhibiting (acetylsalicylic acid) properties. Known representatives of this family are ibuprofen, naproxen and diclofenac. They target cyclooxygenase, an enzyme that has two isoforms and can be found in endothelial cells, kidney tube cells,

platelets, gastric mucosa and at site of inflammation. Important downstream products of cyclooxygenase-1/2 are prostaglandins (PG) and thromboxane (TX). The abundant occurrence of cyclooxygenase and manifold functions of PG and TX in the human body explain why NSAIDs can cause severe adverse effects (Rao and Knaus, 2008). They can affect the gastrointestinal tract causing gastroduodenal ulcers with gastrointestinal bleeding and perforation, or the kidney provoking renal papillary necrosis and acute renal failure. Within the cardiovascular system known side effects include heart failure, myocardial infarction, stroke or even cardiovascular death. Furthermore, NSAIDs can set off allergic reactions like asthma, elevate transaminases or cause cytopenias, seizures or aseptic meningitis (Crofford, 2013). There is a necessity for new pharmaceuticals, that target inflammatory and proalgesic agents more specifically. In recent years, remarkable progress has been made in this field of research. Identified key mediators, like PLC, CREB and MAPK are important to maintain physiological functions and are involved in manifold pain pathways (Gangadharan and Kuner, 2013).

1.1.3 TRPA1 channels as key players in inflammation and pain

Julius and Basbaum (2001) stated in a review in *Nature,* that “the goal for nociceptor research is to elucidate signaling functions for key cell-surface markers and to assign physiological roles to molecularly defined sub-populations of sensory neurons“. Recently, transient receptor potential ankyrin 1 (TRPA1) channels were identified as important molecules in nociceptive pain physiology and were found to be nociceptive sensors for oxidative stress (Bahia et al., 2016). Besides, there is a growing number of studies highlighting the importance of TRPA1 in the development and maintenance of inflammatory hyperalgesia (Kistner et al., 2016; Meseguer et al., 2014).

1.1.3.1 The family of TRP channels

The TRPA1 channel belongs to the TRP family of ion channels, which feature a variety of sensory functions like vision, hearing, touch, pain, thermo- and

mechanosensation. TRP channels count 28 members and are divided into seven subfamilies: TRPC (canonical), TRPV (vanilloid), TRPM (melastatin), TRPP (polycystin), TRPML (mucolipin), TRPA (ankyrin) and TRPN (NOMPC-like). The cytoplasmic domains of the channels are used to define each subfamily (Cvetkov et al., 2011). They are polymodal channels, that work via different gating mechanisms and can be activated mechanically, by ligand binding, changes in voltage or temperature and covalent nucleophilic modification of intracellular residues (Nilius and Owsianik, 2011). TRPV1 is a heat- and capsaicin-sensitive ion channel. Capsaicin is naturally produced by capsicum peppers and conveys the pungency of spicy foods (Caterina et al., 1997).

1.1.3.2 Structural characteristics of TRPA1

The basic molecular structure among all TRP channels is a pore-forming tetramer, with each subunit consisting of six α-helical transmembrane domains S1-S6. S1-S4 make up a sensor module, while the pore-forming region S5-S6 conducts ions. The amino-terminal (N-terminal) as well as the carboxyl-terminal (C-terminal) domain are found within the cell (Owsianik et al., 2006).

The non-selective cation channel TRPA1 is characterized by an extensive N-terminal domain (720 of 1119 amino acids), containing between 14 and 17 ankyrin repeats per subunit and a β-hairpin loop, which serves as a linker. Transmembrane helix 5 and 6 shape a pore, which is non-selectively permeable for cations (Cvetkov et al., 2011; Kadkova et al., 2017). The N-terminus is essential for ligand interaction and channel regulation (Hinman et al., 2006). The cytoplasmic pre-S1 site links the ankyrin repeat domain (ARD) to S1 and contains cysteines, which are crucial for the interaction with electrophiles. The proximal C-terminus contains a TRP-like domain, a putative β-sheet and a long coiled-coil (Paulsen et al., 2015b).

1.1.3.3 TRPA1 expression in nociceptors

Specialized primary sensory neurons that are essential for the perception of pain, are called nociceptors. They function as a first line of defence for the body

against potentially harmful stimuli, as they transmit an unpleasant sensation to the brain (Woolf and Ma, 2007).

TRPA1 is prominently present in the sensory neurons of DRG, trigeminal and nodose ganglia, where it functions as a nociceptive channel (Nilius et al., 2012). Pseudo-unipolar DRG neurons can be divided morphologically into two groups: small diameter neurons (< 27 µm), which tend to have unmyelinated (C-fibers) or thinly myelinated axons (Aδ-fibers) and large diameter neurons (≥ 27 µm) with thickly myelinated axons (Aδ-fibers) (Dirajlal et al., 2003). Small diameter neurons convey nociceptive, thermal and mechanoreceptive stimuli to neurons on lamina I-II of the spinal cord, whereas large diameter neurons convey mechanoreceptive and proprioceptive stimuli to laminae III-V (Maxwell, 1987). TRPA1 is functionally expressed in small diameter C-fiber neurons. Originally, it was described to be found primarily in a subpopulation of small diameter C-fiber neurons, which are IB4-positive and CGRP-negative (Barabas et al., 2012). This classification gave way to a more complex approach, which considers transcriptomic, morphological and functional characteristics for neuron typing. By combining different techniques like high-coverage RNA-sequencing, *in vivo* patch clamp recording and single-cell PCR, mouse DRG neurons could be classified into 6 types (C1-C6) with 10 subtypes of small neurons and 4 types (C7-C10) with 4 subtypes of large neurons, which are distinguished by transcriptional patterns, molecular markers and functional annotations. The expression of different receptors and ion channels is not exclusive to one type of neuron. In the case of TRPA1, it was found to be expressed in neuron subtypes C1-2, C4-2, C5-2, C6-2 and neuron type C10. Conversely, most types of DRG neurons are sensitive to various stimuli, while others show a more exclusive response pattern (Li et al., 2016). Usoskin et al. (2015) performed single-cell RNA sequencing, demonstrating that different classes of sensory neurons can be determined by the variance of gene expression. They distinguish eleven types: NF1 to NF5, NP1 to NP3, PEP1, PEP2 and TH. TRPA1, for example, is expressed by all three NP classes and the TH class. TRPV1 in NP2, NP3 and PEP1. All types are represented by distinct protein markers. They could furthermore relate identified neuronal types to known

modality-specific functions, like low threshold mechanoreception, proprioception, thermosensation, sensation of itch, type C low-threshold mechanoreception and nociception. Most likely, a certain stimulus can activate both, a dedicated neuronal subtype or a set of neurons of different classes.

A growing number of evidence suggests that TRPA1 is widely expressed throughout the whole body, like the heart, brain, skeletal muscles, small intestines, lung, bladder, joints and as a mechanosensor in the inner ear (Nilius et al., 2012).

1.1.3.4 TRPA1 sensing potentially harmful stimuli

TRPA1 is a polymodal sensor for 1. exogenous substances, including environmental irritants, alimentary compounds from natural sources and drugs, 2. endogenous inflammatory metabolites and 3. physical stimuli (Kadkova et al., 2017; Nassini et al., 2014).

Plants have evolved a variety of mechanisms to defend themselves against predators, some of which include pain induction by targeting different molecular sites on nociceptors. Isothiocyanates, like allyl isothiocyanate (AITC), contained in mustard oil, as well as cinnamaldehyde and allicin, the pungent components of cinnamon and garlic, mediate inflammation and pain *in vivo* via TRPA1. Their property as electrophiles allows the formation of covalent adducts with thiols, primary amines and hydroxyl groups (Nassini et al., 2014; Smith M, 2001). They activate TRPA1 by forming a covalent but reversible bond with cysteine chains in the N-terminus of the channel. Hinman et al. (2006) found cysteines C619, C639 and C663 to be decisive for the interaction with electrophiles, while other experimental data showed that TRPA1 cysteine-triple mutant channels lost their sensitivity to electrophilic, sulfhydryl-selective agonists like AITC (Bautista et al., 2013).

Acrolein is an airborne pollutant, which mediates part of its noxiousness by TRPA1 activation. This carcinogenic and α,β-unsaturated aldehyde is found in cigarette smoke as well as in fried foods and causes toxic lung edema, laryngitis, bronchitis and CNS depression (Bautista et al., 2006). General and local anaesthetics were shown to activate TRPA1 and therefore possibly cause

post-operative pain, neurogenic inflammation, airway inflammation and hyperreactivity (volatile anaesthetics) and central sensitization. Therefore, antagonizing TRPA1 could be an approach to inhibit undesirable effects before or during administration of anaesthetics (Leffler et al., 2011). HC-030031, the TRPA1-selective antagonist used in our study, has already proved to attenuate AITC-induced mechanical hypersensitivity and inflammation in the chronic CFA pain model (Eid et al., 2008).

On the other hand, there are diverse endogenous agents that cause inflammation or hyperalgesia via TRPA1. For example prostaglandins, bradykinin, histamine, and trypsin are involved in TRPA1-activating signaling cascades (Kadkova et al., 2017).

TRPA1 channels can directly, or indirectly detect toxic signals of cellular stress. They are directly targeted by reactive oxygen species (ROS), nitric oxide (NO) and peroxynitrite ($ONOO^-$). Further agonists are peroxided or nitrosylated phospholipids such as 4-hydroxy-2-nonenal (4-HNE), 4-hydroxy-2-hexenal (4-HHE), 4-oxo-2-nonenal (4-ONE) and nitrooleic acid. Cyclooxygenase activity induced by inflammatory processes results in the formation of cyclopentenone PGs and isoprostanes (iso-PGs) like 15-deoxy-$\Delta^{12,14}$-prostaglandin J_2 (15d-PGJ_2), PGA_2 and 8-iso-PGA_2. Cyclopentenone PGs and iso-PGs cause inflammatory pain by activating TRPA1 (Nassini et al., 2014; Viana, 2016). 15d-PGJ_2 has already been known as an antiphlogistic compound, before its pro-inflammatory functions were discovered (Cruz-Orengo et al., 2008).

TRPA1 is involved in detecting physical stimuli. There is evidence proposing TRPA1 as a bidirectional thermosensor for warmth, uncomfortable heat and noxious cold (Moparthi et al., 2016), and as crucial for causing cold hyperalgesia (Nassini et al., 2014). Moreover, it mediates mechanosensation *in vitro* (Vilceanu and Stucky, 2010). In rodent models of inflammatory and neuropathic pain, it was found to play an important role in sensing mechanical allodynia (Nassini et al., 2014).

Apart from inflammatory hyperalgesia, scientific insights suggest TRPA1 to be involved in other inflammatory diseases such as airway inflammation (Belvisi et al., 2011), colitis (Engel et al., 2011) and diabetes (Eberhardt et al., 2012). It

was even discovered that a gain-of-function mutation in TRPA1 causes the familial episodic pain syndrome, where physical stress triggers episodes of severe upper body pain (Kremeyer et al., 2010).

1.1.3.5 Involvement in the sensation of inflammatory pain

TRPA1 channels are involved in manifold endogenous signaling pathways of pain transmission. The activation of TRPA1 at nerve terminals of primary sensory neurons induces an influx of cations, like calcium. Downstream sodium influx through voltage-gated sodium channels causes a membrane depolarization and the subsequent generation of an action potential. The increase in intracellular calcium triggers a calcium-dependent exocytosis of vesicles containing neuropeptides like Substance P, CGRP and neurokinin A (Bautista et al., 2013; Kadkova et al., 2017). Substance P is an essential trigger of inflammatory diseases and mediates different phlogistic processes like smooth muscle contractility, vascular permeability and immune function (O'Connor et al., 2004). CGRP is among the strongest vasodilators. It works via cAMP and subsequent activation of protein kinase A and C (PKA, PKC), mechanisms that are also involved in the pathophysiology of migraine and allodynia (Tepper and Stillman, 2008).

Mediators present in injured or inflamed tissue including PGs, serotonin, proteases and bradykinin can initiate proinflammatory signaling cascades via G protein-coupled receptor (GPCR)-mediated TRPA1 activation (Kadkova et al., 2017). Bradykinin, a vasoactive peptide hormone, is one of the most potent algesic agents (Bandell et al., 2004; Petho and Reeh, 2012). The bradykinin receptor, which is one representative of a variety of GPCRs, seems to play an important role in sensitizing TRPA1 to exogenous and endogenous agonists and in mediating TRPA1 activation. One the one hand, bradykinin acts on TRPA1 via the cAMP-PKA pathway (Petho and Reeh, 2012). PKA can phosphorylate TRPA1 and thus lower its activation thresholds for noxious stimuli (Kadkova et al., 2017). On the other hand, bradykinin binding to the bradykinin receptor initiates the phospholipase C (PLC) pathway. PLC catalyzes the hydrolysis of phosphatidylinositol 4,5-bisphosphate (PIP_2) to

inositol 1,4,5-trisphosphate (IP_3) and diacyl glycerol (DAG). IP_3 mediates the liberation of calcium from intracellular stores (Petho and Reeh, 2012). Calcium is a key element for the function of TRPA1. It activates the channel from the cytoplasmic side, potentiates its responses induced by other endogenous or exogenous agonists and subsequently causes an inhibition. Modulating properties of calcium on TRPA1 affect its unitary conductance, ion selectivity, channel opening probability and surface expression levels (Sura et al., 2012). PIP_2 has an inhibitory effect on TRPA1, which is possibly reversed by GPCR-mediated activation of PLC. PLC seems to be crucial for the interaction of TRPA1 with GPCRs in general, while PKA only appears to be involved specifically in the modulation of TRPA1 by the bradykinin receptor (Wang et al., 2008).

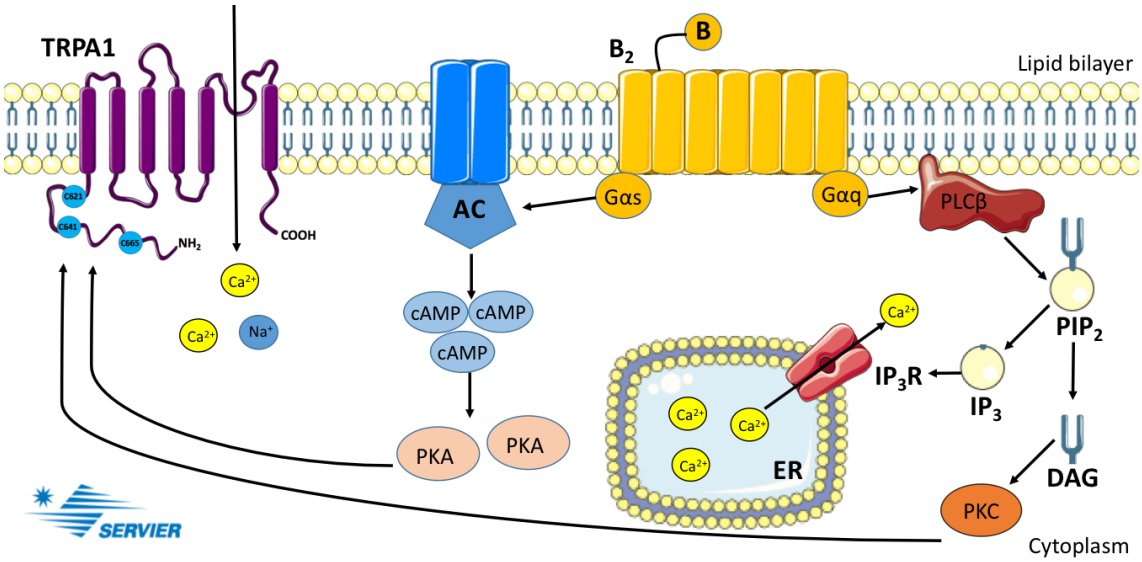

Figure 2: Signaling pathways influencing TRPA1 activity

Shown is the structure of TRPA1 with six α-helical transmembrane domains per subunit, a pore-forming unit for the influx of cations and the intracellular N- and C-terminal domain. The N-terminal domain contains ankyrin repeats as well as cysteine residues. Binding of bradykinin to the bradykinin receptor 2 (B_2) can activate Gαs, a protein that stimulates the adenylate cyclase (AC) to produce cAMP. cAMP-mediated activation of PKA sensitizes TRPA1. The activation of B_2 also causes Gαq to activate the PLCβ-PIP_2 signaling pathway. The resulting IP_3 causes a calcium

efflux from the ER. PKC activated by DAG can sensitize TRPA1 as well. Image modified from (Kadkova et al., 2017)

1.1.4 Generation of proinflammatory agents by ROS

Neutrophil granulocytes and macrophages release ROS, a process called oxidative or respiratory burst. ROS are involved in various physiological functions in the human body, which are part of the innate host defence, such as cellular differentiation, proliferation and cell death programs. As an example, they enable immune cells to phagocytose pathogens (de Oliveira-Junior et al., 2011). Persistent inflammatory processes however, can cause an imbalance between the production of ROS and antioxidant mechanisms, resulting in oxidative stress (Freigang, 2016).

The enzyme NADPH oxidase catalyses the reaction of oxygen and NADPH to O_2^-, a superoxide anion radical. This product is highly reactive itself and an educt for further generation of ROS. The enzyme superoxide dismutase converts O_2^- into hydrogen peroxide (H_2O_2). Hydroxyl radicals (OH^-), and alkoxy radicals (RO^-) are other representatives of the ROS group (Catala, 2009). Physiologically, there is a balance between ROS generation and breakdown. Antioxidant redox enzymes of the glutathione-, catalase- and thioredoxin-dependent systems, as well as the substances α-tocopherol (vitamin E), β-carotene, ascorbate (vitamin C) and glutathione protect the body against a surplus of oxidative activity (Viana, 2016).

The cell membrane consists of 30-80 % lipids, 20-60 % protein and 0-10 % carbohydrates. A large portion of membrane lipids is represented by phospholipids, among them 40-50 % phosphatidylcholine (PC). In higher eukaryotes, polyunsaturated fatty acids in the hydrophobic tail ensure membrane fluidity, flexibility and selectivity (Catala, 2009). Oxidative stress, due to the formation of free radicals, results in oxidative modification of biomolecules, like lipids, proteins and nucleic acids. The polyunsaturated fatty acid side chains of membrane phospholipids are predestined to ROS-induced non-enzymatic lipid peroxidation, generating a variety of bioactive oxidized phospholipids (OxPL) (Freigang, 2016). This process can impair the bilayers function by

altering physiological capacities (Catala, 2009). The peroxidation of lipids launches a cascade of further free radical reactions. Hydroxyl, alkoxyl and peroxyl radicals are among the ROS that are able to initiate peroxidation by creating a lipid radical. Down the road of this chain reaction emerge lipid hydroperoxides (LOOH) and new lipid radicals (Catala, 2006). Lipid hydroperoxides decay into cytotoxic aldehydes like 4-HNE, malondialdehyd and 4-HHE. Andersson et al. (2008) demonstrated in their study that ROS, alkenyl aldehydes and 15d-PGJ_2 triggered TRPA1-dependently 1. an activation of sensory neurons *in vitro* and 2. pain associated behaviour *in vivo* (Andersson et al., 2008).

1.1.5 Oxidized phospholipids as bioactive compounds in inflammation

1.1.5.1 Derivation and formation of oxidized phospholipids

OxPL are not simply by-products of plasma membrane oxidation processes, they are rather key mediators of diverse inflammatory diseases, including atherosclerosis, microbial infections, acute lung injury and neurodegenerative disorders (Freigang, 2016). They are involved in the initiation, amplification, and resolution of inflammatory processes (Bochkov et al., 2010).

PCs represent a class of phospholipids ubiquitously found in the lipid bilayer of animal and plant cells but not in most bacteria. They incorporate choline as a head group. Like the majority of phospholipids, PCs have a glycerol basic structure, which is esterified to a saturated fatty acid in the *sn*-1 position, and to a mono- or polyunsaturated fatty acid in the *sn*-2 position.

The two acyl chains are usually represented by palmitic, stearic, oleic, linoleic, or arachidonic acid (Stemmer and Hermetter, 2012; Thewalt and Bloom, 1992). Free radical attack of acyl chains in the *sn*-2 position of membrane phospholipids causes a series of modifications and fragmentations, thus creating a high diversity of OxPL species (Bochkov et al., 2010). Fragmentation of *sn*-2 fatty acids can generate aldehydophospholipids with a shorter acyl chain and a higher polarity. They are chemically very reactive and can form Schiff bases with proteins and aminophospholipids. Carboxyphospholipids are higher oxidized derivatives of aminophospholipids and due to their low reactivity

only able to interact physically with other molecules (Stemmer and Hermetter, 2012).

Oxidized PCs (OxPCs) have been identified as bioactive lipids in atherosclerosis and inflammatory diseases (Itabe et al., 2003). A well characterized oxidized arachidonic acid-containing phospholipid, extracted from minimally modified LDL, is oxidized 1-palmitoyl-2-arachidonoyl-*sn*-glycero-3-PC (OxPAPC). The un-oxidized PAPC occurs abundantly in mammalian cell membranes. At the site of inflammation, OxPAPC does not exist as a defined OxPL or OxPL mixture. Since ROS-mediated oxidation of the *sn*-2 arachidonic acid is non-specific, a wide range of different bioactive OxPAPC species is created (Bochkov et al., 2010). For instance, modification and fragmentation of PAPC at position *sn*-2 generates the truncated aldehydophospholipd 1-palmitoyl-2-(5'-oxo-valeroyl)-*sn*-glycero-3-PC (POVPC) and the truncated carboxyphospholipid 1-palmitoyl-2-glutaryl-*sn*-glycero-3-PC (PGPC) (Stemmer and Hermetter, 2012). More complex OxPCs with full length oxygenated *sn*-2 residues are 1-palmitoyl-2-epoxyisoprostane-*sn*-glycero-3-PC (PEIPC) and PECPC, which are formed by cyclization, rearrangement and further oxidation (Freigang, 2016).

1.1.5.2 Biological functions of oxidized phospholipids and in particular, OxPAPC

OxPL are associated with a variety of inflammatory and anti-inflammatory processes. They were found to be recognized by toll like receptors (TLRs), scavenger receptors, soluble pattern recognition receptors (PRRs) and natural antibodies (Freigang, 2016).

On the one hand, their strong proinflammatory activity is attributed to cytokine and chemokine-induced inflammatory processes, initiated by the recognition of OxPL by cells of the monocyte lineage. This can be mediated directly via TLR2 on macrophages (Freigang, 2016). Also, the CD36 receptor binds OxPL present on OxLDL, causing the assembly of the dimeric TLR4/6 receptor, which sets off various signaling cascades for the initiation and potentiation of inflammation (Stewart et al., 2010). In general, CD36 serves as a PRR to recognize modified

lipoproteins, apoptotic cells or pathogens. Epitopes, critical for the interaction of OxPL with CD36, are oxidized *sn*-2 fatty acids or peroxidized PCs. OxPC bound by CD36 were found to mediate foam cell formation in atherosclerotic lesions (Podrez et al., 2002).

The direct interaction between OxPAPC and the scavenger receptor B1 (SRB1) favours the development of atherosclerosis by inhibiting reverse cholesterol transport (Gao et al., 2010). Another proatherogenic pathway is initiated by OxPAPC or PEIPC binding to E-type prostaglandin receptors (EP2), causing monocyte adhesion to endothelial cells (Li et al., 2006). In pulmonary endothelial cells, OxPAPC was found to activate PKC, PKA, protein tyrosine phosphorylation and MAP kinase cascades, thereby modifying gene expression and inducing cytoskeletal remodelling (Birukov et al., 2004). OxPAPC and different OxPAPC species activate peroxisome proliferator-activated receptors α and γ (PPAR), which are ligand-activated transcription factors (Bochkov et al., 2010). Moreover, pathogenic conditions like allergy, septic shock, arterial thrombosis and inflammation can be triggered by OxPAPC and POVPC binding to platelet-activating factor (PAF) receptors (Lee et al., 2012). The vascular epithelial growth factor receptor (VEGFR) mediates different effects of OxPAPC on endothelial cells, like the expression of IL-8, tissue factor and the LDL-receptor (Bochkov et al., 2010).

On the other hand, OxPL exert anti-inflammatory activities by interfering with TLR signaling. This effect is not exclusive for individual TLRs. Via TRL4, OxPL can inhibit NFκB activation and the expression of inflammatory adhesion molecules in endothelial cells (Bochkov et al., 2002). This results in an antagonism of LPS-induced adhesion of granulocytes to the endothelium and a downregulation of inflammatory surface receptor expression (Bochkov et al., 2010). Via TLR2, TLR3, TLR4 and TLR9 and CD40, OxPL were shown to restrict the production of the cytokines TNF-α and IL-12 by macrophages and dendritic cells (Bluml et al., 2005; Ma et al., 2004).

Bretscher et al. (2015) identified the two OxPAPC compounds PECPC and PEIPC as anti-inflammatory mediators. The fatty acid epoxycyclopentenone at the *sn*-2 position of PECPC is the determining structure for the activation of the

transcription factor nuclear factor E2-related factor 2 (Nrf2). Nrf2 is responsible for the expression of antioxidant proteins, protecting tissue from oxidative stress caused by injury. Due to the structural resemblance of epoxycyclopentenone to the endogenous, pro-resolving 15d-PGJ_2, it seems possible that PECPC mimics anti-inflammatory physiological functions of this lipid mediator *in vivo* (Bretscher et al., 2015). Moreover, OxPAPC was found to directly impact endothelial cell function on the genetic level, thus regulating inflammation, sterol synthesis, cell division and redox signaling, amongst other things. The resulting overall impact can be both, harming or protective, depending on the time of exposure to OxPAPC (Lee et al., 2012).

It also seems likely that the respective pro- or anti-inflammatory effect of the OxPAPC mixture is a consequence of the composition of OxPL species (Bretscher et al., 2015).

Like demonstrated above, the function of OxPAPC in inflammation has been widely investigated in previous years, but its contribution to inflammatory pain is still unexplored (Bochkov et al., 2010).

1.1.6 ApoA−I and ApoA−I-mimetic peptides mediate anti-inflammatory effects in atherosclerosis

It has been known for many years that atherogenic effects are due to the adhesion of monocytes to vascular endothelium and the release of cytokines (Watson et al., 1997). The role of OxPL in the development of atherosclerotic lesions has just become clearer in previous years. They are no irrelevant by-products found in atherosclerotic plaques, but contribute substantially to the pathophysiology of lesion formation (Lee et al., 2012). As described before, OxPAPC is involved in various proatherogenic pathways.

High plasma levels of low-density lipoproteins (LDL) are associated with atherosclerosis, a chronic inflammation of the intima of arteries, whereas protective functions of the counterpart, high-density lipoprotein (HDL), have been discussed for many years (Hansson and Hermansson, 2011). HDL is a known protective parameter in the pathophysiology of atherosclerosis and its sequelae, like coronary heart disease and apoplexy (Gordon et al., 1989). Other

than mediating reverse cholesterol transport, various functions of HDL have been identified, including the inhibition of LDL oxidation, reduction of chemokine production and support of vascular dilatation (Feig et al., 2008). However, oxidative stress can cause unfavourable modifications to both lipoproteins, causing changes in particle recognition by scavenger receptors. OxPL, like POVPC mask the receptor docking sites in LDL, which facilitates the recognition by scavenger receptors (Stemmer and Hermetter, 2012). As a consequence, scavenger receptor-mediated OxLDL uptake into cells causes an excessive cholesterol uptake into macrophages and foam cell formation (Glass and Witztum, 2001). HDL modified by phospholipid aldehydes is very likely to be recognized by the same receptors as modified LDL and could therefore initiate the same proatherogenic effects (Stemmer and Hermetter, 2012). ROS-induced oxidation of LDL phospholipids also causes atherogenic chemokine expression, thus triggering inflammatory reactions (Getz and Reardon, 2011).

Apolipoprotein A-I (ApoA-I) is the major apoprotein of HDL and known for its anti-atherogenic and anti-inflammatory impact, including a reduction of OxPL (Getz and Reardon, 2011). Derivatives of ApoA-I, ApoA-I-mimetic peptides, supress LDL-induced monocyte migration and are discussed to have HDL-enhancing functions (Degoma and Rader, 2011). Moreover, they promote reverse cholesterol transport (Tang et al., 2006), which possibly contributes to the atherosclerosis-attenuating effect found in the mouse model (Navab et al., 2011). A part of the anti-inflammatory effect of ApoA-I mimetic peptides is due to the reduction of lipid rafts in macrophages, which is correlated with the reduction of cytokines, chemokines and TRL4 expression (Smythies et al., 2010).

ApoA-I mimetic peptides consist of amphiphatic α-helices with opposing polar and non-polar faces, which are hydrophilic and hydrophobic. The structure of the helix complements with phospholipids, which favours protein-lipid complexes to form (Segrest et al., 1994). The first ApoA-I mimetic peptide was created with 18 amino acids by Anantharamaiah et al. in 1985 and named 18A. Since then, this peptide has been modified many times. In order to increase its capacity to bind lipids, the N-terminus was acetylated and the C-terminus was

amidated. The resulting peptide, 2F, contains 2 phenylalanine residues on the hydrophobic face. A further variation with 2 more phenylalanine residues on the non-polar face is 4F, resulting in a peptide with phenylalanine residues at 4 of 8 positions (Getz and Reardon, 2011). 4F has anti-inflammatory properties, binds lipids with a high affinity and promotes reverse cholesterol transport (Wool et al., 2008). Naturally, the peptide contains L-amino acids, which makes it an easy target for degradation by proteases in the gastrointestinal tract. The isomer, D-4F however, is resistant to metabolism and just as effective (Getz and Reardon, 2014). Navab et al. (2011) found that irrespective of the administered way, 4F dose-dependently reduces atherosclerosis, the HDL inflammatory index and plasma biomarkers. They suspect the small intestine as the site of action of 4F.

These findings highlight the importance of D-4F as a potential therapeutic option for inflammatory diseases with a major contribution of oxidized lipids, like asthma, renal inflammation, diabetes and rheumatoid arthritis (Getz and Reardon, 2014).

1.1.7 The monoclonal IgM antibody E06 recognizes immunogenic lipids

Oxidative stress can cause oxidation and modification of phospholipids, creating neo-self determinants, which initiate responses of the innate and adaptive immune system. Especially the oxidation of PC present in LDL and cell membranes generates highly reactive products like 4-HNE and POVPC, which can be considered as neo-epitopes. In animal models of atherosclerosis and in humans, antibodies recognizing OxPL present in OxLDL have been detected (Bochkov et al., 2010). Apo E-deficient mice, which are characterized by extensive hyperlipidaemia and arteriosclerosis, have exceptionally high titres of IgM and IgG autoantibodies binding OxLDL. Palinski et al. (1996) used this as an approach to clone monoclonal antibodies to epitopes of OxLDL. They created hybridomas from spleen B cell isolates, which indeed produced anti-OxLDL IgM monoclonal antibodies, so called “E0 antibodies”. Shaw et al. (2000) discovered by gene sequence analysis and anti-idiotypic studies, that the E06 clone is a germline-encoded antibody identical to T15 natural IgA

antibodies. B1 cells produce T15 anti-PC antibodies against polysaccharides of the bacteria capsule and thereby protect the host organisms from lethal infections with Gram-positive bacteria, like *Streptococcus pneumoniae* (Shaw et al., 2000). E0 antibodies, like E06, have important biological functions like impeding the binding and uptake of OxLDL or the phagocytosis of apoptotic cells by macrophages (Friedman et al., 2002; Horkko et al., 1999). The decisive epitope for the recognition of phospholipids by E06 is the phosphorylcholine head group (Friedman et al., 2002).

1.2 Preliminary work of the research group "Molekulare Schmerzforschung"

The experiments of this thesis were part of the project N261 PI, "Transient Receptor Potential channels (TRPA1 and TRPV1): Oxidized Phospholipids and Mechanisms of Inflammatory Pain", of the Interdisciplinary Center of Clinical Research at the University of Würzburg, under the stewardship of Prof. Dr. med. Heike Rittner, Dr. med. Beatrice Oehler and PD Dr. rer. nat. Robert Blum. The objective of the study was to classify the oxidized phospholipids found in inflamed tissue, evaluate their impact on TRP channels and to find strategies to prevent inflammatory hyperalgesia. Before I started my research, which was exclusively based on calcium imaging as a method to investigate the action of OxPAPC on TRPA1 and furthermore to assess the effect of possible OxPAPC scavengers, there was already a series of experiments performed by the research group "Molekulare Schmerzforschung". The obtained results were the basis for my experiments and are presented in this section. They are important to understand why this thesis specifically focuses on OxPAPC as an agonist of TRPA1 channels.

1.2.1 OxPAPC induced thermal and mechanical hyperalgesia after local injection in rats and was found in inflamed paw tissue

In the beginning of this study we investigated whether the commercially available OxPL mixture OxPAPC could cause hyperalgesia *in vivo*. Diana Pflücke and Milad Mohammadi used the Randall-Selitto and the paw withdrawal latency test to reveal the algesic potential of OxPAPC in contrast to the non-oxidized PAPC and NaCl control. Hyperalgesia persisted over 6 hours after intraplantar injection and showed a dose-dependency in dose-response curves. Lowest mechanical nociceptive thresholds were reached with 500 µg OxPAPC after 1-3 hours (Figure 3a), thermal nociceptive thresholds at this concentration after 6 hours (Figure 3b).

Next, we wanted to analyse the composition of phospholipids and especially of OxPAPC species occurring at the site of inflammation in comparison to

phospholipids found in OxPAPC-treated tissue. CFA injected in rats hindpaws was used to induce localized inflammation (Figure 3e). Matrix-assisted laser desorption and ionization time-of-flight mass spectrometry (MALDI-TOF MS) was used to detect OxPAPC species and OxPAPC metabolites in inflamed tissue and in OxPAPC-treated tissue. The OxPAPC mixture, which was injected in rat paws, contained non-oxidized PAPC (m/z 782), POVPC (m/z 594), PGPC (m/z 610) and PEIPC (m/z 828,). In untreated paw tissue non-oxidized PC species were detected (m/z 734-832). Tissue analysed directly after OxPAPC injection (0 min) contained various OxPAPC components, like POVPV, PGPC and PEIPC, which weren't detectable in tissue treated with OxPAPC for 15 minutes. In this sample only downstream OxPAPC metabolites, like lysophosphatidylcholine (LPC), were present (e.g. m/z 496). These OxPAPC fragments were also found after local CFA injection, as well as OxPAPC peaks in various intensities (e.g. m/z 616, POVPC). These findings suggest that *in vivo*, OxPAPC species like POVPC, are produced in inflammatory settings and that OxPAPC is subject to rapid metabolism (Oehler et al., 2017).

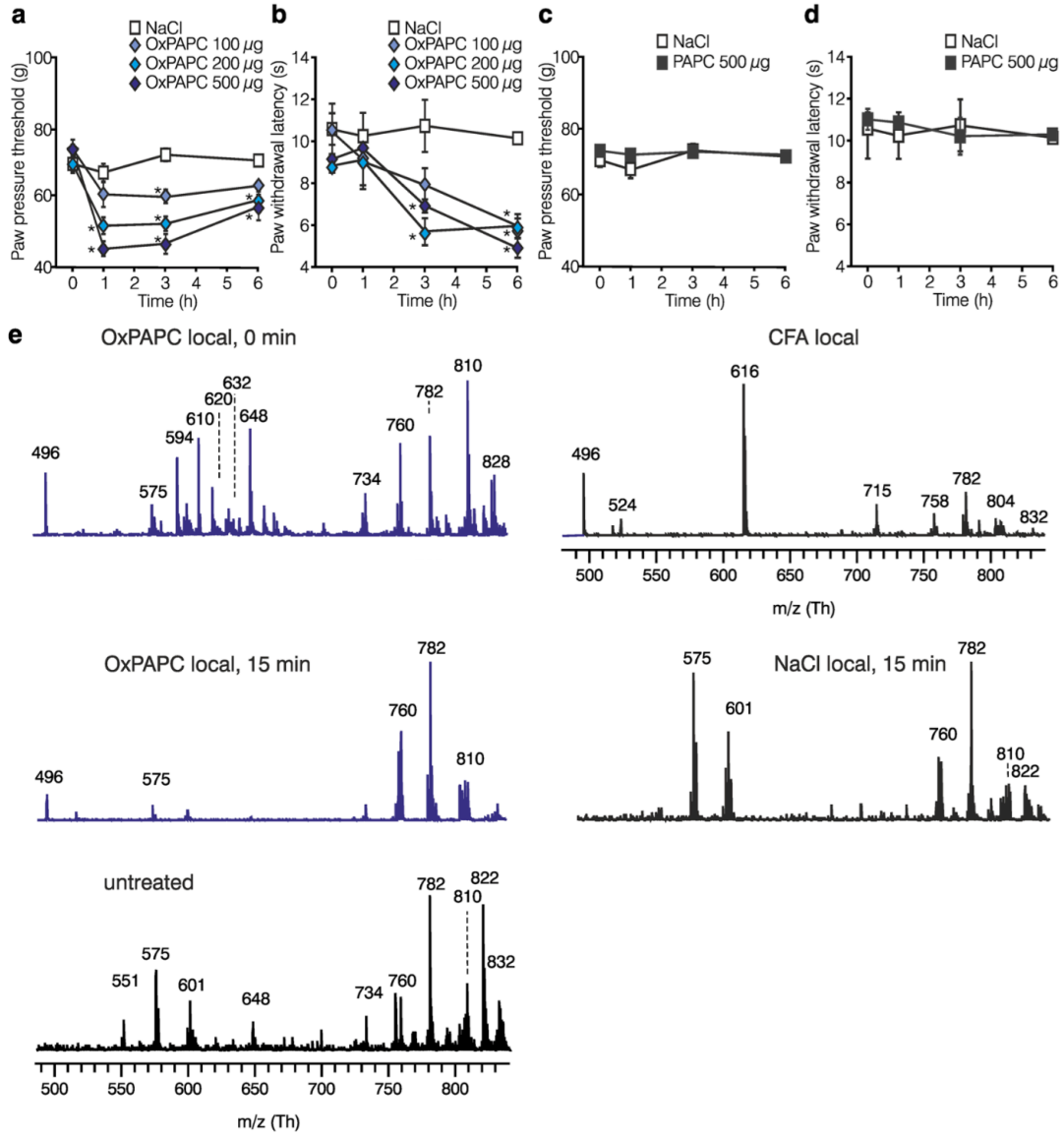

Figure 3: Mechanical and thermal nociceptive thresholds and MALDI-TOF MS of paw tissue extracts

Mechanical paw pressure threshold ***(a, c)*** *and thermal paw withdrawal latencies* ***(b, d)*** *were measured after injection of OxPAPC (concentrations of 100, 200 and 500 µM)* ***(a, b)*** *and PAPC* ***(c, d)*** *into rat hind paws over time. 0.9 % NaCl was used as a negative control. n = 6 Wistar rats per group, mean ± SEM, two-way RM ANOVA, post hoc Holm-Sidak, * p ≤0.05.* ***(e)*** *Positive ion MALDI-TOF (MS) was performed using chloroform tissue extracts from rat paws. Tissue for MS analysis was taken 0 and 15 minutes after intraplantar injection of 500 µg OxPAPC, 3 hours after CFA injection, 15 minutes after injection of 0.9 % NaCl solvent and from untreated paws.*

m/z values represent peaks. The scaling was set to the same intensity for the most intense peak in each measurement. Peaks at m/z 575.5 and 601.5 indicate loss of one fatty acid (sodium salt) from triacylglycerols (asterisks: signals due to 2,5-dihydroxybenzoic acid matrix cluster ions, representative example, n = 3. Figure taken from (Oehler et al., 2017).

Qualification of lipids in the inflammation model by MALDI-TOF MS

The following process of lipid analysis was kindly performed by PD. Dr. Jürgen Schiller, Universität Leipzig.

MALDI-TOF MS is a method for the analysis of biomolecules with high molecular weight and low volatility with a minimal degradation reaction. Mass spectrometry experiments were performed with a Bruker Autoflex mass spectrometer (Bruker Daltonics, Bremen, Germany). A pulsed nitrogen laser emits light in the UV spectral range (337 nm) onto the sample of lipid extracts suspended in a matrix of 20-30 µl 2,5-dihydroxybenzoic acid. The matrix ensures that the molecules in the sample stay apart from each other and absorbs laser energy, thus triggering a heating and evaporation process. Collisions between matrix and sample lead to an attachment of protons to lipids, thus forming positively charged ions (adducts). These adducts are accelerated with an extraction voltage of 20 kV in the electric field according to the following equation:

$$U \times e = \frac{1}{2} m \times v^2$$

U, voltage e, elementary charge m, mass v, velocity

After passing the area of acceleration through a charged grid, the adducts enter the area of ‘time-of-flight’ where they are separated by their different molecular mass corresponding to the formula:

$$\frac{m}{z} = 2\,E_{kin}\frac{t^2}{s^2}$$

m, mass z, charge E_{kin}, kinetic energy t, time of flight s, length of flight tube

Small ions reach the detector faster than big ones, enabling the analysis of the composition of the sample. Gated matrix suppression inhibits a saturation of the detector by matrix ions. 128 single laser shots were averaged for each matrix spectrum (Schiller et al., 2004).

1.2.2 OxPAPC induced calcium influx via TRPA1 but not via other TRP channels

To examine the impact of OxPAPC on different channels of the TRP family, Dr. med. Beatrice Oehler performed calcium imaging experiments of recombinant TRPA1 and TRPV1-4 channels expressed in HEK-293 cells using a fluorescence imaging plate reader (FLIPR). For each channel, typical agonists were used as a reference. OxPAPC could only induce significant calcium influx through TRPA1 channels at concentrations ≥ 6.3 µM. Whereas it could not induce a significant channel activation in concentrations from 0.05-100 µM neither in TRPV1-4 nor in the non-transfected HEK-293 control. TRPA1-mediated calcium influx evoked by OxPAPC was delayed compared to the AITC response at equal concentrations. Dose response curves show that increasing agonist concentrations caused higher F/F_0 ratios, while each agonist had a calcium threshold that was not exceeded.

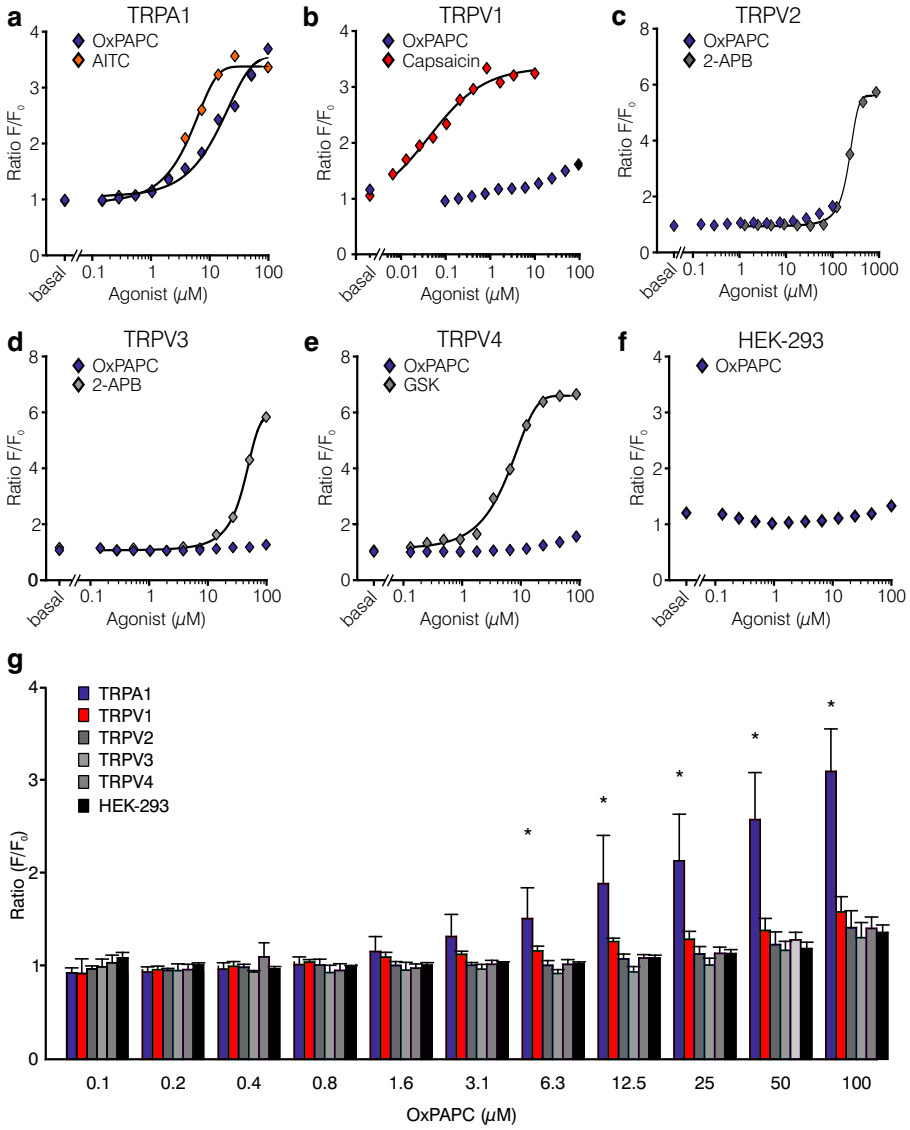

Figure 4: OxPAPC response of different TRP channels

HEK-293 cells stably expressing TRPA1 ***(a)****, TRPV1* ***(b)****, TRPV2* ***(c)****, TRPV3* ***(d)*** *or TRPV4* ***(e)*** *were used for FLIPR assays. Shown are dose-dependency curves of changes in Fluo-4/calcium fluorescence (ratio* F/F_0*) after OxPAPC activation. Non-transfected HEK-293 cells* ***(f)*** *served as negative control. Positive controls for each channel type were realized with a specific agonist (****a****, TRPA1: AITC;* ***b****, TRPV1: capsaicin;* ***c/d****, TRPV2/TRPV3: 2-APB;* ***e****, TRPV4: GSK2193874.* F/F_0 *ratios are represented along the ordinate and the corresponding concentration of OxPAPC, expressed in µM, along the abscissa. n = 3 of quadruple measurements, mean ± SD;*

*two-way ANOVA RM, post hoc Holm-Sidak, * $p \leq 0.05$. Figure taken from (Oehler et al., 2017).*

1.2.3 Stable expression of human TRPA1 in HEK-293 cells

For the investigation of TRPA1 responses to OxPAPC, we needed a cell line stably expressing this channel. We used HEK-293 cells for calcium imaging experiments, because they have a reliable growth and can be transfected efficiently (Wurm, 2004). HEK-293 cells are described in chapter 2.1.

To express human TRPA1 in HEK-293 cells, we used the lentiviral expression vector pCDH1-Ubc-MCS-EF1-Hygro (System biosciences) under the control of an ubiquitin promoter. Human TRPA1 cDNA was cloned to the lentiviral expression vector. Lentiviral particles were produced in HEK-293T cells in the Institute for Clinical Neurobiology with the pseudotyping vector pMD2.G and the packaging vector pCMVΔR8.91. Cell culture supernatants containing lentiviral particles were used to transduce HEK-293 cells. Lentiviral vectors undergo genomic integration. Transduced HEK-293 cells were continuously kept under 400 µg/ml hygromycin and used for calcium imaging experiments.

PD. Dr. Robert Blum and Dr. med. Beatrice Oehler kindly performed the cloning of hTRPA1 DNA to the lentiviral vector and the subsequent transduction into HEK-293 cells.

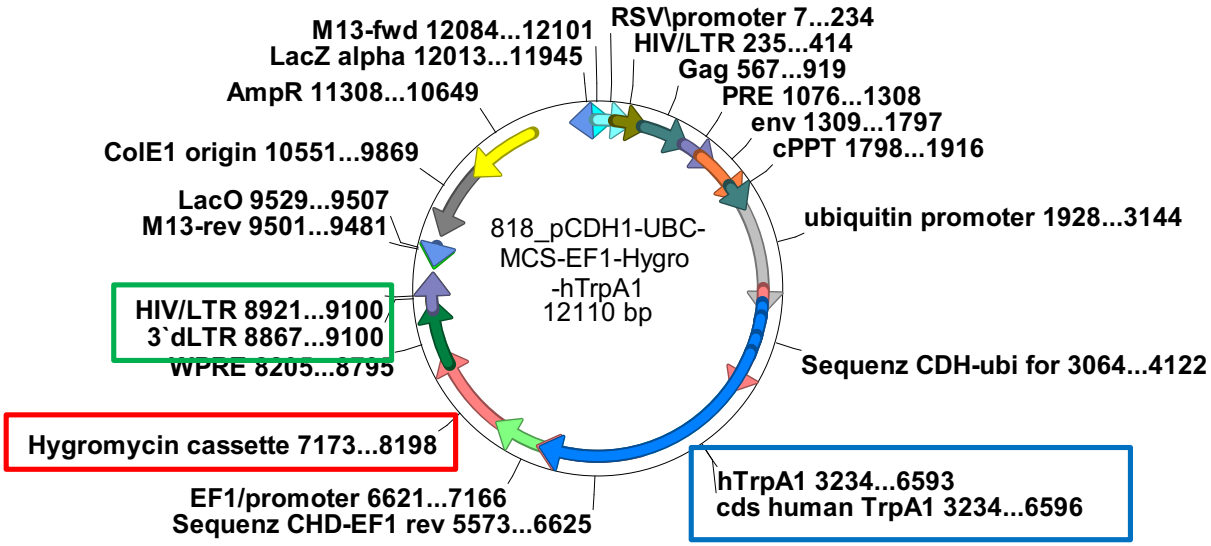

This figure was provided with the kind permission of PD Dr. Robert Blum, Würzburg

Figure 5: Human TRPA1 gene integrated in lentiviral genome

Essential genes are highlighted in the graph: Long Terminal Repeats (LTR, marked in green) support the integration of the vector into the host DNA, the stability within the host cell and the transcription. The hygromycin cassette (marked in red) ensures a selection advantage of the transfected cells over non-transfected cells. The hTRPA1 gene (marked in blue) was integrated into the lentiviral vector for the expression in the cell model.

1.3 Objectives of the dissertation

The aim of this dissertation was to investigate TRPA1-mediated proalgesic properties of oxidized phospholipids at the molecular level and to identify potential neutralizing agents. Following hypotheses were subject of the investigation:

1. OxPAPC is a direct agonist of TRPA1
2. TRPA1 activation is mediated by modification of three decisive cysteines in the intracellular channel domain.
3. D-4F and E06 impede the interaction of OxPAPC with TRPA1 and therefore constitute attractive potential agents for the clinical therapy of inflammatory and postoperative pain.

This figure is a depiction of the hypotheses of this thesis:

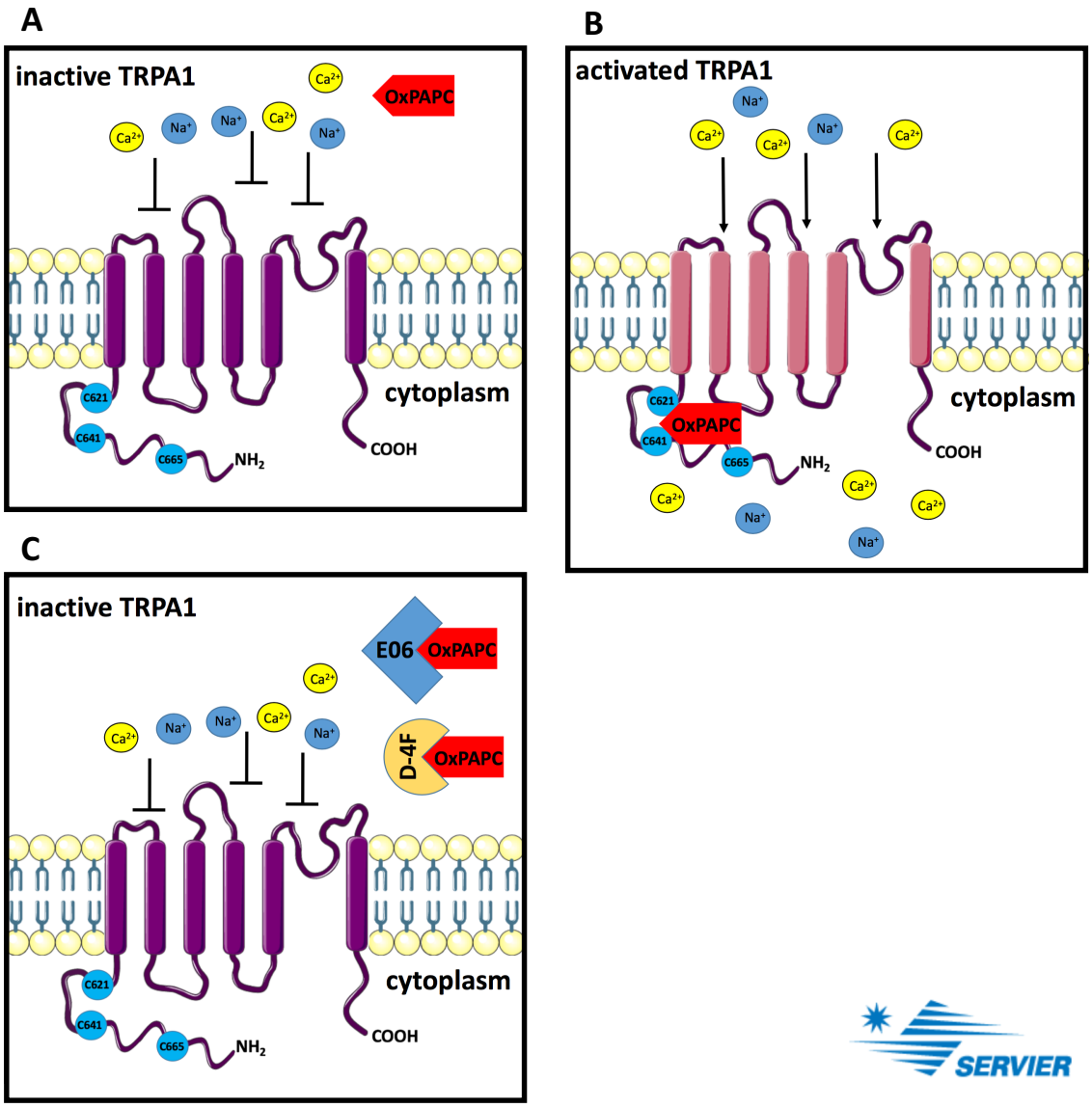

Figure 6: TRPA1 as a target receptor of OxPAPC

***A** shows TRPA1 in an inactive, impermeable state when OxPAPC is not bound to the receptor. Cations, like sodium and calcium, can pass through the activated TRPA1 channel after OxPAPC is bound to three decisive cysteines in the N-terminal part **(B)**. Bound to the scavengers D-4F and E06, OxPAPC cannot activate TRPA1 and the channel remains inactive.*

2 Material and Methods

2.1 HEK-293 cell culture

Human embryonic kidney cells-293 (HEK-293) are frequently used in cell biology or biotechnology. They were originally derived from human embryonic kidney cells and transformed by sheared adenovirus 5 DNA (Graham et al., 1977). They feature many favourable characteristics and are therefore widely used in experiments investigating signal transduction, protein interaction, viral packaging (Lin et al., 2014) or for the heterologous expression of membrane proteins (Ooi et al., 2016). Favourable properties of HEK-293 cells are a high division rate, a low expression of native channels, an efficient transfection as well as a reliable translation and processing of proteins (Wurm, 2004). In this study, we took advantage of these properties and used HEK-293 to stably express TRPA1 and to investigate the channel's properties as a target of OxPAPC.

2.1.1 Maintenance and splitting process

HEK-293 cells were cultured in Dulbecco's Modified Eagle Medium (DMEM) with GlutaMax^{TM} supplemented with 10 % heat-inactivated fetal bovine serum (FBS) and 1 % penicillin-streptomycin (PS) at 37 °C, and 5 % CO_2 in 25 cm^2 tissue culture flasks in a tissue culture incubator. At 70-90 % confluence, cells were sub-cultured in the following manner: the medium was aspirated from the flask and cells were washed with 5 ml of Dulbecco´s Phosphate Buffered Saline (DPBS). Cells were detached by incubation with 500 µl TrypLE Express (diluted 1/10 in DPBS) for 1 minute. The de-attachment was microscopically verified. After being washed once in cell culture medium, cells were re-plated in new tissue flasks. For selection, 400 µg/ml hygromycin was added to the cell culture. For calcium imaging experiments cells were cultivated on 10 mm cover slips in 4-well dishes coated with 20 µg/ml poly-L-lysine (PLL) at 37 °C for 2 hours.

2.1.2 Cryopreservation and thawing process

In order to constantly maintain a back-up of HEK-293 cells with or without TRPA1 channel expression, we always kept a stock of cells under cryopreservation. To prepare the long term storage of one HEK-293$_{TRPA1+/TRPA1-}$ cell culture, the freezing medium containing DMEM, 20 % dimethyl sulfoxide (DMSO) and 10 % FBS was prepared and prewarmed to 37 °C before usage. DMSO prevents crystallization within the cells during the freezing process. When the cell culture reached a confluency of 70-90 %, HEK-293 cells were detached from the cell culture flasks (in analogy to 2.1.1) and re-suspended in cell culture medium before centrifugation at $400 \times g$ for 5 minutes. The supernatant liquid was aspirated and the cell pellet was re-suspended in prewarmed freezing medium with a cell density of 1.5-2.0 $\times$ 10^6 cells/2 ml. This suspension was then filled into cryogenic vials and stored at -80 °C overnight in an isopropanol chamber before being transferred into liquid nitrogen at -196 °C for long term storage.

To re-cultivate the cells for calcium imaging experiments, the vials were thawed in a 37 °C water bath. Time of thawing had to be kept at a minimum, as DMSO in high concentrations destroys the cells when not frozen. To wash out DMSO, 1 ml cell suspension was transferred from the cryogenic vial into a 15 ml Falcon tube with 5 ml DMEM and subsequently centrifuged for 3 minutes at 800 rpm. After the supernatant was withdrawn, the described washing process was repeated once more. As a last step, 5 ml of the cell-DMEM suspension was transferred into a 25 cm^2 cell culture flask in a 1:5 dilution of cell culture medium containing DMEM with GlutaMax^{TM}, 10 % FCS and 1 % PS (in analogy to 2.1).

2.1.3 Transient transfection of HEK-293 with the TRPA1-3C mutant

We used the TRPA1-3C mutant C621S/C641S/C665S for experiments concerning the question whether three cysteines in the N-terminus of the channel were decisive for OxPAPC-mediated activation of TRPA1. Electrophilic agonists, like AITC are known to activate TRPA1 by forming covalent bonds with three intracellular N-terminal cysteine residues (Macpherson et al., 2007). In the mutant we used for our experiments, three cysteines at the positions

mentioned above were exchanged by serines, as serine is a structural homologue of cysteine with a hydroxyl group instead of a thiol group. In order to express TRPA1-3C in HEK-293 cells, we performed a transient transfection, meaning that the introduced DNA only temporally exists in the cell and does not undergo genomic integration (Kim and Eberwine, 2010). The transient transfection of HEK-293 cells was performed using FuGENE® HD Transfection Reagent, which is a non-liposomal formulation, conceived to introduce foreign DNA into the cell. We used FuGENE® HD Transfection Reagent because it has a high transfection and expression efficiency and a low cytotoxicity (Manifava, 2006; Ustek, 2007). 2 µg hTRPA1-3C, 0.2 ng/µl pcDNA3-YFP and 4 µl FuGENE® were diluted in 200 µl DMEM and incubated for 30 minutes at room temperature. The DNA-FuGENE mixture was added to a 35 mm dish with cultured HEK-293 cells. By microscopically visualizing the fluorescence, co-transfection with the yellow fluorescent protein (YFP) plasmid served as a transfection control of hTRPA1-3C. Calcium imaging was realized 48 hours after transfection.

2.2 Animals

To investigate the effect of OxPAPC on naturally TRPA1-expressing cells, we obtained DRG neurons from C57BL/6 wild type mice. Mice were bred in an unsterile environment in accordance to local Animal Care and Use Guidelines in the Institute of Clinical Neurobiology, University of Würzburg, Germany. For experiments mice were euthanized in a CO_2 chamber.

2.3 Preparation and culture of naive DRG neurons from C57BL/6 mice

100 ml of DRG medium was prepared beforehand. The medium consisted of the following: 75 ml of 1:1 DMEM + GlutaMAX™ and Ham's F12 Nutrient Mix, 2 ml HEPES 750 mM, 3 ml Glucose 10 %, 20 ml FBS, 100 µl gentamicin 50 mg/ml and NaOH until the medium had a pH of 7,4 (or until the medium's colour turned tomato red). DMEM contains amino acids and vitamins, thus supporting the growth of cells. It is supplemented with GlutaMAX™ to avoid the

accumulation of ammonia and to enhance cell viability and growth (Gibco™ DMEM, high glucose, GlutaMAX™ Supplement). The medium was furthermore enriched with Ham's F12 Nutrient Mix*,* which *Thermo Fisher Scientific* declares to ensure "superior quality, greater reliability, and improved consistency in mammalian cell culture" (Ham's F12 Nutrient Mixture, a). It contains components for the enhancement of cell growth like zinc, hypoxanthine, thymidine and putrescine (Ham's F12 Nutrient Mixture, b). Latter is a growth factor involved in cell division (Pohjanpelto and Raina, 1972). To avoid harming changes of the pH in our cell culture, we used HEPES, a zwitterionic organic chemical buffer with a pKa value between 6.0 and 8.0. It is well soluble, chemically and enzymatically stable, does not permeate the cell membrane, nor interfere critically with biochemical reactions. It is furthermore important for calcium imaging that HEPES has a very low ultraviolet light absorbance, as during the measurements, the cells and the medium were exposed to light within the ultraviolet range (Good et al., 1966). Extra glucose was added to the medium to ensure that DRGs were able to maintain their energy metabolism. FBS was supplemented to provide nutrient, growth and attachment factors for the cell culture and to protect them from oxidative damage and apoptosis (Fetal Bovine Serum). Gentamicin, a broad-spectrum antibiotic from the group of aminoglycosides, was used to prevent the growth of bacterial strains in the cell culture. Its antibacterial spectrum includes Gram-positive and Gram-negative bacteria like Pseudomonas, Proteus, Staphylococcus and Streptococcus (Gentamicin, 1967).

The medium was sterile-filtered with a 0.2 µm filter. Primary DRG cultures were obtained from 6 to 12 weeks old C57BL/6 mice of either sex. The mouse was asphyxiated in a CO_2 chamber and prepared in the following manner: for reduced spreading of germs, the fur was moistened with the disinfectant liquid terralin®. It is bactericidal and helps to avoid contamination of the cell culture. The fur was then lifted from the muscle beneath. The spine was cut through at the skull and the pelvis and subsequently separated from all adjoining organs and tissue. In order to expose the DRGs, the spine was opened at the level of the processi transversi. After mobilization of the spinal cord, ganglia were found

in the foramina intervertebralia between two vertebrae. DRGs were detached with very fine tweezers and kept in HBSS buffer supplemented with gentamycin in a 35 mm petri dish. Of all ganglia, as many as possible should be found in order to get a sufficient amount of neurons for imaging experiments. Ganglia were separated from attached nerves with a scissor and kept in a 15 ml Falcon. The suspension was centrifuged for 3 minutes at 600 rpm, the supernatant was then removed and discarded. To separate the connective tissue from DRG neurons, the ganglia were incubated with 0,5 ml collagenase (1,5 mg/ml) and dispase (3,0 mg/ml) for 20 minutes in a water bath at 37 °C. Thereafter, 0,5 ml Trypsin (0,25 %) was added for another 5 minutes to the suspension. For Trypsin inactivation, 4 ml medium was added and the suspension was triturated and then centrifuged for 5 minutes at 1000 rpm. The supernatant was removed and discarded and the remaining cell mass was re-suspended in about 80 µl 'final' medium (= medium + 1:100 ITS + 1:1000 nerve growth factor (100 µg/ml)). DRGs grew at an approximate density of 7×10^3 per 10 mm glass cover slip (coated with poly-L-lysine (PLL, 20 µg/ml)) with 10 µl of suspension. For 1-2 h, neurons adhered to the glass cover in the incubator at 37 °C and 5 % CO_2 atmosphere, before flooding them with 2 ml of 'final' medium. Calcium imaging was scheduled after 24 hours.

2.4 Calcium imaging

Calcium is one of the most abundant elements on earth and serves several functions like transmission of information through second messenger cascades, glycogen metabolism in hepatocytes or neuronal axonal growth (Berridge et al., 2000). Intracellular calcium levels have to be kept at a very low level since it has highly cytotoxic effects like aggregation of proteins and nucleic acids, precipitation of phosphates and damage of the lipid bilayer at high levels. In order to ensure intracellular calcium homeostasis, the cell has developed several systems like calcium-binding proteins (EF-hand) and active transporters. This way cytosolic calcium concentrations can be kept at about 50-100 nM, enabling us to display an increase in intracellular calcium with a fluorescent dye (Blumenfeld et al., 1992).

2.4.1 Fura-2/AM

Fura-2 is a ratiometric, fluorescent dye, which we used in our experiments to determine changes of intracellular calcium concentrations. Its chelate-building properties permit a photometric determination of calcium concentrations within the cell. Calcium saturated Fura-2 is excited at 340 nm, non-saturated at 380 nm, light is emitted at 512 nm. The ratiometric properties of Fura-2 allow direct conclusions to changes of the intracellular calcium concentrations (Barreto-Chang and Dolmetsch, 2009). The derivate, Fura-2/acetoxymethyl ester (AM) can cross the cell membrane by passive diffusion and is converted into Fura-2 by cellular esterases (Grynkiewicz et al., 1985). Fura-2/AM was prepared as 2 mM stock solution by adding 500 µL of 20 % Pluronic® F-127 plus DMSO to 1 mg Fura-2/AM. 3 µL aliquots were made for dye loading, 1 mL of calcium imaging buffer was added.

2.4.2 Preparation and performance of calcium imaging experiments

We used the fact that TRPA1 channels are conductive for cations like sodium and calcium (Kadkova et al., 2017) to investigate whether OxPAPC was able to activate TRPA1 and to evaluate the benefit of different OxPAPC scavengers. We visualized changes of intracellular calcium concentrations after the addition of different agonists by performing calcium imaging experiments. Previous to the measurements, HEK-293 cells were plated on a PLL-coated glass cover slips and loaded with 6 µM Fura-2/AM (dissolved in DMSO + 20 % Pluronic) dissolved in buffer containing 10 mM HEPES, 134 mM NaCl, 6 mM KCl, 1 mM $MgCl_2$, 1 mM $CaCl_2$, 5.5 mM Glucose, pH 7.4. After 30 minutes of incubation at 37 °C and 5 % CO_2 in a standard cell culture incubator, the cells were washed with buffer and positioned into a custom-made measuring chamber containing 100 µl buffer solution. Through the microscope, with a 10-fold magnification, we selected a field of vision in which we estimated a sufficient cell density of at least 100 cells. This selected area was then recorded during the calcium imaging. The measurements were performed at room temperature and in complete darkness with a Nikon TE2000-E inverted microscope with a CFI S-Fluor 10x/0.5 objective and a cooled EMCCD Andor iXon camera. In intervals

of 2 seconds, the samples were exposed to 340/380 nm of light for 100 ms with a Lambda DG 4/17 wavelength switch. Data was collected by NIS Elements Software and analysed with the ImageJ 1.42l software (Schneider et al., 2012).

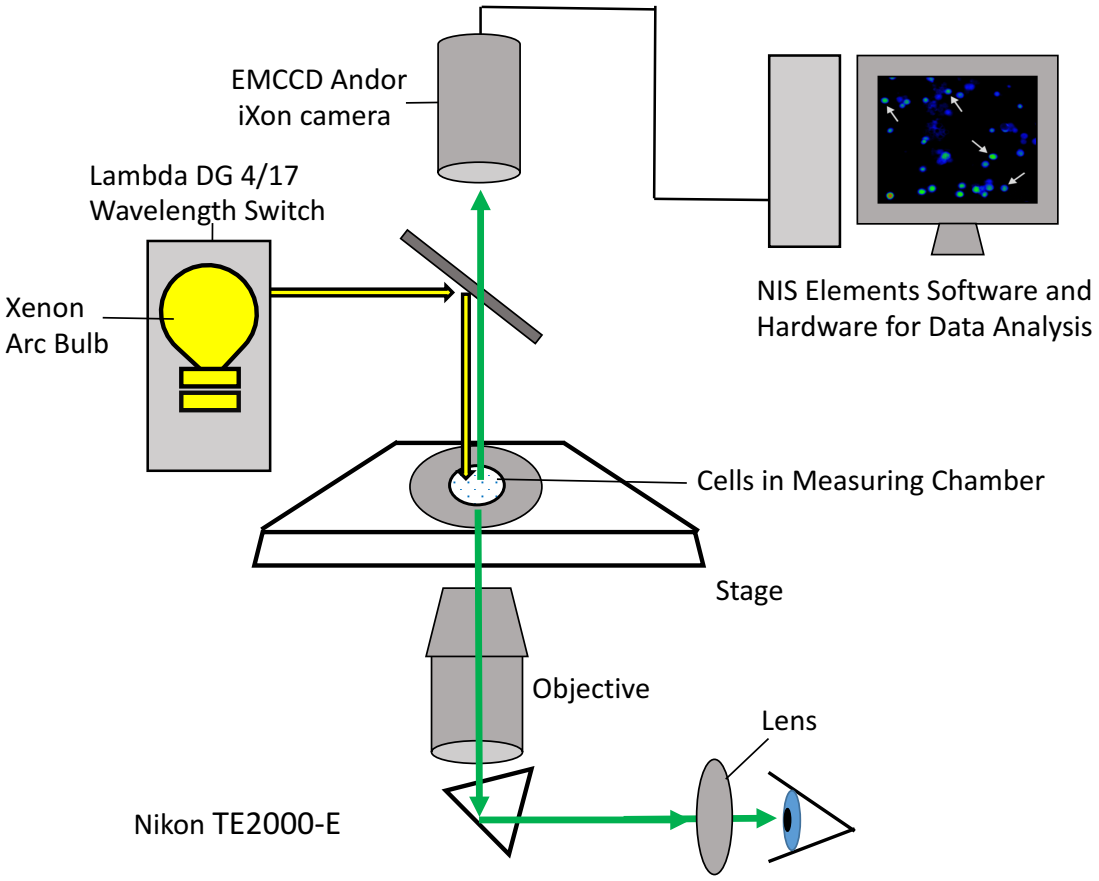

Figure 7: Schematic representation of the experimental setup for calcium imaging

Through the Nikon TE2000-E inverted microscope, we can see the cells in the measuring chamber in a 100-fold magnification. The Lambda DG 4/17 wavelength switch, equipped with a xenon arc bulb, exposes the cells alternating to 340 and 380 nm of light. The light emitted by the cells loaded with Fura-2/AM is recorded by a EMCCD Andor iXon camera and demonstrated graphically on a computer by NIS Elements Software.

The cell density on glass cover slips was not counted, as for the analysis of Fura-2 ratios we always selected 100 cells within the recorded area randomly. For each measurement, one new glass cover slip with either HEK-293 cells or

DRG neurons was used. For channel modulation following substances were tested:

Table 1: Time points of agonist/antagonist addition

Substance	Time point of Addition*		Concentration**
	HEK-293	DRG	
OxPAPC	120 seconds	120 seconds	10 µM
AITC	120 seconds	540 seconds	10 µM
Capsaicin	—	720 seconds	1 µM
Carvacrol	540 seconds	—	250 µM
KCl	—	900 seconds	50 mM
HC-030031	540 seconds	preincubation with cells	10 µM
E06 mAb	preincubation with OxPAPC, addition: 120 s		1/3000
IgM	preincubation with OxPAPC, addition: 120 s		1/500
D4F	preincubation with cells		100 µg/ml
	preincubation with OxPAPC, addition: 120 s		

* Time point of addition of substances to the measuring chamber after starting the measurements of HEK-293 cells or DRGs

** Final concentration in measuring chamber

2.4.3 Evaluation and analysis

In ImageJ ROIs (regions of interest) were positioned on 100 different cells. The analysis of the film taken during calcium-imaging experiments contained data about quantification of light intensities that were emitted by the cells after excitation with 340 and 380 nm of light (as described in 2.4.2). These data were transferred into Excel tables, where the quotient of light intensities at different time points at 340 nm and 380 nm (Ratio F(340/380)) was calculated after background subtraction. This ratio allows indirect conclusions about intracellular calcium levels during the measurement.

The area under the curve (AUC) was calculated from the mean response of 100 cells in different intervals:

- for all HEK-293 cell experiments between 120-570 seconds
- for DRG experiments: OxPAPC between 360-540 seconds, AITC 540-720 seconds, capsaicin 720-900 seconds.

Responding cells (%) were defined as cells that showed an increased Fura-2 ratio of:

a) ≥ 1.5 times in HEK-293 cell experiments

b) ≥ 1.3 times in DRG experiments

over base line after the addition of an agonist.

2.5 Statistics

Mean ± SD/SEM over all ROIs at each time point was calculated. Single measurements were analysed with a t-test, whereas multiple measurements with one or two variables were analysed by one-way ANOVA or by two-way ANOVA repeated measurements (RM). Differences were considered significant when $p \leq 0.05$. Statistical analysis was performed with OriginPro 9.0.

2.6 Chemicals and buffers

All standard chemicals were obtained from Sigma-Aldrich Chemie GmbH (Steinheim, Germany)

Table 2: Company directions

A. Hartenstein Laborbedarf GmbH, Würzburg, Deutschland
Addgene, Cambridge, USA
Avanti Polar Lipids, Alabaster, USA
Biomol GmbH, Hamburg, Germany
Bruker Daltonics, Bremen, Germany
Calbiochem, San Diego, USA/BD Bioscience, San Jose, USA
Greiner bio one GmbH, Frickenhausen, Germany
Hycultech GmbH, Beutelsbach, Germany
IKW®-Werke, Staufen, Germany
Life Technologies GmbH, Darmstadt, Germany
OriginLab Corporation, Northampton, MA, USA
Peptide Specialty Laboratories GmbH, Heidelberg, Germany
Sarstedt inc. , Newton, NC, USA
Schülke & Mayr GmbH, Norderstedt, Deutschland
Sigma-Aldrich, Taufkirchen, Germany

Table 3: Chemicals, buffers and solutions

Chemical	Company	Productno.
0,25 % Trypsin-EDTA	Life Technologies	25200056
AITC	Sigma-Aldrich	36682
Capsaicin	Sigma-Aldrich	M2028
Carvacrol	Sigma-Aldrich	282197
CFA	Calbiochem /BD Bioscience	344289

Collagenase D	Sigma-Aldrich	COLLD-RO
D-4F peptide	Peptide Specialty Laboratories	Custom made
Dimethylsulfoxid (DMSO)	Sigma-Aldrich	276855
Dispase II	Sigma-Aldrich	D4693
Dulbecco´s Modified Eagle´s Medium (DMEM), high glucose, GlutaMAX^{TM} Supplement	Life Technologies	61965026
Dulbecco´s Phosphate Buffered Saline (DPBS)	Life Technologies	14190144
E06 mAb	Avanti Polar Lipids	330001
FuGENE® HD Transfection Reagent	Promega	E2311
Fura-2/AM	Life Technologies	F1201
Gentamicin solution	Sigma-Aldrich	G1397
Gibco® Fetal bovine serum (FBS)	Life Technologies	10500064
Ham's F12 Nutrient Mix	Life Technologies	21765029
Hank's Balanced Salt Solution, HBSS, no Ca^{2+}, no Mg^{2+}	Life Technologies	14170138
HC-030031	Sigma-Aldrich	H4415
HEPES	Sigma-Aldrich	H3375
Hygromycin B solution from Streptomyces hygroscopicus	Sigma-Aldrich	H0654

ITS Liquid Media Supplement (100x)	Sigma-Aldrich	I3146
Mouse IgM isotype	Biomol	WS0803M
Nerve growth factor-7s (NGF)	Sigma-Aldrich	N0513
OxPAPC	Hycultech	HC4036
pcDNA3-YFP	Addgene	13033
Penicillin-Streptomycin	Life Technologies	15070063
Pluronic® F-127	Sigma-Aldrich	P2443
Poly-L-lysine hydrobromid, PLL	Sigma-Aldrich	P2636
terralin® liquid	Schülke & Mayr	
TrypLE™ Express Enzyme, phenol Red	Life Technologies	12605036

Table 4: Other material, software and devices

4-well cellstar cell culture dishes	Greiner bio one
Bruker Autoflex mass spectrometer	Bruker Daltonics
EMCCD Andor iXon	Andor Technology Ltd., Belfast, UK
IKA® RW 14 lab mixer	IKW®-Werke
Lambda DG4/17 wavelength switch	Sutter Instruments, Novato, CA, USA
Microscope cover glasses, ∅ 10 mm	A. Hartenstein Laborbedarf
Nikon TE2000-E	Nikon Instruments Europe B.V., Amsterdam, Netherlands
NIS-Elements Advanced Software	Nikon Instruments Europe B.V.

Origin Pro 9.0	OriginLab Corporation, Northampton, MA, USA
Tissue culture flask, 25 cm^2	Sarstedt inc.

3 Results

3.1 OxPAPC induced a calcium influx in HEK-293 cells stably expressing hTRPA1

Ratiometric calcium imaging experiments were used to explore whether the commercially available OxPAPC mixture could activate TRPA1 channels. First of all, we performed calcium measurements on HEK-293 cells which, by means of a lentiviral vector, stably expressed this channel on their surface. After the addition of OxPAPC to the measuring chamber, the alteration of intracellular calcium levels was determined.

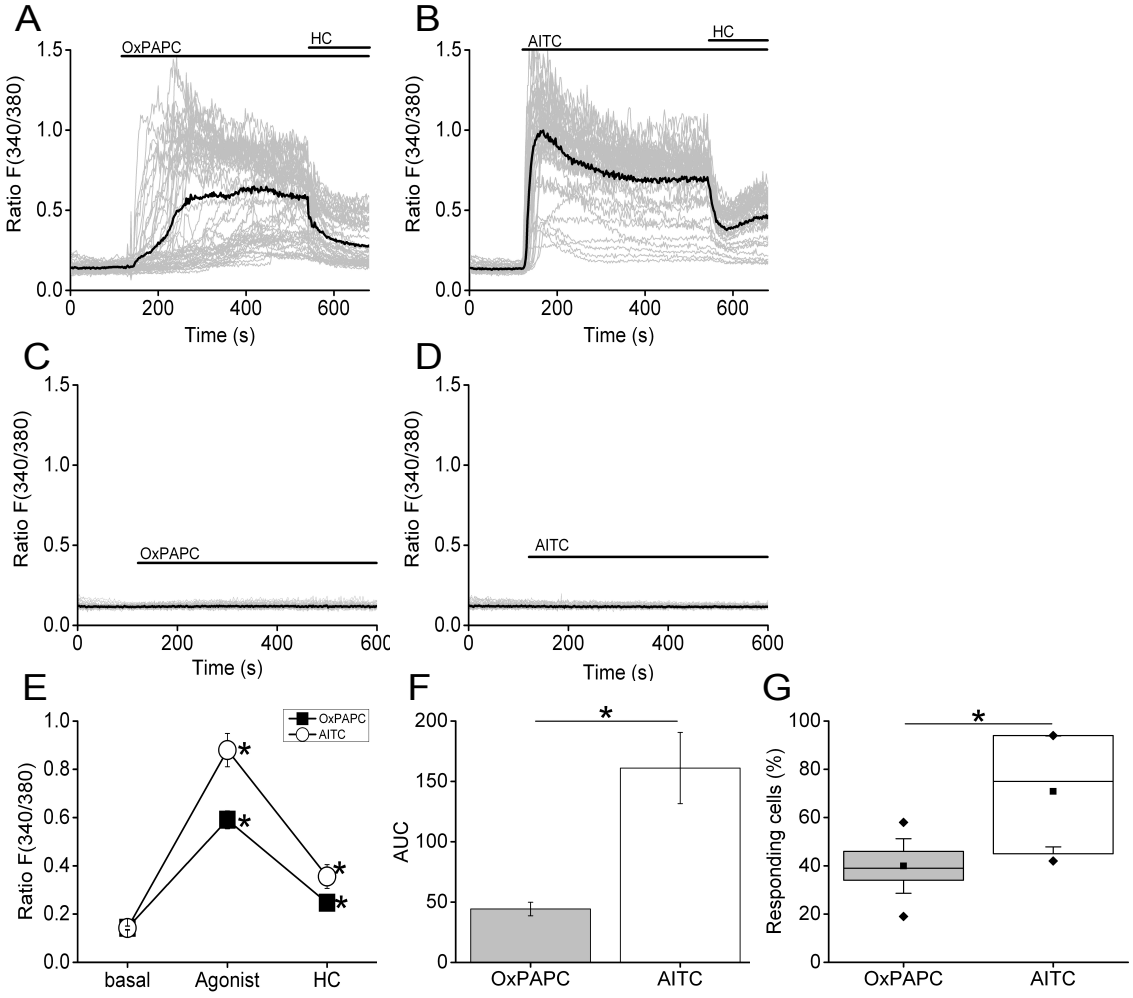

Figure 8: OxPAPC triggered an activation of hTRPA1 channels in HEK-293 cells.

*Graphs **A-D** represent Fura-2/AM-based calcium imaging measurements. F(340/380) ratios are depicted on the abscissa, time (h) on the ordinate. Grey lines show intracellular calcium changes of single cells, black lines the average activation of about 100 cells. Experiments in **A** and **B** were performed on HEK-293 cells stably expressing hTRPA1, **C** and **D** on non-transfected HEK-293 cells. All measurements of this set of experiments were carried out on 24 days in total. OxPAPC, AITC and HC-030031 were used in concentrations of 10 µM. OxPAPC and AITC were added after 120 seconds, HC-030031 after 540 seconds. Non-transfected HEK-cells served as a negative control and were stimulated with 10 µM OxPAPC **(C)** and 10 µM AITC **(D)**. Summary graph **E** shows a comparison of peaks of mean responses after activation with OxPAPC (black square) and AITC (white circle) and blocking with HC-030031. Statistical analysis: 'n' refers to the number of implemented calcium imaging measurements: n(OxPAPC) = 15, n(AITC) = 11, n(OxPAPC, HC-030031) = 9, n(AITC, HC-030031) = 6; two-way ANOVA RM, post hoc Bonferroni, * p ≤ 0.05 **(E)**. Box-plot and bar graph **(F and G):** n(OxPAPC) = 13, n(AITC) = 6; one-way ANOVA, post hoc Bonferroni, * p ≤ 0.05.*

Calcium imaging measurements of HEK-293 cells stably expressing hTRPA1 revealed an OxPAPC-triggered, TRPA1-dependent increase in intracellular calcium. Average Fura-2 ratios F(340/380) after OxPAPC stimulation were about 4 times higher than base line values (0.59 versus 0.14). Ratios are indirect measures of cytosolic calcium concentrations. A significantly higher activation was induced by mustard oil (AITC; mean ratio 0.88). The addition of the specific TRPA1 antagonist HC-030031 blocked calcium influx instantly and caused an immediate decrease of Fura-2 ratios after previous OxPAPC or AITC stimulation (Figure 8 **E**). Cytosolic calcium levels showed an initial boost after OxPAPC (Figure 8 **A**) and AITC (Figure 8 **B**) addition, which decreased thereafter and evened out on a plateau of activation before being blocked by HC-030031. Comparing both agonists, the increase in intracellular calcium levels caused by OxPAPC was delayed and less pronounced. Both, the area under the curve (AUC) as well as the number of responding cells were significantly lower after OxPAPC stimulation than after activation by AITC.

OxPAPC raised the AUC to only about one third of the AUC reached by AITC (Figure 8 **F**). 56 % of all cells responding to AITC were also responsive to OxPAPC (Figure 8 **G**). No response to OxPAPC (Figure 8 **C**) or AITC (Figure 8 **D**) was measured in non-transfected HEK-293 control cells.

In calcium imaging experiments using calcium-free buffer solution, neither OxPAPC (Figure 9 **A**) nor AITC (Figure 9 **B**) evoked a cytoplasmic calcium increase as summarized in the statistical analysis (Figure 9 **C**).

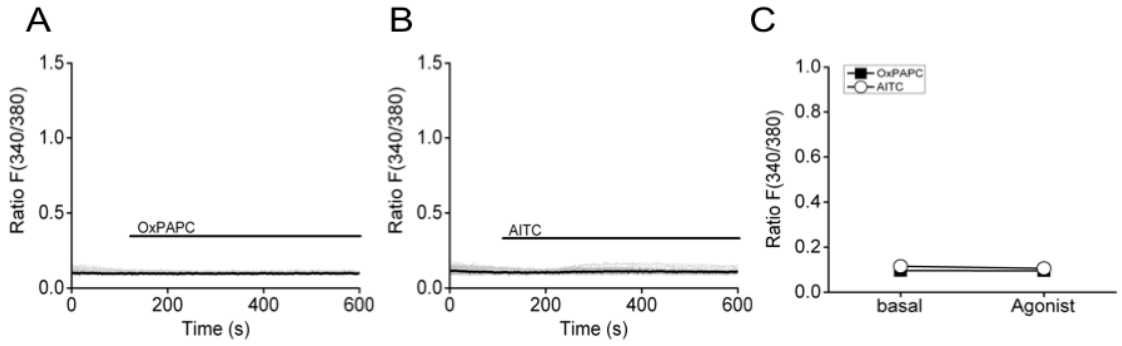

Figure 9: Intracellular calcium levels could not be increased by the TRPA1 agonists OxPAPC and AITC, when the measurements were performed in calcium-free buffer solution.

Stimulation of HEK-293$_{hTRPA1}$ in a calcium-free buffer solution with 10 µM OxPAPC ***(A)*** *and 10 µM AITC* ***(B)*** *in Fura-2-based imaging experiments. OxPAPC and AITC were added after 120 seconds.* ***C*** *is a summary graph of all OxPAPC and AITC measurements performed with a calcium-free buffer: n = 3 per group, performed on 2 different days. Statistical analysis: two-way ANOVA RM, post hoc Bonferroni, * $p \leq 0.05$.*

3.2 hTRPA1-3C mutant channels showed a minimal response to OxPAPC

In the HEK-293 cell line, which was transiently transfected with the triple TRPA1-3C mutant, AITC did not triggered any calcium influx. OxPAPC could not cause a significant activation of TRPA1-3C, but there were still some cells responding with a slight increase in intracellular calcium (Figure 10 **A**). In

contrast, carvacrol, a non-electrophilic TRPA1 agonist, set off a 2.6 times higher calcium increase than OxPAPC or AITC in these experiments (Figure 10 **D**). Carvacrol-triggered activation of TRPA1-3C confirmed that the function of the channel was still intact. For comparison, stimulation of the wild-type hTRPA1 channel in HEK-293 cells with OxPAPC is shown (Figure 10 **C**).

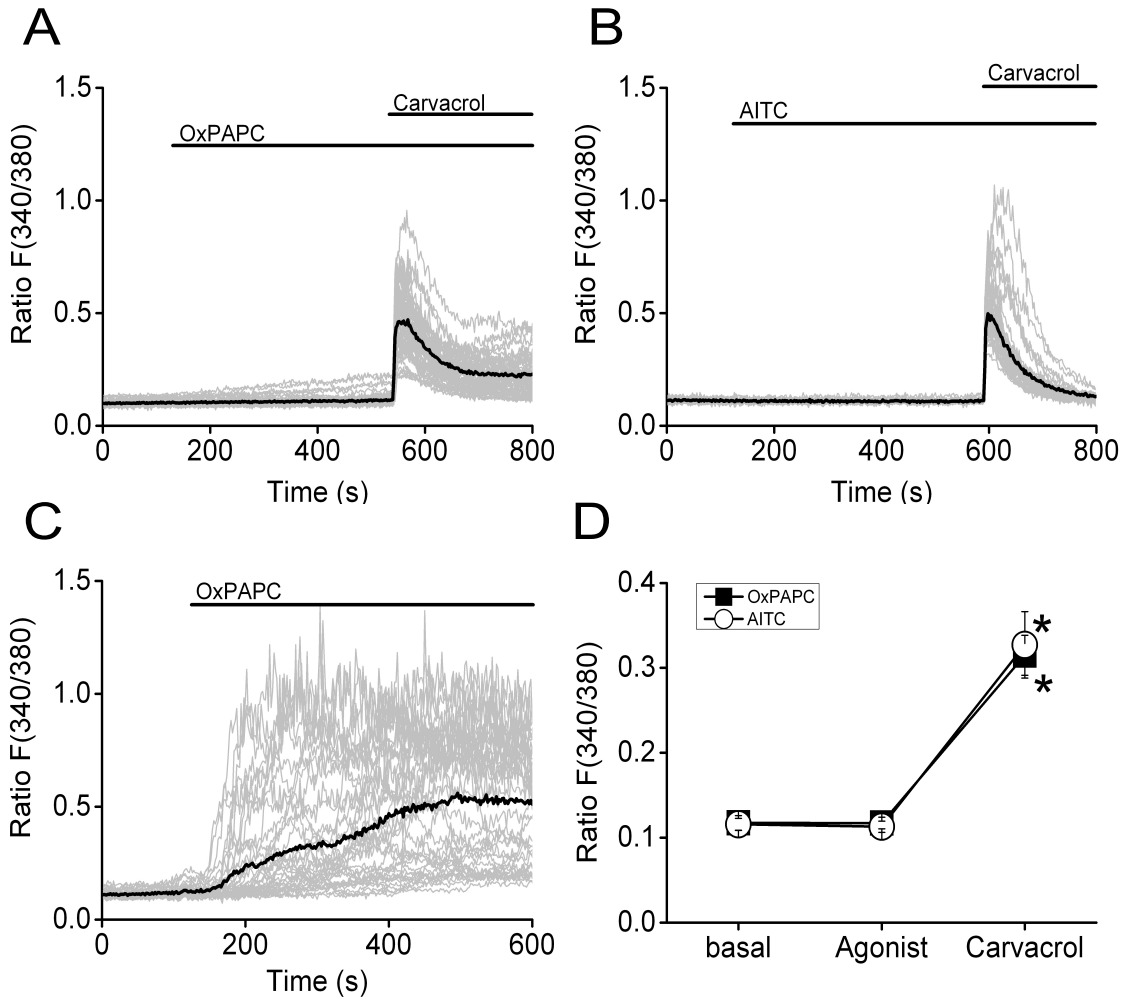

Figure 10: HEK-293 cells transiently transfected with the hTRPA1-3C mutant channel responded only slightly to the stimulation with the electrophilic agonists OxPAPC and AITC.

hTRPA1 C621S/C641S/C665S triple mutant transiently expressed in HEK-293 cells was used for calcium imaging ***(A, B, D)****. HEK-293 cells were stimulated with the agonists OxPAPC (10 µM)* ***(A)****, AITC (10 µM)* ***(B)*** *and carvacrol (250 µM)* ***(A and B)*** *during the experiments. OxPAPC and AITC were added after 120 seconds of imaging,*

carvacrol after 540 seconds. 10 µM OxPAPC was used for HEK-293 cells stably expressing TRPA1 as a positive control ***(C)****. Summary graph* ***D:*** *n(OxPAPC, carvacrol) = 6, n(AITC, carvacrol) = 3; the measurements were performed on 2 different days. Statistical analysis: two-way ANOVA RM, post hoc Bonferroni, * p ≤ 0.05.*

3.3 Blockade of the agonistic capacities of OxPAPC on hTRPA1 by D-4F and E06

After providing experimental evidence that the commercially available OxPAPC mixture could set off an influx of calcium in hTRPA-expressing HEK-293 cells, we investigated possibilities to neutralize OxPAPC. Therefore, we assessed whether D-4F, an apolipoprotein A-I mimetic peptide, as well as the monoclonal antibody (mAb) E06 were able to prevent OxPAPC-induced calcium influx in HEK-293 cells.

After a 30-minute preincubation of OxPAPC and D-4F, hTRPA1 activation was decreased significantly (Figure 11 **A**). The percentage of responding cells was decreased by about 72 % compared to the activation induced by OxPAPC only. The AUC after co-incubation with D-4F was even lowered by 82 %. In the second setting (Figure 11 **B**), OxPAPC stimulation evoked a minor increase in Fura-2 ratios, too (Figure 11 **C**). After preincubation with D-4F, only 12.4 % of HEK-293 cells responded to OxPAPC addition, with an overall average AUC of 11.9. In another set of measurements, HEK-293 cells underwent a 30-minute D-4F preincubation before being exposed to AITC (Figure 11 **D**). Comparing Figure 11 **D** and Figure 11 **E**, there is no difference of calcium influx in both experiments. Statistical analysis of the AUC and percentage of responding cells confirmed that previous addition of D-4F could not inhibit AITC-induced activation of hTRPA1.

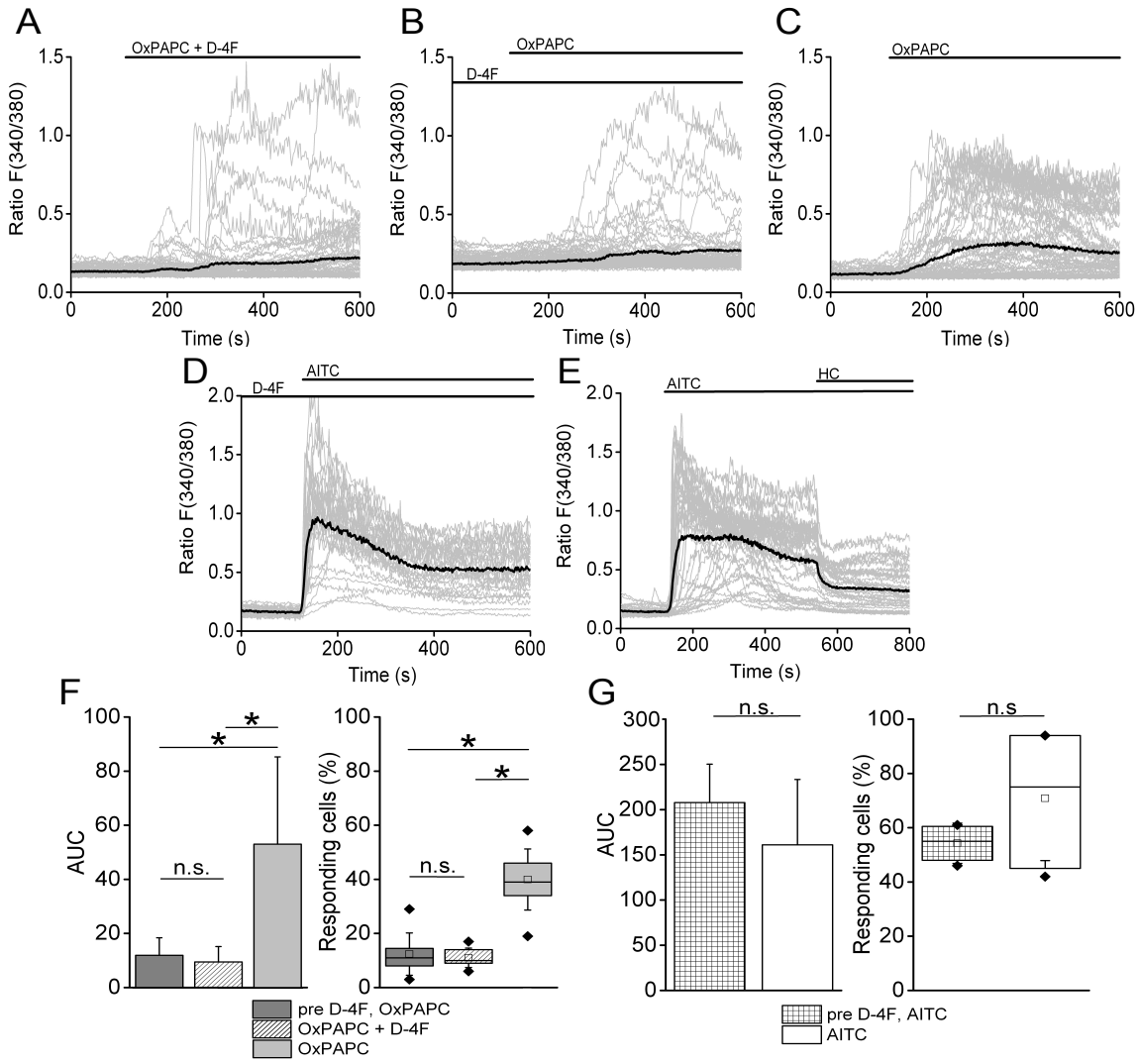

Figure 11: D-4F diminished the hTRPA1 response evoked by OxPAPC.

The effect of D-4F was tested in 2 different setups: In ***A,*** *100 µM OxPAPC + 1 mg/ml D-4F were preincubated in imaging buffer for 30 minutes at 37 °C. The solution was added after 120 seconds to the measuring chamber and diluted by factor 10. In* ***B,*** *Fura-2/AM loaded cells were incubated with 100 µg/ml D-4F in imaging buffer for 30 minutes. During the measurement, the cells were stimulated with 10 µM OxPAPC after 120 seconds.* ***C*** *shows an experiment where only OxPAPC was added at a final concentration of 10 µM after 120 seconds.* ***(D)*** *HEK-293 cells were preincubated with D-4F peptide as described in* ***B****, followed by an AITC stimulation (10 µM). For comparison,* ***E*** *illustrates a measurement of HEK-293 cells stimulated with 10 µM AITC and blocked with 10 µM HC-030031 (as described*

*in **3.1 B**). **F** and **G** show the AUC (bar graph) and percentage of responding cells (box plot) for OxPAPC **(F)** and AITC **(G)** measurements. n(pre D-4F, OxPAPC) = 8, n(OxPAPC + D-4F) = 7, n(OxPAPC) = 13, n(pre D-4F, AITC) = 4, n(AITC) = 6. All measurements including D-4F were performed on 9 days in total. Statistical analysis: one-way ANOVA, post hoc Bonferroni, * p ≤ 0.05.*

In our second approach to reduce OxPAPC-induced activation of hTRPA1, we used the monoclonal antibody E06 to bind and neutralize OxPAPC. Our experiments demonstrated that the influx of calcium in HEK-293 cells was considerably reduced when OxPAPC was incubated with E06 prior to the measurement (Figure 12 **A**). The isotype control antibody IgM was used to rule out unspecific effects as shown in Figure 12 **B**. Regarding the AUC, statistics revealed that E06 could significantly lower hTRPA1 channel activation by 70 %, when preincubated with OxPAPC, compared to measurements where only OxPAPC was added (Figure 12 **G**). Furthermore, only 37 % of all OxPAPC-sensitive cells were still responsive after preincubation with E06. The AUC of OxPAPC + IgM measurements was 62 % higher than the AUC of OxPAPC + E06 measurements. The same tendency resulted from the percentage of responding cells in these measurements, as 58 % more cells were activated by OxPAPC in the presence of IgM. The percentage of cells responding to OxPAPC stimulation and the resulting AUC were not significantly different from the percentage responding to the OxPAPC-IgM-solution and the AUC calculated from these measurements (Figure 12 **G**).
AITC was preincubated with each, E06 (Figure 12 **D**) and IgM (Figure 12 **E**) for 30 minutes prior to the measurements. AITC only was used as positive control (Figure 12 **F**). The AUC was significantly reduced by 51 % by E06 and by 58 % by IgM, compared to AITC only (Figure 12 **H**). The difference between E06 and IgM was not significant. Moreover, E06 lowered the percentage of cells responding to AITC in a non-significant manner, while IgM decreased the values significantly.

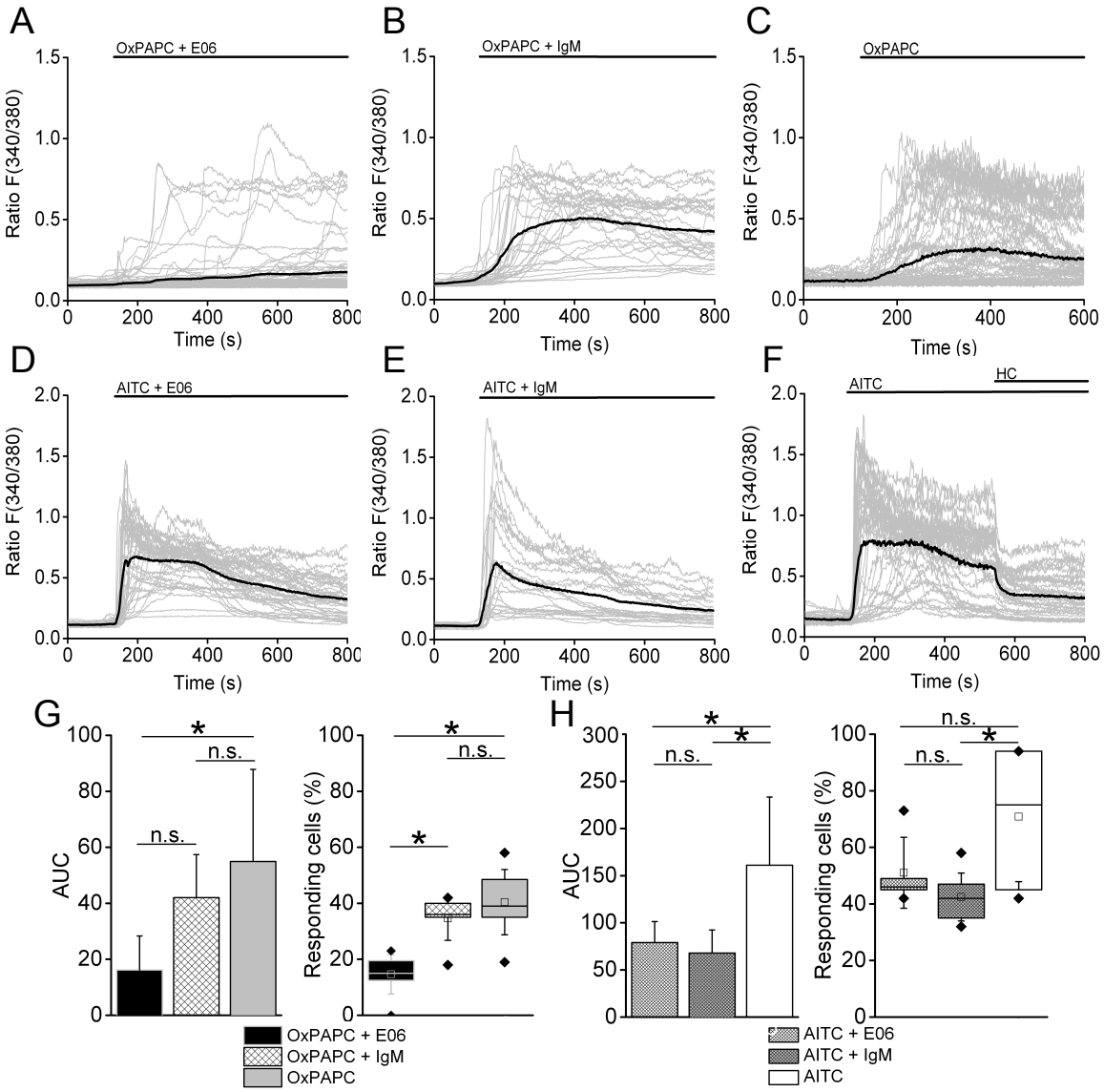

Figure 12: E06 neutralized OxPAPC and subsequently reduced hTRPA1 activation.

(A) *E06 (1/300) was preincubated with OxPAPC (100 µM) for 30 minutes at 37 °C. After 120 seconds of measurement, the solution was added with final concentrations of 10 µM OxPAPC and 1/3000 E06 mAb.* ***(B)*** *IgM (1/50) and OxPAPC (100 µM) were preincubated for 30 minutes and assessed during the experiment in concentrations of 10 µM OxPAPC and 1/500 IgM. To draw a comparison,* ***C*** *shows an OxPAPC measurement performed as described in* ***3.1****. AITC (100 µM) was preincubated with either* ***(D)*** *E06 mAb (1/300) or* ***(E)*** *IgM (1/50) for 30 minutes. During the measurements AITC was used with a concentration of 10 µM, E06 of 1/3000 and IgM*

of 1/500. ***F*** *shows an AITC measurement (10 µM final concentration) with a HC-030031 block (10 µM final concentration).* ***G*** *demonstrates the AUC and the percentage of responding cells of OxPAPC-related assays. Compared were OxPAPC + E06 to OxPAPC + IgM and OxPAPC only.* ***H*** *follows the same schema comparing AITC + E06 to AITC + IgM and AITC only. n(OxPAPC + E06) = 8, n(OxPAPC + IgM) = 7, n(OxPAPC) = 13, n(AITC + E06) = 5, n(AITC + IgM) = 7, n(AITC) = 6. All experiments including E06 were performed on 10 days in total. Statistical analysis: one-way ANOVA, post hoc Bonferroni, * p ≤ 0.05.*

3.4 OxPAPC induced a TRPA1-dependent calcium influx in cultured DRG neurons, which was reduced by the OxPAPC scavengers D-4F and E06

After confirming experimentally that OxPAPC was an agonist of TRPA1 channels in HEK-293 cells, we asked whether these findings were reproducible in native cells. TRPA1 is naturally expressed by sensory DRG neurons (Bautista et al., 2013). Therefore, we used rodent DRG neurons to investigate whether OxPAPC could activate TRPA1 and to evaluate the extent of calcium influx compared to HEK-293 cells.

In calcium imaging experiments of DRG neurons, the addition of OxPAPC doubled the Fura-2 ratio. The increase in cytoplasmic calcium after OxPAPC addition was less pronounced in naïve cells with Fura-2 ratios of 0.36 compared to 0.59 in the cell model (DRG < HEK-293$_{hTRPA1}$). 16 % of neurons were responsive to OxPAPC, whereas 40 % of HEK-293$_{hTRPA1}$ cells reacted with an influx of calcium ions (compare to **3.1**) The more potent TRPA1 agonist AITC enhanced intracellular calcium levels by a Fura-2 ratio of 0.1, when cells were already activated by OxPAPC. In total, 25 % of DRGs were activated after the addition of AITC. DRGs were also tested for their response to capsaicin, a specific TRPV1 agonist. TRPA1 and TRPV1 channels are known to be co-expressed in DRGs (Bautista et al., 2006). Calcium levels after capsaicin stimulation differed significantly from OXPAPC values but non-significantly from AITC values. Potassium served as control for neurons **(**Figure 13 **A, D).** The addition of potassium to the medium surrounding the cells causes an absolute

surplus extracellularly. High concentrations of extracellular potassium, in comparison to intracellular concentrations, result in an increasing membrane potential of neuronal cells. These changes in potential activate voltage gated sodium and calcium channels, which in turn leads to an influx of these ions. Calcium imaging experiments show how preincubation of DRG neurons with the specific TRPA1 blocker HC-030031 almost completely suppressed OxPAPC and AITC-mediated calcium influx **(**Figure 13 **C)**. HC-030031 diminished the number of cells responding to OxPAPC cells by 75 %. The AUC in this setting was also significantly decreased by 26 % **(**Figure 13 **E)**. The statistical evaluation of AITC-correlated results revealed a HC-030031-caused, significant reduction of the AUC and the percentage of responding cells.

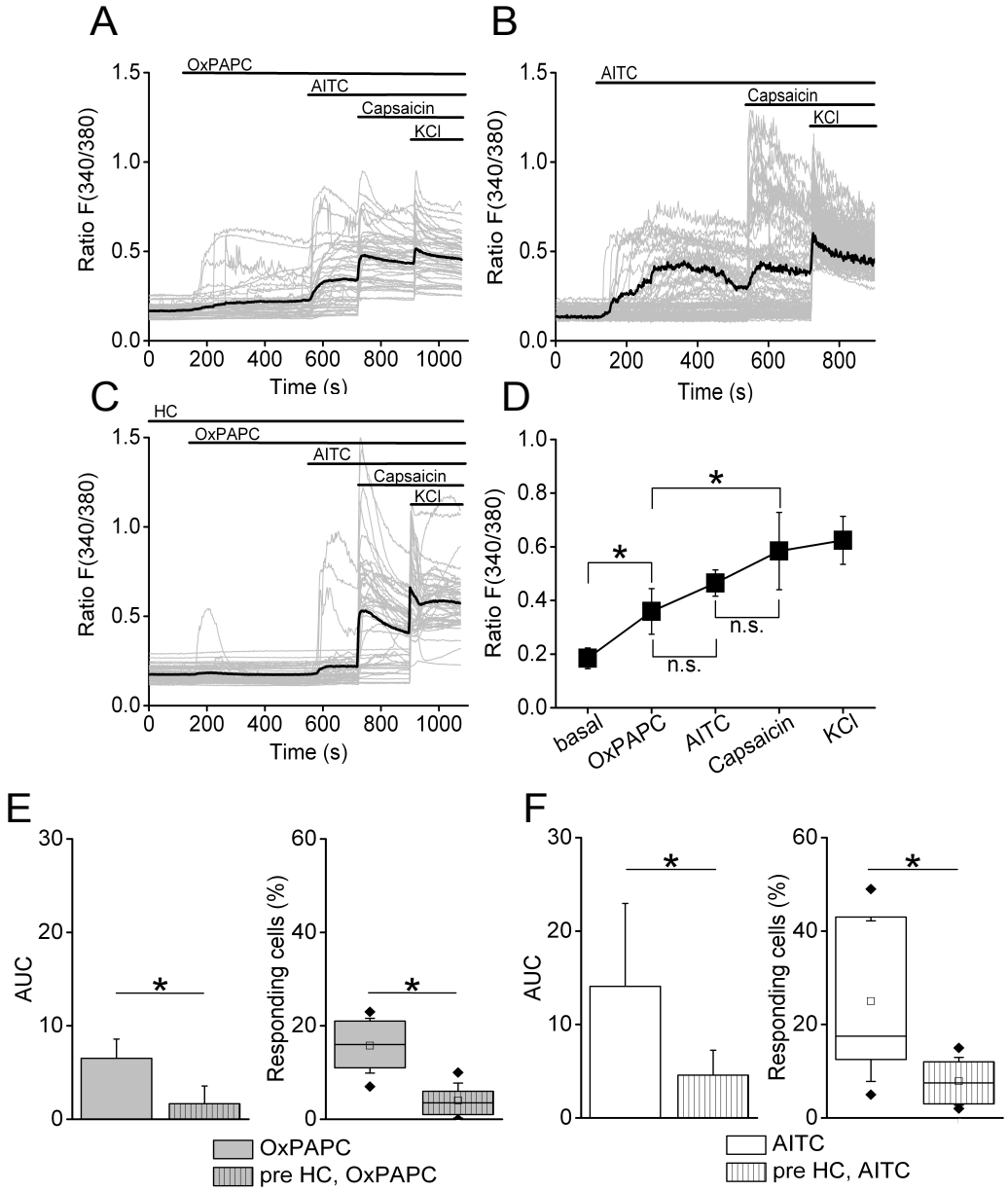

Figure 13: Neurons from DRGs of C57BL/6 WT mice showed a TRPA1-dependent activation by OxPAPC in calcium imaging.

DRGs were stimulated with the following agonists at the corresponding time points: OxPAPC (10 µM) after 120 seconds, AITC (10 µM) after 540 seconds, capsaicin (1 µM) after 720 seconds, KCl (50 mM) after 900 seconds. In measurements without OxPAPC, the cells were stimulated at different time points: AITC after 120 seconds, capsaicin after 540 seconds, KCl after 720 seconds ***(A, B)****.* ***C*** *shows a measurement of DRG neurons with a five minutes preincubation in buffer + HC-030031 (10 µM), followed by a stimulation as indicated in* ***A****. Black lines in graphs* ***A-C*** *show the average*

activation of about 50 cells, depending on the yield of cells after preparation. ***D*** *demonstrates a summary graph of the average increase of Fura-2 ratios F(340/380) after stimulation with each agonist. Statistics* ***(D)****: n = 8, one-way ANOVA RM, post hoc Bonferroni, * p ≤ 0.05. For the statistical analysis of* ***E*** *and* ***F****, the AUC and the percentage of cells responding to OxPAPC and AITC were compared to approaches with HC-030031 preincubation. These measurements were carried out on 9 different days with a number of measurements of: n(OxPAPC) = 8, n(AITC) = 4, n(pre HC) = 6. DRG neurons for all measurements shown in Figure 13, Figure 14 and Figure 15 were obtained from 10 mice in total. Statistical analysis: one-way ANOVA, post hoc Bonferroni, * p ≤ 0.05.*

After preincubation of OxPAPC with D-4F, DRG neurons reacted with decreased calcium levels, compared to OxPAPC-induced activation shown in Figure 14 **A**. AITC and capsaicin triggered a strong and immediate increase of Fura-2 ratios without being influenced by D-4F in their TRPA1-stimulating properties (Figure 14 **A**). A previous incubation of OxPAPC with D-4F for 30 minutes could reduce the AUC significantly by 62 %. The percentage of OxPAPC-sensitive cells also showed a significant reduction by 66 % when previously incubated with D-4F (Figure 14 **B**). AITC (Figure 14 **C**) and capsaicin-mediated (Figure 14 **D**) calcium influx remained unaffected by D-4F as shown in statistical analysis.

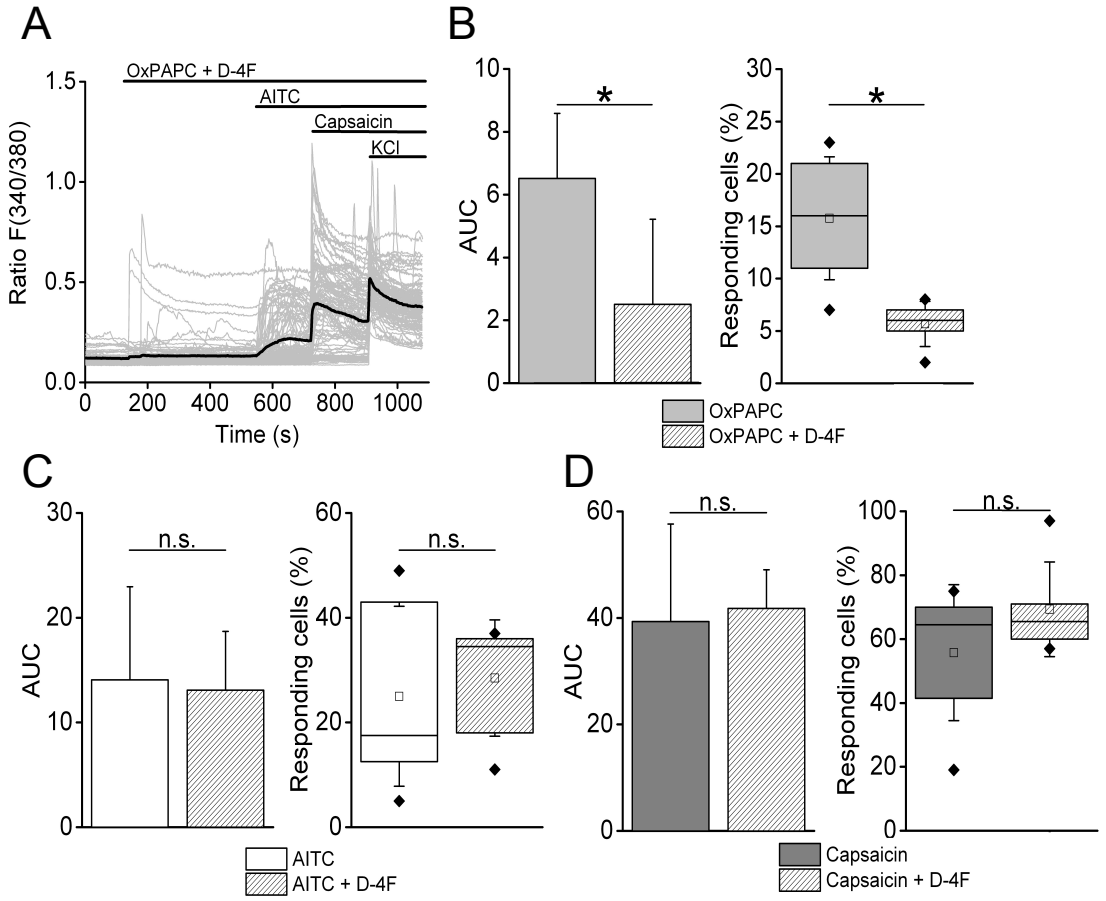

Figure 14: Reduction of OxPAPC-induced TRPA1 channel activation by D-4F peptide in DRGs

Before the measurement, 100 µM OxPAPC was preincubated for 30 minutes at room temperature with 1 mg/ml D-4F, followed by a stimulation with 1/10 of the concentrations ***(A)****. Compared were the AUC and the percentage of responding cells to OxPAPC* ***(B)****, AITC* ***(C)*** *and capsaicin* ***(D)*** *to measurements with D-4F. n = 6 measurements with D-4F preincubation on 3 days. n = 8 measurements with agonist stimulation only. Statistical analysis: one-way ANOVA, post hoc Bonferroni, * p ≤ 0.05.*

The stimulation of DRG neurons with OxPAPC + E06 caused only a very weak activation (Figure 15 **A**). After the addition of AITC, there was just a slight increase in intracellular calcium, compared to measurements which did not include any blocking substances (see Figure 13 **A**). After incubating OxPAPC with the control IgM antibody, a similar channel response was triggered as by

OxPAPC alone. The subsequent addition of AITC induced an immediate cell activation with Fura-2 ratios up to 0.6 (Figure 15 **B**). The AUC of OxPAPC + E06 was 35 % lower than the AUC reached after OxPAPC activation (4.2 versus 6.5). A previous incubation of IgM with OxPAPC resulted in an AUC of 4.8, which did not differ significantly from the AUC of OxPAPC or OxPAPC + E06 measurements. 42 % of all OxPAPC-sensitive cells were still responsive after previous incubation with E06, whereas 87 % of all OxPAPC-sensitive cells were also activated by IgM + OxPAPC (Figure 15 **C**). AITC caused a minor calcium influx when either E06 or IgM were present in the measuring chamber. E06 decreased the AUC by 42 %, IgM by 14 %. Likewise, 42 % less cells responded to AITC when E06 was added in the same measurement, whereas IgM did not have an impact on the percentage of responding cells (Figure 15 **D**). Comparing the effects of E06 on the AUC and the percentage of DRGs activated by capsaicin, measurements with previous E06 addition resulted in the lowest values of all 3 assessments as well. E06 decreased the AUC by 6.3 units, the number of cells sensitive to capsaicin by 10 %. IgM did not have any considerable impact on the action of capsaicin (Figure 15 **E**).

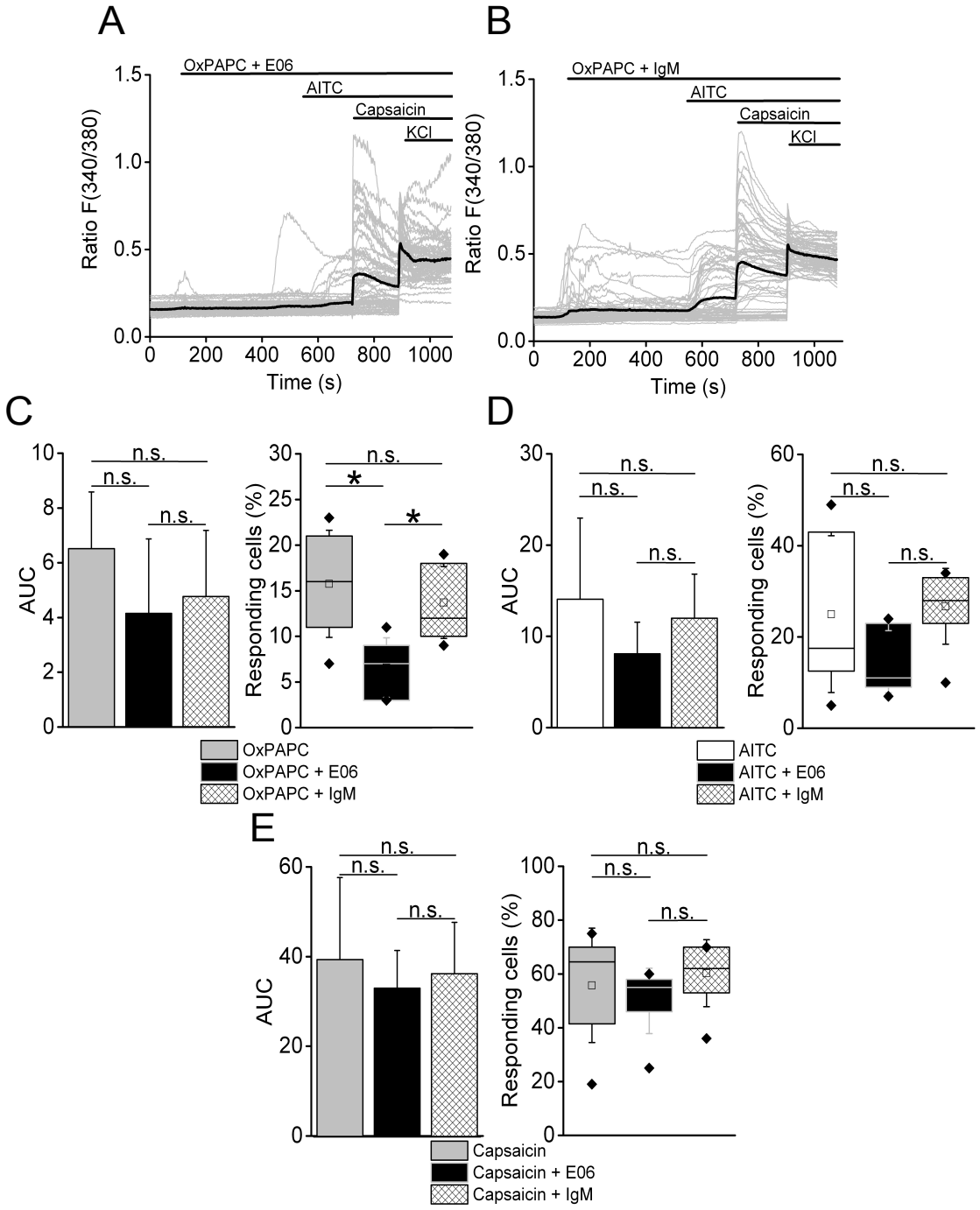

Figure 15: Reduction of the OxPAPC-triggered TRPA1 activation by E06

100 µM OxPAPC was incubated for 30 minutes at room temperature with 1/300 E06 ***(A)*** *and 1/50 IgM* ***(B)*** *prior to the measurement and added 1/10 to the measuring chamber after 120 seconds from the start of the measurement. AITC was added after 540 seconds, capsaicin after 720 seconds. Statistical analysis was performed comparing the AUC and the percentage of cells responding to OxPAPC* ***(C)****, AITC* ***(D)***

*and capsaicin **(E)** to values in measurements where OxPAPC was previously incubated with E06 or IgM. n = 7 measurements with E06 mAb/IgM preincubation performed on 3 days. n = 8 measurements with agonist stimulation only. Statistical analysis: one-way ANOVA, post hoc Bonferroni, * p ≤ 0.05.*

4 Discussion

4.1 Summary of results

The results of this thesis confirmed that OxPAPC is an important activator of TRPA1 channels. OxPAPC caused a considerable and sustained calcium influx in hTRPA1-expressing HEK-293 cells, while no response was seen when the outside medium lacked calcium. In comparison to AITC, OxPAPC induced a temporally delayed and less pronounced, but still significant cell response at equimolar concentrations. The activation of the mutant hTRPA1-3C channel by OxPAPC was either considerably reduced or even absent, while still being sensitive to the non-electrophilic substance carvacrol. In addition, hTRPA1-3C did not respond to AITC stimulation at all. The potential of OxPAPC to activate hTRPA1 was significantly diminished when either the cells or OxPAPC itself were preincubated with the apolipoprotein analogue D-4F. It had no effect on AITC-induced cell response. Another potential OxPAPC inhibitor tested was E06. Measured calcium influx was significantly lower when OxPAPC was incubated with E06 previous to experiments, whereas IgM had no effect on the OxPAPC action. Interestingly, calcium influx evoked by AITC was reduced as well after preincubation with either E06 or IgM. OxPAPC not only worked as a TRPA1 agonist in our cell model, but also in DRG neurons from C57BL/6 wild type mice. It led to a distinct calcium influx, which could be blocked by D-4F and E06. In this case however, E06 did not show an effect as distinctive as D-4F. The AITC-mediated DRG activation was diminished by E06, as observed in HEK-293 cells as well.

4.2 Discussion of methods

4.2.1 Expression of hTRPA1 in HEK-293T cells

To investigate TRPA1 responsiveness to the agonists OxPAPC, AITC and carvacrol, we used HEK-293T cells 1. stably expressing hTRPA1 and 2. transiently transfected with hTRPA1-3C. Advantages of virus-mediated

transfection of HEK-293T cells for stable expression of TRPA1 are a high transfection efficiency and a sustainable transgene expression (Kim and Eberwine, 2010). On the other hand, it is cytotoxic can induce inflammatory reactions, which may either add to the effects of OxPAPC on TRPA1 or disrupt normal cell function. Occurring virus-induced insertional mutations may disrupt gene activity of the host cell (Woods et al., 2003).

Chemicals for transient transfection of HEK-293 cells have a variable transfection efficacy, but do not cause mutagenesis or cytotoxicity. Variation of transfection efficacy between the two transfection methods we used may confine the comparability of our experiments (Kim and Eberwine, 2010).

Introducing foreign DNA into HEK-293 cells may alter transcript abundance of other genes and hence induce changes of mechanisms, which influence TRPA1 function. Differential expression of transcripts is often attributed to transfection chemicals. A comparison between FuGENE HD, which we used for transient transfection, and other reagents like Lipofectamine 2000 and Effectene, showed that FuGENE HD causes the fewest alterations of transcript levels (Jacobsen et al., 2009).

More recently developed, physiological methods for cell transfection are electroporation and laser-based transfection (Mehier-Humbert and Guy, 2005). These methods deliver nucleic acids into the cell by causing the formation of holes or pores in the cell membrane. Electroporation is easy to use and rapid, whereas laser-based transfection enables an exact transfection of single cells (Kim and Eberwine, 2010). Therefore, electroporation could be an alternative to virus-mediated transfection in our future experiments.

Elicited calcium influx was much stronger in the HEK-293 cell model than in DRG neurons, indicating that transfected HEK-293 cells express TRPA1 more abundantly than DRG neurons. The ubiquitin C promoter of our lentiviral expression vector probably caused an overexpression of hTRPA1, as it was found to drive ubiquitous gene expression in transgenic mice before (Schorpp et al., 1996). The overexpression of TRPA1 in HEK-293 cells ensures a higher sensitivity of the measurements for the detection of agonist-induced channel activation. In this study, we evaluated TRPA1 expression by measuring

agonist-induced calcium influx. Moreover, TRPA1 channel expression can be visualized by transducing HEK-293 cells with a lentiviral expression vector containing an internal ribosome entry site (IRES) and the coding sequence for a fluorescent protein, like green fluorescent protein (GFP). The IRES ensures the simultaneous transcription of the TRPA1 and GFP genes (Mancia et al., 2004). We isolated our stably TRPA1-expressing cells with a hygromycin resistance gene. This method using antibiotic markers is generally accompanied by highly variable expression levels of the gene of interest. Therefore, a GFP-based selection method could be used to produce a stable HEK-293_{TRPA1} cell line with a constantly high channel expression (Mancia et al., 2004).

Interestingly, HEK-293 cells seem to descend from neuronal cells within the original kidney tissue, since they have many characteristics of immature neurons (Shaw et al., 2002). This fact is beneficial for our study, since this cell type is a closer correlate to primary sensory neurons, which express TRPA1 *in vivo*. Therefore, our data gathered in the cell model are more likely to be transferable to physiologically occurring processes.

TRPA1 is not found in untreated HEK-293 cells, whereas TRPC1, TRPC3, TRPC4 and TRPC6 are commonly expressed (Zagranichnaya et al., 2005). An unselective OxPAPC-induced activation of various members of the TRP family was excluded by two lines of evidence: 1. non-transfected HEK-293 cells did not respond to OxPAPC stimulation and 2. the TRPA1 specific blocker HC-030031 eliminated calcium influx (compare to **3.1**).

In this study, we focused on the action of OxPAPC on TRPA1. OxPAPC is known to mediate its effects *in vivo* via various other mechanisms (Bochkov et al., 2010). OxPAPC itself can activate TRPV1 (Oehler et al., 2017) and TRPV1 activity is modulated by TRPA1 (Spahn et al., 2014). Hence, investigating the effects of OxPAPC on TRPA1 only, provides a limited view of the mode of action of OxPAPC. Co-expressing TRPA1 and TRPV1 in a heterologous expression system to analyse the influence of OxPAPC on both channels and their mutual impact, could open up further insights in OxPAPC-mediated pain transduction (Hsu and Lee, 2015). Moreover, acid-sensing ion channels (ASICs) are present in nociceptive neurons and are associated with pain

sensing. Besides being activated by extracellular acidosis, they interact with many substances, like endogenous regulators or plant compounds (Baron and Lingueglia, 2015; Wemmie et al., 2013). Whether OxPAPC can mediate nociception via ASICs is unknown. Therefore, it could be revelatory to include ASICs in our investigation and to explore possible interactions with OxPAPC and TRPA1.

In measurements of this work, we investigated the action of a commercially available OxPAPC mixture on TRPA1. As literature describes a wide variety of OxPAPC activity, including pro- and anti-inflammatory properties, it might be important to study defined OxPAPC species in future experiments (Bretscher et al., 2015).

4.2.2 Visualization of calcium gradients by a fluorescence-based assay

In order to visualize TRPA1 activation in HEK-293 cells, we used calcium imaging. The ratiometric dye Fura-2/AM allows for measuring relative changes of cytosolic calcium concentrations. TRPA1 channels are non-selective ion channels, preferentially conducting calcium.

Calcium imaging enables real-time measurements in living cells during channel stimulation with different agonists and a direct tracing of the effects. This method is a valuable approach to detect functional channel expression and responsiveness. Another advantage is the possibility to monitor both, the response of a larger selection of cells as well as every cell individually.

One point of criticism is that this method delivers cumulative results of the response of many channels expressed in one cell. The response of individual channels cannot be evaluated. Therefore, calcium imaging is an efficient concept to get a first overview of the general effect of a substance on the target structure but unsuitable to determine exact kinetics of TRPA1. Patch-clamp recordings enable the measurement of currents of single ion channels in the cell membrane (Neher and Sakmann, 1992). Our group used this method to get a deeper insight in electric and kinetic properties of TRPA1 activation by OxPAPC, but it was not part of this thesis. For patch-clamp recordings, a micropipette filled with an electrolyte solution, dipped in an electrode is adhered

to the cell membrane. The creation of a vacuum causes a sealed connection between the pipette and the cell membrane with a high resistance. A second electrode then enables the measurement of currents. Patch-clamp fluorometry could provide additional understanding of the interaction between OxPAPC and TRPA1, since ligand binding and channel activation can be analysed simultaneously by using a confocal laser scanning microscope (Biskup et al., 2007; Zheng and Zagotta, 2000). Additionally, it could be important to visualize OxPAPC cellular uptake in a further set of experiments. Intracellular OxPAPC can be quantified by flow cytometry in order to investigate time-dependent intracellular OxPAPC concentrations (Chu et al., 2018). In combination with calcium imaging, we could establish a dose-response curve, showing the dimension of TRPA1 activation in relation to intracellular OxPAPC concentrations. Furthermore, we could establish intracellular OxPAPC concentration curves depending on the time of preincubation in order to optimize temporal resolution and time of measurement in calcium imaging experiments. Moreover, fluorescent oxidized phospholipid species could enable the visualization of OxPAPC uptake and the investigation of primary protein targets of OxPAPC in HEK-293 cells and DRG neurons (Stemmer et al., 2012b). Stemmer et al. (2012b) used the reporter fluorophore BODIPY bound to the nitrogen atom of the head group of a POVPC analogue for the detection of labelled protein targets by a laser scanner on electrophoresis gels. Thus, we could visualize, whether OxPAPC primarily targets TRPA1 from intracellular, or if the extracellular part of the channel is involved in the interaction with OxPAPC as well, and furthermore identify other target channels.

In our calcium imaging experiments, we used Fura-2/AM as a ratiometric calcium indicator. It has one of the highest calcium affinities among other high affinity calcium indicators, like Fluo-4 and Oregon Green 488 BAPTA and hence, is well suited to depict changes in calcium concentrations in compartments with low calcium levels, like the cytosol. It shows only slight photo-bleaching, but can become compartmentalized and is excited by phototoxic UV wavelengths, like most ratiometric dyes. As a dual excitation dye, it requires alternation of

excitation and emission wavelengths, which impedes the use of confocal microscopy and restricts temporal resolution of measurements. In contrast, Fluo-4 and Oregon Green 488 BAPTA are single wavelength dyes and can be easily used with an argon laser for confocal microscopy (Lock et al., 2015; Paredes et al., 2008). We performed our measurements with an imaging rate of 0.5 Hz. Calcium imaging using Fluo-4 and Oregon Green 488 BAPTA can be performed at a 10 times higher frequency, allowing a more precise depiction of the increase in intracellular calcium, which can indicate the kinetics of TRPA1 channel activation. The ratio of 340/380 nm in our data analysis only represents a direct dimension of cytosolic calcium concentrations. It is possible to calibrate the experimental setup and fit Fura-2 ratios in order to obtain absolute values of the calcium concentration (Loading and Calibration of Intracellular Ion Indicators).

In our experimental setup we did not use a perfusion system, but added the substances manually to the buffer in the measuring chamber during the measurements. This implies various potential disadvantages: 1) during the measurement we could not control pH and temperature within the measuring chamber. There is evidence suggesting that cytosolic acidification activates TRPA1 (Garrity, 2011; Wang et al., 2011). A temperature dependency of TRPA1 is only known for cold temperatures below 17° C, whereas TRPV1 is sensitive for noxious heat > 42° C (Bandell et al., 2004; Story et al., 2003). Our experiments never exceeded 20 minutes, a substantial change in pH or temperature seems unlikely, especially because the ambient temperature was constant. Temperatures necessary for TRPA1 or TRPV1 (TRPV1 in DRG measurements) activation are unlikely to be attained in given circumstances. 2) Since we added the agents manually with a pipette, a contribution of mechanical stimuli to TRPA1 activation cannot be excluded. By evaluating TRPA1 channel responses after the addition of buffer solution only, this effect can be precluded. Vilceanu et al. (2010) described a mechanosensitivity of TRPA1. However, they found that TRPA1 alone is not sufficient to mediate mechanically activated currents and concluded that co-expressed proteins in native neurons are necessary for sensitivity to mechanical stimuli (Vilceanu and

Stucky, 2010). 3) The buffer was not exchanged during measurements. Hence, we could not evaluate whether the effect of OxPAPC was reversible upon the removal of agonist-containing buffer solution. As a consequence, the effect of individual agonists in measurements with various substances cannot be accredited reliably to one specific substance, since all added substances accumulated in the measuring chamber. This was primarily the case in experiments with DRG neurons, where we used OxPAPC, AITC, capsaicin and potassium within the same measurement. However, we focused on OxPAPC-mediated effects and therefore always added it as the first agonist in each measurement.

4.3 Discussion of results

4.3.1 OxPAPC is an important agonist of nociceptive TRPA1 channels

Noxious chemicals like the exogenous agonist AITC depolarize nociceptors via TRPA1 and cause neurogenic inflammation and pain hypersensitivity (Bautista et al., 2006; Bautista et al., 2005). *In vivo* data validated that thermal and mechanical hyperalgesia due to AITC injection are diminished by a pharmacological TRPA1 block (Bautista et al., 2013).

An endogenous agent, we identified at site of inflammation, was the oxidized PI OxPAPC (see **1.2.1**.). Jordt et al. have already assumed that lipid second messengers could possibly excite TRPA1 channels (Jordt et al., 2004). Our results provide prove that OxPAPC causes immediate and sustained hyperalgesia when injected in rat or mouse paws. While mechanical hyperalgesia was both, TRPA1 and TRPV1-mediated, thermal hyperalgesia was attributable to TRPV1. Stimulation of TRPA1 and V1 by OxPAPC caused a CGRP release from paw skin (Oehler et al., 2017). CGRP itself sets off cascades of molecular mechanisms leading to a sensitization of nociceptors and to an intensification of inflammatory and neuropathic pain (Iyengar et al., 2016).

The results of this thesis demonstrate that OxPAPC is a potent activator of TRPA1 channels *in vitro*. Micromolar concentrations of OxPAPC triggered a strong calcium influx into the cytoplasm of HEK-293_{hTRPA1} cells. Furthermore, we demonstrated that OxPAPC impact is specific for TRPA1 and measured effects were not subject to unspecific changes in membrane permeability for cations. This was verified by two lines of evidence: 1) the A1 antagonist HC-030031 significantly lowered high endoplasmic concentrations of calcium after OxPAPC addition; 2) non-transfected HEK-293 cells did not respond to OxPAPC stimulation. There are various studies pointing out that TRPA1 detects harmful chemicals by its cytoplasmic N-terminal domain (Hinman et al., 2006; Paulsen et al., 2015a). Therefore, it is possible that OxPAPC crosses the cell membrane and causes a TRPA1 activation from the inside of the cell. This is in line with the finding that the OxPAPC compounds PGPC and POVPC are taken

up rapidly into the cell (Moumtzi et al., 2007). Oxidized phospholipids are very polar and can be transferred to the cells through the aqueous phase, followed by an incorporation into the plasma membrane and a subsequent internalization (Stemmer and Hermetter, 2012). Another observation we made was a delayed OxPAPC-induced response of TRPA1 channels compared to AITC. This may be due to its chemical properties like a higher molecular weight and lower membrane permeability.

Moreover, our results showed that OxPAPC and AITC triggered an initial vast boost of cytosolic calcium in most HEK-293$_{hTRPA1}$ cells, which in the course of the measurement decreased notably. In accordance to previous investigation, this could be a consequence of intracellular calcium-mediated TRPA1 inactivation, which restricts the sensory activation by painful agents (Wang et al., 2008). However, a potentiating effect of calcium on agonist-induced TRPA1 activation has also been described in prior studies (Jordt et al., 2004; Zurborg et al., 2007). It was even reported that in the absence of an agonist, calcium influx through spontaneously open TRPA1 channels could cause a channel activation. The putative binding site for calcium is an EF-hand domain in the N-terminal ankyrin repeat of TRPA1 (Doerner et al., 2007). In general, a great number of calcium-interacting proteins contain an EF-hand calcium binding domain, which consists of twelve residues with only six of them being involved in calcium-binding. The calcium-coordinating pentagonal pyramidal configuration is a helix-loop-helix motif (Lewit-Bentley and Rety, 2000). In calcium imaging experiments, we cannot exclude a secondary effect of calcium on OxPAPC-induced TRPA1 activation. An exact contemplation of single cell responses in our experiments showed that most cells reacted to OxPAPC with a rapid calcium influx, but some cells increased rather slowly in intracellular calcium (Figure 8). This could be explained through an initial OxPAPC-triggered calcium influx, which itself causes a further channel opening. Whole cell patch clamp recordings of HEK-293$_{hTRPA1}$ of our group also showed slightly ascending currents over time after OxPAPC application (Oehler et al., 2017).

4.3.2 Calcium influx caused by TRPA1 activation originates from extracellular sources and not from intracellular depots

Calcium sets off a variety of inflammatory processes after entering through TRPA1 channels in sensory neurons (Ruparel et al., 2008). It also plays an important role in potentiating and inactivating TRPA1 channel function, which requires the entry of calcium ions and cannot be mediated from extracellular (Wang et al., 2008). We pursued the question whether it was necessary for calcium to enter the cells after agonist stimulation in order to be measurable in calcium imaging. We further asked, whether TRPA1 activation could liberate calcium from intracellular depots. To resolve this question, we used calcium free buffer solution and examined if OxPAPC and AITC could trigger an increase in cytosolic calcium levels in HEK-293 cells. Another, possibly more precise approach would be to directly measure changes of calcium concentrations within intracellular departments after TRPA1 activation. This can be realized by combining patch clamp recordings and optical imaging. Cells have to be loaded with a calcium-sensitive fluorescent indicator, which has to be removed from the cytosol by e.g. two-photon permeabilization in order to keep it trapped in cellular compartments. The patch clamp technique is used to measure ion currents after TRPA1 activation (Gerasimenko Julia et al., 2014).

In our measurements, neither of the agonists evoked a measurable TRPA1 response. Consistent with our findings were results of Jordt el al. (2004), where AITC-mediated activation was abolished when extracellular calcium was removed. Nevertheless, they demonstrated that TRPA1 activation is not calcium-dependent, but augmented by rising calcium levels (Jordt et al., 2004). Our data suggest, that there is no TRPA1-mediated calcium release from intracellular stores in HEK-293 cells, occurring during the 10 minute measurement. Shang et. Al (2016) found that in mouse DRG neurons, AITC activates TRPA1 channels localized in endolysosomes, causing an intracellular calcium release, which accounts for about 40 % of the overall calcium increase induced by AITC. They failed to reproduce these findings in TRPA1-overexpressing HEK-293 cells und proposed that this might be due to their non-neuronal properties and different protein modification systems. The

release of lysosomal calcium is dependent on the AITC concentration. For example, 10 µM AITC can trigger a hardly detectable calcium increase of few nM (Shang et al., 2016). Considering that Fura-2/AM has a sensitivity ranging from about 100 nM to about 100 µM (Paredes et al., 2008), we probably would not have detected lysosomal calcium release in our imaging experiments. Moreover, exocytosis of neuropeptides is triggered by AITC activation in lysosomes and *in vivo*, AITC-induced hyperalgesia is partly lysosome-dependent (Shang et al., 2016).

Taking these results into account, we suggest that in HEK-293 cells, calcium enters through activated TRPA1 channels localized in the cell membrane.

4.3.3 OxPAPC can activate TRPA1 via cysteine residues in the intracellular part of the channel

Nociception caused by oxidative stress can be mediated by TRPA1 channels through the highly reactive cysteine C621. For the interaction with electrophiles, the proximity of K620 and the function of C665 seem to be crucial (Bahia et al., 2016). Paulsen et al. (2015a) revealed through their structural analysis of TRPA1, that cysteines C621, C641 and C665 in the pre-S1 region of TRPA1 contribute to sensitivity to electrophiles like AITC. Therefore, we asked whether these cysteines were crucial for the interaction of TRPA1 with OxPAPC or if there was more than one mechanism involved. Springstead et al. (2012) emphasized the role of cysteines in OxPAPC-mediated gene regulation and protein interactions. The most reactive component of OxPAPC, PEIPC, is an electrophile that can interact with cysteines by Michael addition or by forming Schiff bases (Domingues et al., 2013; Springstead et al., 2012). In general, oxidized phospholipids are able to generate covalent bonds with biomolecules due to their electrophilicity and high reactivity in general (Domingues et al., 2013; Stemmer and Hermetter, 2012). However, PEIPC only makes up a small fraction of the commercially available OxPAPC mixture and the two truncated phospholipids PGPC and POVPC, which are also OxPAPC compounds, are not electrophilic.

In our measurements, the hTRPA1 triple mutant C621S/C641S/C665S did not respond to AITC at all and agonistic effects of OxPAPC were drastically diminished or even completely abolished. hTRPA1-3C retained sensitivity to carvacrol, an agonist structurally unrelated to oxidized phospholipids or AITC (compare to **3.2**). Carvacrol, a phenol, is produced by oregano, thyme and other aromatic plants and functions i.a. as a non-electrophilic TRPA1 agonist, forming non-covalent bonds to structures outside of cysteine residues (Meents et al., 2016; Mihara and Shibamoto, 2015). Our results suggest that electrophilic interaction of OxPAPC with three cysteines is an important activation mechanism of TRPA1. Nevertheless, the residual activity of hTRPA1-3C, which we saw in our measurements after OxPAPC stimulation, indicates that there are other, cysteine-independent mechanisms involved.

TRPA1 peptide binding studies performed by our research group indicate the function of individual OxPAPC compounds as two-electron oxidants, what enables an oxidation of cytosolic N-terminal domains (Oehler et al., 2017). It is likely that these covalent bonding forces of electrophilic OxPAPC compounds cause a channel transformation, which repeals steric impediments and electrostatic repulsive forces (Paulsen et al., 2015a).

The fact that PGPC is a non-electrophilic, end-stage oxidation product of PAPC, excludes the possibility that PGPC activates TRPA1 through the mechanisms discussed above. Anyhow, our calcium imaging experiments of HEK-293_{TRPA1} cells revealed that PGPC and POVPC could cause a channel activation, which was even slightly higher than the one observed in OxPAPC measurements. Moreover, PGPC caused a calcium influx in hTRPA1-3C-expressing HEK-293 cells, which verified that PGPC can activate TRPA1 in an indirect and cysteine-independent manner. (Oehler et al., 2017). Due to its properties as a negatively charged phospholipid, PGPC can add electrostatic charges to the phospholipid monolayer of lipoprotein particles (Stemmer et al., 2012a). It is conceivable that this results in conformational changes of the lipid bilayer and integrated proteins. POVPC, on the other hand, can react with proteins and aminophospholipids by Schiff base formation. Incurred adducts can destabilize the lipid bilayer (Stemmer et al., 2012a). Therefore, PGPC and POVPC could

cause mechanical alterations of the cell membrane, thus activating TRPA1 indirectly, as the mechanosensory function of TRPA1 was described before (Brierley et al., 2011).

Furthermore, it is possible that OxPAPC activates TRPA1 indirectly through signaling cascades, causing a channel phosphorylation, for example by PKA. PKA itself can be activated by OxPAPC (Birukov et al., 2004), but was also found to mediate TRPA1 activation (Kadkova et al., 2017).

4.3.4 Primary sensory DRG neurons are activated by algesic oxidized phospholipids through TRPA1

Using rodent DRG neurons, we investigated whether our findings in the HEK-293 cell model were reproducible in native cells. Our results confirmed the function of OxPAPC as a ligand of TRPA1 in primary sensory neurons. In total, 40 % less DRG neurons than HEK-293_{hTRPA1} cells were responsive to OxPAPC stimulation. 25 % of sensory neurons were activated by AITC, which is consistent with Caspani et al. (2009) reporting 28 % of adult mouse DRG neurons to express TRPA1 mRNA (Caspani et al., 2009). The increase in cytoplasmic calcium after OxPAPC stimulation was about 66 % more pronounced in HEK-293 cells than in naïve cells (HEK-293_{hTRPA1} > DRG). It seems likely that transfected HEK-293 cells express the gene product more abundantly than sensory neurons. These differences indicate that the potent agonism of OxPAPC we measured in HEK-293 cells is not completely transferable into naturally occurring neuronal processes. Nonetheless, our group demonstrated that this OxPAPC-mediated cation influx through TRPA1 in primary sensory neurons is still enough to cause considerable pain behaviour *in vivo* (Oehler et al., 2017). Keszthelyi et al. (2016) express their concern that *in vitro* data and *in vivo* animal studies are difficult to be translated into the function of TRPA1 in the human organism.

The experiments of this study revealed that DRG neurons respond to OxPAPC stimulation in a diverse manner. Some neurons reacted with a prompt calcium influx, whereas others showed a rather linear increase in intracellular calcium (see Figure 13). This could be a consequence of the diverse expression of

TRPA1 in different types of neurons, like described by Li et al. (2016, see chapter 1.1.3). Our group demonstrated by fast calcium imaging that PGPC triggers a spike-like calcium response in about three-quarters, and a transient-like response in about a quarter of all evaluated neurons (Martin et al., 2018). Here, we used an OxPAPC mixture containing various OxPL components, which possibly activate TRPA1 through different mechanisms. Therefore, we cannot conclude which of the possible causes of diverse response patterns was important in this study, or if it was even a combination.

Within the TRP family, A1 is co-expressed with the capsaicin-sensitive V1 channel in DRG, trigeminal and nodose ganglion neurons (Nagata et al., 2005; Weller et al., 2011). Therefore, we additionally tested capsaicin-mediated TRPV1 activation. 56 % of all DRG neurons were sensitive to this agonist. In literature, values ranging from 32 % to 58 % can be found (Kobayashi et al., 2005). Fura-2 ratios were 20 % higher after capsaicin stimulation, compared to AITC (see Figure 13). This could be caused by an additional activation of TRPV1 on top of A1 channels, subsequently facilitating a higher calcium influx. Or it could arise from the fact that neuron types C4, C5 and C6, express TRPV1 at higher levels than TRPA1, while in C1 neurons both are equally high expressed (Li et al., 2016). Further experiments by our group revealed that OxPAPC can also act via recombinant TRPV1. But to induce an activation, threefold higher concentrations of OxPAPC were needed and the response thereafter was still modest and delayed. In DRG neurons, the TRPV1-specific antagonist BCTC could only partly reduce OxPAPC-induced activation (Oehler et al., 2017), whereas HC-030031 blocked the OxPAPC-response almost completely. The very limited effect of OxPAPC on TRPV1 *in vitro* stands in contrast to *in vivo* data of our group, demonstrating that TRPV1 was clearly involved in hyperalgesia and CGRP release caused by OxPAPC (Oehler et al., 2017). These controversial findings might be due to a TRPA1-dependent sensitization of TRPV1, which can be mediated by the following sequence of reactions: calcium influx through TRPA1, an increase in adenylyl cyclase activity producing a surplus of cAMP, causing an activation of PKA and a

subsequent phosphorylation and channel opening of TRPV1 (Spahn et al., 2014).

Besides TRPA1 and TRPV1, OxPAPC has various other target receptors. Among them another member of the TRP family: the calcium-permeable TRP canonical 5 (TRPC5) channel (Al-Shawaf et al., 2010). Other known receptors for OxPAPC are CD36, PPAR, SRB1, EP2, PAF receptors, VEGFR and various TLR (Bochkov et al., 2010; Lee et al., 2012; Li et al., 2006).

Receptors and ion channels expressed by DRG neurons, but which are not known to be direct targets of OxPAPC, include neuropeptide Y (NPY) receptors (Zhang et al., 1997), MAS-related G-protein-coupled (MRGPC) receptors (Liu et al., 2008), voltage-gated Na^+ channels VGSC (Baker and Wood, 2001), acid-sensing ion channels ASICs (Li and Xu, 2011) and ATP receptors (Kobayashi et al., 2013). DRG neurons also express the tyrosine kinase receptor VEGFR (Selvaraj et al., 2015), which was shown to be a target of OxPAPC in other studies (see above). It was described before that ligand binding to VEGFR activates phospholipase-C (PLC) on endothelial cells (Abhinand et al., 2016). Through the PLC/IP3 pathway, calcium can be released from internal stores (Han et al., 2001). In principle, it seems possible that this pathway also exists in DRG neurons. However, it seems unlikely to have influenced our measurements, as it includes various reactions and calcium influx in DRG neurons after OxPAPC stimulation occurs within less than one minute (see Figure 13).

There is a variety of TRP channels present in DRG neurons (Li et al., 2016). Like discussed before, OxPAPC can stimulate TRPA1 and TRPV1 in cultured sensory neurons. TRPC5, as one target receptor of OxPAPC, was discovered in DRG neurons as well (Zimmermann et al., 2011). Hence, this channel possibly mediated calcium influx in our experiments as well. But since the specific TRPA1 antagonist HC-030031 reduced the responsiveness of neurons to OxPAPC by 75 %, the impact of TRPC5 has to be rather tiny.

Interestingly, our group demonstrated in a recent study that the VGSC $Na_V1.9$ is involved in potentiating PGPC-induced responses in DRG neurons in an

inflammatory setting and might therefore serve as a master switch (Martin et al., 2018).

4.3.5 Potential treatment options for OxPAPC-mediated inflammatory hyperalgesia

ApoA-I mimetic peptides, like D-4F, are important new treatment options for inflammatory diseases, like microbial infections, autoimmune diseases and atherosclerosis (Getz and Reardon, 2014). They were also found to positively influence cancer, probably by reducing cellular oxidative stress. 4F could inhibit tumour growth, tumorigenicity and tumour invasiveness (Reddy et al., 2014).

In this study we evaluated, whether D-4F is also suitable to attenuate inflammatory pain. ApoA-I mimetic peptides, in comparison to ApoA-I, were shown to have a four to six orders of magnitude greater affinity for oxidized fatty acids, cholesterol and oxidized phospholipids. Also, the affinity of D-4F to OxPAPC is much higher than to the non-oxidized PAPC (Van Lenten et al., 2008).

We asked whether D-4F could prevent TRPA1-mediated hyperalgesia by neutralizing OxPAPC in a scavenger-like manner. Therefore, we performed calcium imaging experiments to find out if D-4F could reduce OxPAPC-mediated TRPA1 activation *in vitro*. Our results showed that D-4F effectively interferes with the OxPAPC ligand function on TRPA1, thereby attenuating calcium influx in HEK-293 cells and DRG neurons. At this juncture two mechanisms of OxPAPC binding are conceivable: 1) D-4F could interact with functional groups of OxPAPC components, which prevents the activation of the channel or 2) considering the molecular mass of 2.3 kDa (Van Lenten et al., 2008) and electrical charge of the peptide (Getz and Reardon, 2011), it might even impede the lipid-peptide complex to penetrate the cell membrane. Van Lenten et al. (2008) suggested that the binding of oxidized lipids to 4F is due to the fact that polar oxidized lipids prefer the thermodynamically more favourable microenvironment that the peptides provide, over the lipid or aqueous environment in which they are formed.

In vivo data from our group revealed that a single shot of D-4F injected locally, reduces mechanical hyperalgesia in the rat model of acute, CFA-induced hindpaw inflammation. When treated with daily intraperitoneal D-4F injections in the same inflammation model, rats developed less paw edema and showed a reduced mechanical hyperalgesia for 2 days after the last administration. D-4F also had an efficient and sustained ameliorating effect in the model of chronic inflammatory pain caused by collagen-induced arthritis. Furthermore, our group analysed the occurrence of proalgesic phospholipids in paw tissue after CFA injection and found that D-4F impedes the formation of PAPC oxidation fragments (Oehler et al., 2017).

In a clinical study on high-risk coronary artery disease patients, a single oral dose of D-4F significantly reduced the HDL inflammatory index. D-4F was safe and well-tolerated, but had a low bioavailability (Bloedon et al., 2008). A study by Watson et al. (2011), designed to test whether comparable effects could be obtained by intravenous or subcutaneous injection, failed to demonstrate any improvement using L-4F. It might be that the dose achieved in the small intestine, which is the possible site of action of ApoA-I mimetic peptides, was too low and in that in addition L-4F is degraded priorly (Getz and Reardon, 2014; Navab et al., 2011; Reddy et al., 2014). D-4F in contrast, cannot be metabolized and bears the risk to accumulate in the human body (White et al., 2014). Interestingly, the ApoA-I mimetic peptide 6F was expressed in transgenic tomatoes. Tomatoes fed to mice attenuated systemic inflammation and dyslipidaemia possibly by reducing plasma levels of oxidized lipids and unsaturated fatty acids (Navab et al., 2013).

Due to the promising findings *in vitro and in vivo* by other groups, we propose that D-4F is a potential and effective treatment option for inflammatory pain. Following of our results support this proposal: D-4F 1. antagonized OxPAPC-mediated TRPA1 activation in the cell model, 2. attenuated hyperalgesia in the animal model and 3. reduced the occurrence of OxPAPC fragments in the inflammatory soup.

After treating mice with 4F, antibodies against oxidation-specific epitopes of OxPL were found in plasma sera. Titres of the IgM natural antibody E06 were especially high (Wool et al., 2011). Considering the ability of E06 to bind OxPL, we asked whether this was another approach to inhibit OxPAPC-triggered inflammatory pain. Experiments of this thesis performed on HEK-293 cells and DRG neurons demonstrated that E06 antagonizes OxPAPC-mediated TRPA1 activation. Our group furthermore revealed that E06 reduces thermal and mechanical hyperalgesia induced by OxPAPC injection, as well as mechanical hyperalgesia caused by CFA. In analogy to D-4F, proalgesic oxidized fragments of PAPC were not found in E06-treated tissue (Oehler et al., 2017).

Although the phosphorylcholine head group is vital for recognition of OxPL by E06, changes of OxPL conformation by Schiff base formation and aldol condensation are determining factors for immunogenicity (Friedman et al., 2002). Friedman et al. (2002) discovered that POVPC has to undergo an aging process in order to be bound by E06. Within weeks, intermolecular interactions generate an aldol condensation product of the initial POVPC, which is antigenic. But not all Schiff base reactions create epitopes for E06. As an example, the product of Schiff base formation between POVPC and dipalmitoyl phosphatidylethanolamine is not recognized by E06 (Friedman et al., 2002). These findings might explain, why in our experiments some cells were still activated by OxPAPC after preincubation with E06.

Interestingly, we found that E06 lowers the potential of AITC to activate TRPA1 channels in HEK-293 cells. A direct recognition of AITC by E06 seems unlikely, since the phosphorylcholine head group is essential for antigen binding to E06 (Friedman et al., 2002). The electrophilic character of AITC allows coalescences with nucleophilic amino acids (Cejpek et al., 2000). Therefore, AITC could react with E06 outside of the antigen binding site, making it unavailable for electrophilic interactions with TRPA1. In contrast, E06 did not affect AITC-induced TRPA1 activation in DRG neurons significantly, although the responsiveness was slightly decreased. It is conceivable that due to the preincubation with OxPAPC, most E06 antibodies were already bound and hence, could not interact with many AITC molecules.

Further experiments by our group showed that E06 attenuates prolonged mechanical hyperalgesia caused by AITC, 4-HNE and capsaicin *in vivo* and blocks TRPA1 activation by 4-HNE *in vitro*. In contrast, neither free 4-HNE nor 4-HNE protein adducts bound to E06 in binding assays. The finding that in rats, intraplantar injections of AITC, 4-HNE, H_2O_2 and capsaicin lead to local generation of OxPC, gives rise to the idea that in *vivo*, these irritants indirectly elicit the formation of proalgesic OxPL, which can be bound by E06 (Mohammadi et al., 2018). The underlying mechanism could be the following: the activation of TRPA1 or TRPV1 by these agonists can trigger a CGRP and substance P release from nociceptor terminals, which can stimulate a subsequent mast cell and neutrophil degranulation (McMahon et al., 2015). The released proinflammatory agents can contribute to the generation of OxPC (Freigang, 2016), which are directly recognized by E06.

In this study, the control IgM antibody reduced the potential of AITC to activate HEK-293_{hTRPA1} as well. Here, we used the control antibody in a concentration of 1/50, while later our group repeated the same measurements with a concentration of 1/300 and found that IgM did not influence AITC-mediated TRPA1 activation. Possibly, high concentrations of the control antibody caused a competitive antagonism between IgM and TRPA1 for electrophilic interactions with AITC (Cejpek et al., 2000).

In literature, E06 is mainly used as a diagnostic tool, to detect OxPC and evaluate its role in different inflammatory diseases, such as acute lung injury (Imai et al., 2008) and atherosclerosis (Ravandi et al., 2014). Recently, Yeang et. al (2016) showed that the expression of E06 in hyperlipidemic mice reduces the progression of aortic sclerosis, hence proposing it as a therapeutic agent for the treatment of atherosclerosis in humans. Treating inflammatory hyperalgesia with E06 is a novel and promising strategy. By demonstrating that E06 reduces OxPAPC-mediated TRPA1 activation, we support this proposal.

The following figure illustrates a summary of the insights of this work in connection with the current state of research:

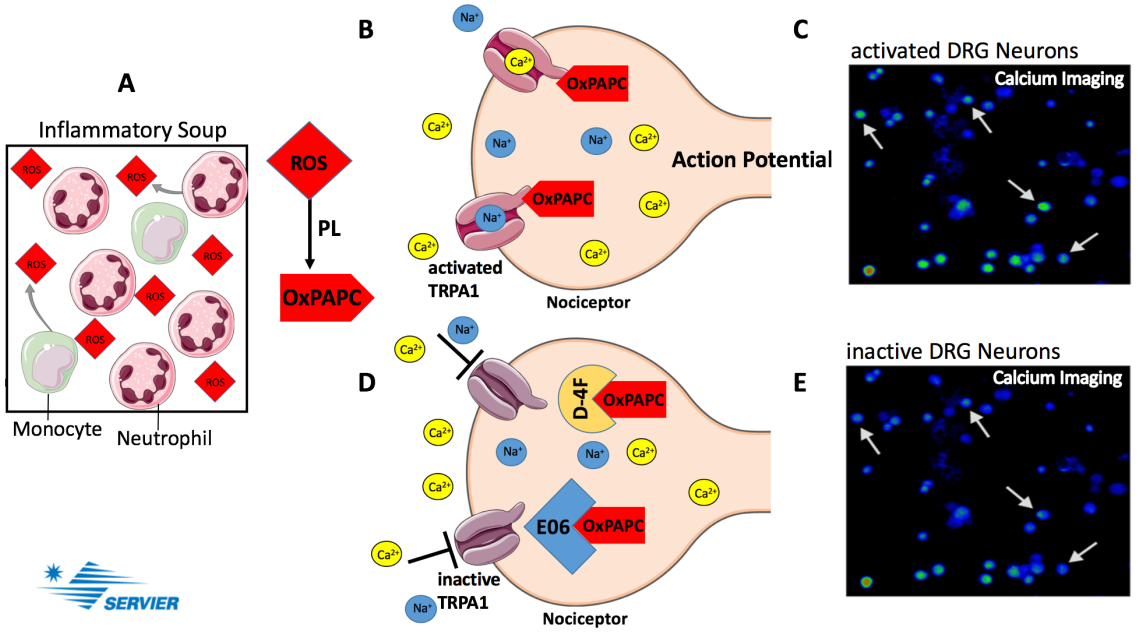

Figure 16: OxPAPC in inflammatory settings contributes to the depolarization of nociceptors.

Different species of leucocytes, e.g. monocytes or neutrophils, found in inflamed tissue, produce a variety of proalgesic mediators, among them ROS. ROS interact with phospholipids of the cell membrane in an oxidizing manner. Products of this reaction are OxPL, like OxPAPC and its compounds ***(A)****. OxPAPC activates TRPA1 channels in nociceptors and causes an influx of cations like calcium and sodium, generating an action potential, possibly through a cascade of further channel and second messenger activation* ***(B)****. In our calcium imaging experiments, OxPAPC caused an influx of calcium in DRG neurons and in HEK-293$_{TRPA1}$ cells* ***(C)****. The scavengers E06 and D-4F bind OxPAPC and hence inhibit an OxPAPC-mediated TRPA1 activation* ***(D)****.* ***E*** *shows DRG neurons in an non-activated state. Images* ***C*** *and* ***E*** *are adapted from (Oehler et al., 2017).*

4.4 Future prospects

Findings acquired in the cell model and in primary sensory neurons indicate that both approaches to neutralize oxidized phospholipids constitute potential

pharmaceuticals to treat inflammatory pain. Apolipoprotein ApoA-I was tested in a clinical study for its effect on coronary atherosclerosis. Not only did it cause a statistically significant improvement, but it was also well tolerated by patients (Tardif et al., 2007). Hence, the treatment of inflammatory or post-surgical pain with D-4F and E06 could be accompanied by less adverse effects than conventional with NSAIDS or opioids. Nevertheless, further studies on OxPAPC, its interaction with TRPA1, D-4F and E06 are needed. One question to resolve is: what impact do different compounds of OxPAPC have on its proalgesic effect? As shown in Figure 3 and described in chapter 1.2.1, our research group analysed the composition of oxidized phospholipids in an inflammatory setting, as well OxPAPC compounds after intraplantar injection by MALDI-TOF mass spectrometry. Considering that OxPAPC has potent pro- and anti-inflammatory properties (Bretscher et al., 2015), it is important to precisely understand interaction mechanisms of all OxPAPC compounds with TRPA1 and to identify further mechanisms that are involved in OxPAPC-mediated transmission of pain. Assessing the effect of all individual OxPAPC compounds on primary sensory neurons could open up new insights about proalgesic properties of different OxPAPC species. In recent years, great progress has been made in the investigation of second messenger cascades downstream of TRPA1 (Kadkova et al., 2017; Petho and Reeh, 2012). Further findings can help to understand, which cellular mechanisms are attenuated by blocking OxPAPC *in vivo*. Since at this moment, the mechanism of OxPAPC neutralization by E06 and D-4F can only be anticipated, it is necessary to perform further studies. Most animal and clinical studies investigate the effect of D-4F and E06 on atherosclerosis (Bloedon et al., 2008; Navab et al., 2013; Yeang et al., 2016). Our group was one of the first investigating the potential of D-4F and E06 to attenuate inflammatory and chronic pain. Considering that D-4F is well-tolerated by humans (Bloedon et al., 2008), clinical studies using D-4F as a pharmaceutical for the treatment of pain could be performed soon.

Generally speaking, OxPAPC not only holds great potential as a target to treat different inflammatory diseases, but is also promising for scientific research as it still has manifold functions and interactions to discover.

5 Abstract

Non-steroidal antiinflammatory drugs are most commonly used for inflammatory and postoperative pain. But they lack effectiveness and specificity, leading to severe side effects, like gastric ulcers, asthma and severe bleeding. Oxidized 1-palmitoyl-2-arachinidonoyl-*sn*-glycero-3-phosphocholine (OxPAPC) plays an important role in inflammatory pain. PAPC is a common phosphatidylcholine of membranes, which can be oxidized by reactive oxygen species. In preliminary experiments, our group found that local injection of OxPAPC in rat paws induces hyperalgesia.

In this study we examined the effect of OxPAPC on transient receptor potential A1 (TRPA1), an ion channel expressed in C-fiber neurons. Furthermore, we investigated if intracellular cysteine residues of TRPA1 were necessary for agonist-channel-interactions and if a subsequent TRPA1 activation could be prevented by OxPAPC scavengers.

To answer these questions, we performed calcium imaging using HEK-293 cells stably expressing hTRPA1, or transiently expressing the triple mutant channel hTRPA1-3C and naïve DRG neurons. Cells were incubated with the ratiometric, fluorescent dye Fura-2/AM and stimulated with OxPAPC. The change of light emission after excitation with 340 and 380 nm wavelengths allowed conclusions regarding changes of intracellular calcium concentrations after TRPA1 activation.

In our investigation we proved evidence that OxPAPC activates TRPA1, which caused a flow of calcium ions into the cytoplasm. The TRPA1-specific channel blocker HC-030031 eliminated this agonist-induced response. TRPA1-3C was not completely sensitive to OxPAPC. The peptide D-4F and the monoclonal antibody E06 neutralized OxPAPC-induced TRPA1 activation.

In this work, the importance of OxPAPC as a key mediator of inflammatory pain and as a promising target for drug design is highlighted. Our results indicate that TRPA1 activation by OxPAPC involves cysteine-dependent mechanisms, but there are other, cysteine-independent activation mechanisms as well. Potential pharmaceuticals for the treatment of inflammatory pain are D-4F and

E06, whose efficiency has recently been confirmed in the animal model by our research group.

Zusammenfassung

Nichtsteroidale Antiphlogistika werden bei Entzündungs- und postoperativen Schmerzen eingesetzt. Ihre mangelnde Effektivität und Spezifität kann jedoch starke Nebenwirkungen wie Magen-Darmulzera, Analgetikaasthma und Blutungen hervorgerufen. Hyperalgesie kann in Entzündungsprozessen lokal durch das oxidierte Phospholipid 1-Palmitoyl-2-Arachinidonoyl-*sn*-Glycero-3-Phosphocholin (OxPAPC) induziert werden, welches durch Oxidation mit reaktiven Sauerstoffspezies entsteht. Vorarbeiten unserer Arbeitsgruppe zeigten, dass OxPAPC nach intraplantarer Injektion in Rattenpfoten Hyperalgesie hervorruft.

In dieser Arbeit steht die Interaktion zwischen OxPAPC und dem „transient receptor potential A 1“ Kanal (TRPA1), einem Ionenkanal von C-Faser-Neuronen, im Fokus. Es wurde untersucht, ob intrazelluläre Cysteinreste zur Aktivierung durch oxidierte Phospholipide beitragen und ob diese durch einen OxPAPC-spezifischen Antagonismus verhindert werden kann. Zur Klärung der Fragestellung verwendeten wir HEK-293 Zellen, die entweder hTRPA1 stabil oder den an drei Positionen mutierten hTRPA1-C3 transient exprimierten und native DRG Neurone. Die Änderung der intrazellulären Kalziumionenkonzentration nach Kanalmodulation mit OxPAPC wurde mittels ratiometrischer Fura-2/AM-Experimente bestimmt.

Wir zeigten, dass OxPAPC zur Aktivierung von TRPA1 führt, welche sich nach Zugabe des spezifischen Antagonisten HC-030031 als reversibel erwies. Sind drei Cysteine des intrazelllulären Aminoterminus von TRPA1 mutiert, wurde ein Anstieg der intrazellulären Kalziumkonzentration durch OxPAPC verringert. Das Peptid D-4F und der monoklonale Antikörper E06 neutralisierten die Wirkung von OxPAPC auf den Kanal.

Das in Entzündungsprozessen gebildete OxPAPC ist ein endogener Agonist von TRPA1 Kanälen und stellt damit eine potentielle pharmakologische Zielsubstanz für die Entwicklung von Analgetika dar. Naheliegend ist, dass die Aktivierung von TRPA1 durch OxPAPC über Cysteinbindungsstellen erfolgen

kann. Jedoch sind weitere, cysteinunabhängige Mechanismen ebenfalls wahrscheinlich. D-4F und E06 sind vielversprechende neuartige Substanzen für die Behandlung von Entzündungsschmerz. Ihre analgetische Wirkung wurde bereits im Tiermodell durch unsere Arbeitsgruppe bestätigt.

6 References

Abhinand, C.S., Raju, R., Soumya, S.J., Arya, P.S., and Sudhakaran, P.R. (2016). VEGF-A/VEGFR2 signaling network in endothelial cells relevant to angiogenesis. Journal of Cell Communication and Signalling *10*, 347-354.

Al-Shawaf, E., Naylor, J., Taylor, H., Riches, K., Milligan, C.J., O'Regan, D., Porter, K.E., Li, J., and Beech, D.J. (2010). Short-term stimulation of calcium-permeable transient receptor potential canonical 5-containing channels by oxidized phospholipids. Arteriosclerosis, Thrombosis, and Vascular Biology *30*, 1453-1459.

Anantharamaiah, G.M., Jones, J.L., Brouillette, C.G., Schmidt, C.F., Chung, B.H., Hughes, T.A., Bhown, A.S., and Segrest, J.P. (1985). Studies of synthetic peptide analogs of the amphipathic helix. Structure of complexes with dimyristoyl phosphatidylcholine. Journal of Biological Chemistry *260*, 10248-10255.

Andersson, D.A., Gentry, C., Moss, S., and Bevan, S. (2008). Transient receptor potential A1 is a sensory receptor for multiple products of oxidative stress. Journal of Neuroscience *28*, 2485-2494.

Bahia, P.K., Parks, T.A., Stanford, K.R., Mitchell, D.A., Varma, S., Stevens, S.M., Jr., and Taylor-Clark, T.E. (2016). The exceptionally high reactivity of Cys 621 is critical for electrophilic activation of the sensory nerve ion channel TRPA1. Journal of General Physiology *147*, 451-465.

Baker, M.D., and Wood, J.N. (2001). Involvement of Na+ channels in pain pathways. Trends in Pharmacological Sciences *22*, 27-31.

Bandell, M., Story, G.M., Hwang, S.W., Viswanath, V., Eid, S.R., Petrus, M.J., Earley, T.J., and Patapoutian, A. (2004). Noxious cold ion channel TRPA1 is activated by pungent compounds and bradykinin. Neuron *41*, 849-857.

Barabas, M.E., Kossyreva, E.A., and Stucky, C.L. (2012). TRPA1 is functionally expressed primarily by IB4-binding, non-peptidergic mouse and rat sensory neurons. PloS One *7*, e47988.

Baron, A., and Lingueglia, E. (2015). Pharmacology of acid-sensing ion channels - Physiological and therapeutical perspectives. Neuropharmacology *94*, 19-35.

Barreto-Chang, O.L., and Dolmetsch, R.E. (2009). Calcium imaging of cortical neurons using Fura-2 AM. Journal of Visualized Experiments.

Bautista, D.M., Jordt, S.E., Nikai, T., Tsuruda, P.R., Read, A.J., Poblete, J., Yamoah, E.N., Basbaum, A.I., and Julius, D. (2006). TRPA1 mediates the inflammatory actions of environmental irritants and proalgesic agents. Cell *124*, 1269-1282.

Bautista, D.M., Movahed, P., Hinman, A., Axelsson, H.E., Sterner, O., Hogestatt, E.D., Julius, D., Jordt, S.E., and Zygmunt, P.M. (2005). Pungent products from garlic activate the sensory ion channel TRPA1. Proceedings of the National Academy of Sciences of the United States of America *102*, 12248-12252.

Bautista, D.M., Pellegrino, M., and Tsunozaki, M. (2013). TRPA1: A gatekeeper for inflammation. Annual Review of Physiology *75*, 181-200.

Belvisi, M.G., Dubuis, E., and Birrell, M.A. (2011). Transient receptor potential A1 channels: insights into cough and airway inflammatory disease. Chest *140*, 1040-1047.

Berridge, M.J., Lipp, P., and Bootman, M.D. (2000). The versatility and universality of calcium signalling. Nature Reviews: Molecular Cell Biology *1*, 11-21.

Birukov, K.G., Leitinger, N., Bochkov, V.N., and Garcia, J.G. (2004). Signal transduction pathways activated in human pulmonary endothelial cells by OxPAPC, a bioactive component of oxidized lipoproteins. Microvascular Research *67*, 18-28.

Biskup, C., Kusch, J., Schulz, E., Nache, V., Schwede, F., Lehmann, F., Hagen, V., and Benndorf, K. (2007). Relating ligand binding to activation gating in CNGA2 channels. Nature *446*, 440-443.

Bloedon, L.T., Dunbar, R., Duffy, D., Pinell-Salles, P., Norris, R., DeGroot, B.J., Movva, R., Navab, M., Fogelman, A.M., and Rader, D.J. (2008). Safety, pharmacokinetics, and pharmacodynamics of oral apoA-I mimetic peptide D-4F in high-risk cardiovascular patients. Journal of Lipid Research *49*, 1344-1352.

Blumenfeld, H., Zablow, L., and Sabatini, B. (1992). Evaluation of cellular mechanisms for modulation of calcium transients using a mathematical model of fura-2 Ca2+ imaging in Aplysia sensory neurons. Biophysical Journal *63*, 1146-1164.

Bluml, S., Kirchberger, S., Bochkov, V.N., Kronke, G., Stuhlmeier, K., Majdic, O., Zlabinger, G.J., Knapp, W., Binder, B.R., Stockl, J.*, et al.* (2005). Oxidized phospholipids negatively regulate dendritic cell maturation induced by TLRs and CD40. Journal of Immunology *175*, 501-508.

Bochkov, V.N., Kadl, A., Huber, J., Gruber, F., Binder, B.R., and Leitinger, N. (2002). Protective role of phospholipid oxidation products in endotoxin-induced tissue damage. Nature *419*, 77-81.

Bochkov, V.N., Oskolkova, O.V., Birukov, K.G., Levonen, A.L., Binder, C.J., and Stockl, J. (2010). Generation and biological activities of oxidized phospholipids. Antioxidants & Redox Signaling *12*, 1009-1059.

Bretscher, P., Egger, J., Shamshiev, A., Trotzmuller, M., Kofeler, H., Carreira, E.M., Kopf, M., and Freigang, S. (2015). Phospholipid oxidation generates potent anti-inflammatory lipid mediators that mimic structurally related pro-resolving eicosanoids by activating Nrf2. EMBO Molecular Medicine *7*, 593-607.

Brierley, S.M., Castro, J., Harrington, A.M., Hughes, P.A., Page, A.J., Rychkov, G.Y., and Blackshaw, L.A. (2011). TRPA1 contributes to specific mechanically activated currents and sensory neuron mechanical hypersensitivity. Journal of Physiology *589*, 3575-3593.

Caspani, O., Zurborg, S., Labuz, D., and Heppenstall, P.A. (2009). The contribution of TRPM8 and TRPA1 channels to cold allodynia and neuropathic pain. PloS One *4*, e7383.

Catala, A. (2006). An overview of lipid peroxidation with emphasis in outer segments of photoreceptors and the chemiluminescence assay. International Journal of Biochemistry and Cell Biology *38*, 1482-1495.

Catala, A. (2009). Lipid peroxidation of membrane phospholipids generates hydroxy-alkenals and oxidized phospholipids active in physiological and/or pathological conditions. Chemistry and Physics of Lipids *157*, 1-11.

Caterina, M.J., and Julius, D. (2001). The vanilloid receptor: a molecular gateway to the pain pathway. Annual Review of Neuroscience *24*, 487-517.

Caterina, M.J., Schumacher, M.A., Tominaga, M., Rosen, T.A., Levine, J.D., and Julius, D. (1997). The capsaicin receptor: a heat-activated ion channel in the pain pathway. Nature *389*, 816-824.

Cejpek, K., Valusek, J., and Velisek, J. (2000). Reactions of allyl isothiocyanate with alanine, glycine, and several peptides in model systems. Journal of Agricultural and Food Chemistry *48*, 3560-3565.

Chu, L.H., Indramohan, M., Ratsimandresey, R.A., Gangopadhyay, A., Morris, E.P., Monack, D.M., Dorfleutner, A., and Stehlik, C. (2018). The oxidized phospholipid oxPAPC protects from septic shock by targeting the non-canonical inflammasome in macrophages. Nature Communications *9*, 996.

Crofford, L.J. (2013). Use of NSAIDs in treating patients with arthritis. Arthritis Research & Therapy *15*.

Cruz-Orengo, L., Dhaka, A., Heuermann, R.J., Young, T.J., Montana, M.C., Cavanaugh, E.J., Kim, D., and Story, G.M. (2008). Cutaneous nociception evoked by 15-delta PGJ2 via activation of ion channel TRPA1. Molecular Pain *4*, 30.

Cvetkov, T.L., Huynh, K.W., Cohen, M.R., and Moiseenkova-Bell, V.Y. (2011). Molecular architecture and subunit organization of TRPA1 ion channel revealed by electron microscopy. Journal of Biological Chemistry *286*, 38168-38176.

de Oliveira-Junior, E.B., Bustamante, J., Newburger, P.E., and Condino-Neto, A. (2011). The human NADPH oxidase: primary and secondary defects impairing the respiratory burst function and the microbicidal ability of phagocytes. Scandinavian Journal of Immunology *73*, 420-427.

Degoma, E.M., and Rader, D.J. (2011). Novel HDL-directed pharmacotherapeutic strategies. Nature Reviews: Cardiology *8*, 266-277.

Dirajlal, S., Pauers, L.E., and Stucky, C.L. (2003). Differential response properties of IB(4)-positive and -negative unmyelinated sensory neurons to protons and capsaicin. Journal of Neurophysiology *89*, 513-524.

Doerner, J.F., Gisselmann, G., Hatt, H., and Wetzel, C.H. (2007). Transient receptor potential channel A1 is directly gated by calcium ions. Journal of Biological Chemistry *282*, 13180-13189.

Domingues, R.M., Domingues, P., Melo, T., Perez-Sala, D., Reis, A., and Spickett, C.M. (2013). Lipoxidation adducts with peptides and proteins: deleterious modifications or signaling mechanisms? Journal of Proteomics *92*, 110-131.

Eberhardt, M.J., Filipovic, M.R., Leffler, A., de la Roche, J., Kistner, K., Fischer, M.J., Fleming, T., Zimmermann, K., Ivanovic-Burmazovic, I., Nawroth, P.P.*, et al.* (2012). Methylglyoxal activates nociceptors through transient receptor potential channel A1 (TRPA1): a possible mechanism of metabolic neuropathies. Journal of Biological Chemistry *287*, 28291-28306.

Eid, S.R., Crown, E.D., Moore, E.L., Liang, H.A., Choong, K.C., Dima, S., Henze, D.A., Kane, S.A., and Urban, M.O. (2008). HC-030031, a TRPA1 selective antagonist, attenuates inflammatory- and neuropathy-induced mechanical hypersensitivity. Molecular Pain *4*, 48.

Engel, M.A., Leffler, A., Niedermirtl, F., Babes, A., Zimmermann, K., Filipovic, M.R., Izydorczyk, I., Eberhardt, M., Kichko, T.I., Mueller-Tribbensee, S.M.*, et al.* (2011). TRPA1 and substance P mediate colitis in mice. Gastroenterology *141*, 1346-1358.

Feig, J.E., Shamir, R., and Fisher, E.A. (2008). Atheroprotective effects of HDL: beyond reverse cholesterol transport. Current Drug Targets *9*, 196-203.

Fetal Bovine Serum, SIGMA-ALDRICH, (Online in the Internet) URL: https://www.sigmaaldrich.com/catalog/product/sigma/f7524?lang=de&region=DE, Status from: 19.06.2018, 04:30 p.m.

Freigang, S. (2016). The regulation of inflammation by oxidized phospholipids. European Journal of Immunology *46*, 1818-1825.

Friedman, P., Horkko, S., Steinberg, D., Witztum, J.L., and Dennis, E.A. (2002). Correlation of antiphospholipid antibody recognition with the structure of synthetic oxidized phospholipids. Importance of Schiff base formation and aldol condensation. Journal of Biological Chemistry *277*, 7010-7020.

Gangadharan, V., and Kuner, R. (2013). Pain hypersensitivity mechanisms at a glance. Disease Models & Mechanisms *6*, 889-895.

Gao, D., Ashraf, M.Z., Kar, N.S., Lin, D., Sayre, L.M., and Podrez, E.A. (2010). Structural basis for the recognition of oxidized phospholipids in oxidized low density lipoproteins by class B scavenger receptors CD36 and SR-BI. Journal of Biological Chemistry *285*, 4447-4454.

Garrity, P.A. (2011). Weakly acidic, but strongly irritating: TRPA1 and the activation of nociceptors by cytoplasmic acidification. Journal of General Physiology *137*, 489-491.

Gentamicin. (1967). British Medical Journal *1*, 158-159.

Gerasimenko Julia, V., Petersen Ole, H., and Gerasimenko Oleg, V. (2014). Monitoring of intra‐ER free Ca2+. Wiley Interdisciplinary Reviews: Membrane Transport and Signaling *3*, 63-71.

Getz, G.S., and Reardon, C.A. (2011). Apolipoprotein A-I and A-I mimetic peptides: a role in atherosclerosis. Journal of Inflammation Research *4*, 83-92.

Getz, G.S., and Reardon, C.A. (2014). The structure/function of apoprotein A-I mimetic peptides: an update. Current Opinion in Endocrinology, Diabetes, and Obesity *21*, 129-133.

Gibco™ DMEM, high glucose, GlutaMAX™ Supplement, ThermoFisher Scientific, (Online in the Internet) URL: https://www.thermofisher.com/order/catalog/product/61965240?SID=srch-srp-61965240 Status from: 19.06.2018, 03:08 p.m.

Glass, C.K., and Witztum, J.L. (2001). Atherosclerosis. the road ahead. Cell *104*, 503-516.

Good, N.E., Winget, G.D., Winter, W., Connolly, T.N., Izawa, S., and Singh, R.M. (1966). Hydrogen ion buffers for biological research. Biochemistry *5*, 467-477.

Gordon, D.J., Probstfield, J.L., Garrison, R.J., Neaton, J.D., Castelli, W.P., Knoke, J.D., Jacobs, D.R., Jr., Bangdiwala, S., and Tyroler, H.A. (1989). High-density lipoprotein cholesterol and cardiovascular disease. Four prospective American studies. Circulation *79*, 8-15.

Graham, F.L., Smiley, J., Russell, W.C., and Nairn, R. (1977). Characteristics of a human cell line transformed by DNA from human adenovirus type 5. Journal of General Virology *36*, 59-74.

Grynkiewicz, G., Poenie, M., and Tsien, R.Y. (1985). A new generation of Ca2+ indicators with greatly improved fluorescence properties. Journal of Biological Chemistry *260*, 3440-3450.

Ham's F12 Nutrient Mixture, a, ThermoFisher Scientific (Online in the Internet) URL: https://www.thermofisher.com/ch/en/home/life-science/cell-culture/mammalian-cell-culture/classical-media/f-12-nutrient-mixture.html, Status from: 19.06.2018 04:02 p.m.

Ham's F12 Nutrient Mixture, b, ThermoFisher Scientific, (Online in the Internet) URL: https://www.thermofisher.com/order/catalog/product/21765029?SID=srch-hj-21765029 Status from: 19.06.2018 04:21 p.m.

Han, M.H., Kawasaki, A., Wei, J.Y., and Barnstable, C.J. (2001). Miniature postsynaptic currents depend on Ca2+ released from internal stores via PLC/IP3 pathway. Neuroreport *12*, 2203-2207.

Hansson, G.K., and Hermansson, A. (2011). The immune system in atherosclerosis. Nature Immunology *12*, 204-212.

Hinman, A., Chuang, H.H., Bautista, D.M., and Julius, D. (2006). TRP channel activation by reversible covalent modification. Proceedings of the National Academy of Sciences of the United States of America *103*, 19564-19568.

Horkko, S., Bird, D.A., Miller, E., Itabe, H., Leitinger, N., Subbanagounder, G., Berliner, J.A., Friedman, P., Dennis, E.A., Curtiss, L.K.*, et al.* (1999). Monoclonal autoantibodies specific for oxidized phospholipids or oxidized phospholipid-protein adducts inhibit macrophage uptake of oxidized low-density lipoproteins. Journal of Clinical Investigation *103*, 117-128.

Hsu, C.C., and Lee, L.Y. (2015). Role of calcium ions in the positive interaction between TRPA1 and TRPV1 channels in bronchopulmonary sensory neurons. J Appl Physiol (1985) *118*, 1533-1543.

Imai, Y., Kuba, K., Neely, G.G., Yaghubian-Malhami, R., Perkmann, T., van Loo, G., Ermolaeva, M., Veldhuizen, R., Leung, Y.H., Wang, H.*, et al.* (2008). Identification of oxidative stress and Toll-like receptor 4 signaling as a key pathway of acute lung injury. Cell *133*, 235-249.

Itabe, H., Mori, M., Fujimoto, Y., Higashi, Y., and Takano, T. (2003). Minimally modified LDL is an oxidized LDL enriched with oxidized phosphatidylcholines. Journal of Biochemistry *134*, 459-465.

Iyengar, S., Ossipov, M.H., and Johnson, K.W. (2016). The role of CGRP in peripheral and central pain mechanisms including migraine. Pain.

Jacobsen, L., Calvin, S., and Lobenhofer, E. (2009). Transcriptional effects of transfection: the potential for misinterpretation of gene expression data generated from transiently transfected cells. Biotechniques *47*, 617-624.

Jordt, S.E., Bautista, D.M., Chuang, H.H., McKemy, D.D., Zygmunt, P.M., Hogestatt, E.D., Meng, I.D., and Julius, D. (2004). Mustard oils and cannabinoids excite sensory nerve fibres through the TRP channel ANKTM1. Nature *427*, 260-265.

Julius, D., and Basbaum, A.I. (2001). Molecular mechanisms of nociception. Nature *413*, 203-210.

Kadkova, A., Synytsya, V., Krusek, J., Zimova, L., and Vlachova, V. (2017). Molecular basis of TRPA1 regulation in nociceptive neurons. A review. Physiological Research *66*, 425-439.

Keszthelyi, D., van Avesaat, M., Troost, F.J., and Masclee, A.A. (2016). Translational Difficulties in Studying the TRPA1 Receptor. Nutrients *8*.

Kim, T.K., and Eberwine, J.H. (2010). Mammalian cell transfection: the present and the future. Analytical and Bioanalytical Chemistry *397*, 3173-3178.

Kistner, K., Siklosi, N., Babes, A., Khalil, M., Selescu, T., Zimmermann, K., Wirtz, S., Becker, C., Neurath, M.F., Reeh, P.W.*, et al.* (2016). Systemic desensitization through TRPA1 channels by capsazepine and mustard oil - a novel strategy against inflammation and pain. Scientific Reports *6*, 28621.

Kobayashi, K., Fukuoka, T., Obata, K., Yamanaka, H., Dai, Y., Tokunaga, A., and Noguchi, K. (2005). Distinct expression of TRPM8, TRPA1, and TRPV1 mRNAs in rat primary afferent neurons with adelta/c-fibers and colocalization with trk receptors. Journal of Comparative Neurology *493*, 596-606.

Kobayashi, K., Yamanaka, H., and Noguchi, K. (2013). Expression of ATP receptors in the rat dorsal root ganglion and spinal cord. Anatomical Science International *88*, 10-16.

Kremeyer, B., Lopera, F., Cox, J.J., Momin, A., Rugiero, F., Marsh, S., Woods, C.G., Jones, N.G., Paterson, K.J., Fricker, F.R*., et al.* (2010). A gain-of-function mutation in TRPA1 causes familial episodic pain syndrome. Neuron *66*, 671-680.

Lee, S., Birukov, K.G., Romanoski, C.E., Springstead, J.R., Lusis, A.J., and Berliner, J.A. (2012). Role of phospholipid oxidation products in atherosclerosis. Circulation Research *111*, 778-799.

Leffler, A., Lattrell, A., Kronewald, S., Niedermirtl, F., and Nau, C. (2011). Activation of TRPA1 by membrane permeable local anesthetics. Molecular Pain *7*, 62.

Lewit-Bentley, A., and Rety, S. (2000). EF-hand calcium-binding proteins. Current Opinion in Structural Biology *10*, 637-643.

Li, C.L., Li, K.C., Wu, D., Chen, Y., Luo, H., Zhao, J.R., Wang, S.S., Sun, M.M., Lu, Y.J., Zhong, Y.Q*., et al.* (2016). Somatosensory neuron types identified by high-coverage single-cell RNA-sequencing and functional heterogeneity. Cell Research *26*, 83-102.

Li, R., Mouillesseaux, K.P., Montoya, D., Cruz, D., Gharavi, N., Dun, M., Koroniak, L., and Berliner, J.A. (2006). Identification of prostaglandin E2 receptor subtype 2 as a receptor activated by OxPAPC. Circulation Research *98*, 642-650.

Li, W.G., and Xu, T.L. (2011). ASIC3 channels in multimodal sensory perception. ACS Chemical Neuroscience *2*, 26-37.

Lin, Y.C., Boone, M., Meuris, L., Lemmens, I., Van Roy, N., Soete, A., Reumers, J., Moisse, M., Plaisance, S., Drmanac, R*., et al.* (2014). Genome dynamics of the human embryonic kidney 293 lineage in response to cell biology manipulations. Nature Communications *5*, 4767.

Liu, Y., Yang, F.C., Okuda, T., Dong, X., Zylka, M.J., Chen, C.L., Anderson, D.J., Kuner, R., and Ma, Q. (2008). Mechanisms of compartmentalized expression of Mrg class G-protein-coupled sensory receptors. Journal of Neuroscience *28*, 125-132.

Loading and Calibration of Intracellular Ion Indicators—Note 19.1, ThermoFisher Scientific, (Online in the Internet) URL: http://www.lifetechnologies.com/de/de/home/references/molecular-probes-the-handbook/technical-notes-and-product-highlights/loading-and-calibration-of-intracellular-ion-indicators.html - head2, Status from: 27.05.2018, 07:03 p.m.

Lock, J.T., Parker, I., and Smith, I.F. (2015). A comparison of fluorescent Ca(2)(+) indicators for imaging local Ca(2)(+) signals in cultured cells. Cell Calcium *58*, 638-648.

Ma, Z., Li, J., Yang, L., Mu, Y., Xie, W., Pitt, B., and Li, S. (2004). Inhibition of LPS- and CpG DNA-induced TNF-alpha response by oxidized phospholipids. American Journal of Physiology: Lung Cellular and Molecular Physiology *286*, L808-816.

Macpherson, L.J., Dubin, A.E., Evans, M.J., Marr, F., Schultz, P.G., Cravatt, B.F., and Patapoutian, A. (2007). Noxious compounds activate TRPA1 ion channels through covalent modification of cysteines. Nature *445*, 541-545.

Mancia, F., Patel, S.D., Rajala, M.W., Scherer, P.E., Nemes, A., Schieren, I., Hendrickson, W.A., and Shapiro, L. (2004). Optimization of protein production in mammalian cells with a coexpressed fluorescent marker. Structure *12*, 1355-1360.

Manifava, M. (2006). Fugene® HD Transfection Reagent: Superior Performance for Challenging Expression Studies Biochemica, 26-27.

Martin, C., Stoffer, C., Mohammadi, M., Hugo, J., Leipold, E., Oehler, B., Rittner, H.L., and Blum, R. (2018). NaV1.9 Potentiates Oxidized Phospholipid-Induced TRP Responses Only under Inflammatory Conditions. Frontiers in Molecular Neuroscience *11*, 7.

Maxwell, D.J., Réthely, M. (1987). Ultrastructure and synaptic connections pf cutaneous afferent fibres in the spinal cord. Trends in Neuroscience *10*, 117-123.

McMahon, S.B., La Russa, F., and Bennett, D.L. (2015). Crosstalk between the nociceptive and immune systems in host defence and disease. Nature Reviews: Neuroscience *16*, 389-402.

Meents, J.E., Fischer, M.J., and McNaughton, P.A. (2016). Agonist-induced sensitisation of the irritant receptor ion channel TRPA1. Journal of Physiology.

Mehier-Humbert, S., and Guy, R.H. (2005). Physical methods for gene transfer: improving the kinetics of gene delivery into cells. Advanced Drug Delivery Reviews *57*, 733-753.

Meseguer, V., Alpizar, Y.A., Luis, E., Tajada, S., Denlinger, B., Fajardo, O., Manenschijn, J.A., Fernandez-Pena, C., Talavera, A., Kichko, T.*, et al.* (2014). TRPA1 channels mediate acute neurogenic inflammation and pain produced by bacterial endotoxins. Nature Communications *5*, 3125.

Mihara, S., and Shibamoto, T. (2015). The role of flavor and fragrance chemicals in TRPA1 (transient receptor potential cation channel, member A1) activity associated with allergies. Allergy, Asthma, and Clinical Immunology *11*, 11.

Mohammadi, M., Oehler, B., Kloka, J., Martin, C., Brack, A., Blum, R., and Rittner, H.L. (2018). Antinociception by the anti-oxidized phospholipid antibody E06. British Journal of Pharmacology.

Moparthi, L., Kichko, T.I., Eberhardt, M., Hogestatt, E.D., Kjellbom, P., Johanson, U., Reeh, P.W., Leffler, A., Filipovic, M.R., and Zygmunt, P.M. (2016). Human TRPA1 is a heat sensor displaying intrinsic U-shaped thermosensitivity. Scientific Reports *6*, 28763.

Moumtzi, A., Trenker, M., Flicker, K., Zenzmaier, E., Saf, R., and Hermetter, A. (2007). Import and fate of fluorescent analogs of oxidized phospholipids in vascular smooth muscle cells. Journal of Lipid Research *48*, 565-582.

Nagata, K., Duggan, A., Kumar, G., and Garcia-Anoveros, J. (2005). Nociceptor and hair cell transducer properties of TRPA1, a channel for pain and hearing. Journal of Neuroscience *25*, 4052-4061.

Nassini, R., Materazzi, S., Benemei, S., and Geppetti, P. (2014). The TRPA1 channel in inflammatory and neuropathic pain and migraine. Reviews of Physiology Biochemistry and Pharmacology *167*, 1-43.

Navab, M., Hough, G., Buga, G.M., Su, F., Wagner, A.C., Meriwether, D., Chattopadhyay, A., Gao, F., Grijalva, V., Danciger, J.S.*, et al.* (2013). Transgenic 6F tomatoes act on the small intestine to prevent systemic inflammation and dyslipidemia caused by Western diet and intestinally derived lysophosphatidic acid. Journal of Lipid Research *54*, 3403-3418.

Navab, M., Reddy, S.T., Anantharamaiah, G.M., Imaizumi, S., Hough, G., Hama, S., and Fogelman, A.M. (2011). Intestine may be a major site of action for the apoA-I mimetic peptide 4F whether administered subcutaneously or orally. Journal of Lipid Research *52*, 1200-1210.

Neher, E., and Sakmann, B. (1992). The patch clamp technique. Scientific American *266*, 44-51.

Nilius, B., Appendino, G., and Owsianik, G. (2012). The transient receptor potential channel TRPA1: from gene to pathophysiology. Pflügers Archiv European Journal of Physiology *464*, 425-458.

Nilius, B., and Owsianik, G. (2011). The transient receptor potential family of ion channels. Genome Biology *12*, 218.

O'Connor, T.M., O'Connell, J., O'Brien, D.I., Goode, T., Bredin, C.P., and Shanahan, F. (2004). The role of substance P in inflammatory disease. Journal of Cellular Physiology *201*, 167-180.

Oehler, B., Kistner, K., Martin, C., Schiller, J., Mayer, R., Mohammadi, M., Sauer, R.S., Filipovic, M.R., Nieto, F.R., Kloka, J.*, et al.* (2017). Inflammatory pain control by blocking oxidized phospholipid-mediated TRP channel activation. Scientific Reports *7*, 5447.

Ooi, A., Wong, A., Esau, L., Lemtiri-Chlieh, F., and Gehring, C. (2016). A Guide to Transient Expression of Membrane Proteins in HEK-293 Cells for Functional Characterization. Frontiers in Physiology *7*, 300.

Owsianik, G., Talavera, K., Voets, T., and Nilius, B. (2006). Permeation and selectivity of TRP channels. Annual Review of Physiology *68*, 685-717.

Palinski, W., Horkko, S., Miller, E., Steinbrecher, U.P., Powell, H.C., Curtiss, L.K., and Witztum, J.L. (1996). Cloning of monoclonal autoantibodies to epitopes of oxidized lipoproteins from apolipoprotein E-deficient mice. Demonstration of epitopes of oxidized low density lipoprotein in human plasma. Journal of Clinical Investigation *98*, 800-814.

Paredes, R.M., Etzler, J.C., Watts, L.T., Zheng, W., and Lechleiter, J.D. (2008). Chemical calcium indicators. Methods *46*, 143-151.

Paulsen, C.E., Armache, J.P., Gao, Y., Cheng, Y., and Julius, D. (2015a). Structure of the TRPA1 ion channel suggests regulatory mechanisms. Nature *520*, 511-517.

Paulsen, C.E., Armache, J.P., Gao, Y., Cheng, Y., and Julius, D. (2015b). Structure of the TRPA1 ion channel suggests regulatory mechanisms. Nature *525*, 552.

Petho, G., and Reeh, P.W. (2012). Sensory and signaling mechanisms of bradykinin, eicosanoids, platelet-activating factor, and nitric oxide in peripheral nociceptors. Physiological Reviews *92*, 1699-1775.

Podrez, E.A., Poliakov, E., Shen, Z., Zhang, R., Deng, Y., Sun, M., Finton, P.J., Shan, L., Febbraio, M., Hajjar, D.P.*, et al.* (2002). A novel family of atherogenic oxidized phospholipids promotes macrophage foam cell formation via the scavenger receptor CD36 and is enriched in atherosclerotic lesions. Journal of Biological Chemistry *277*, 38517-38523.

Pohjanpelto, P., and Raina, A. (1972). Identification of a growth factor produced by human fibroblasts in vitro as putrescine. Nature: New Biology *235*, 247-249.

Rao, P., and Knaus, E.E. (2008). Evolution of nonsteroidal anti-inflammatory drugs (NSAIDs): cyclooxygenase (COX) inhibition and beyond. Journal of Pharmacy & Pharmaceutical Sciences *11*, 81s-110s.

Ravandi, A., Leibundgut, G., Hung, M.Y., Patel, M., Hutchins, P.M., Murphy, R.C., Prasad, A., Mahmud, E., Miller, Y.I., Dennis, E.A.*, et al.* (2014). Release and capture of bioactive oxidized phospholipids and oxidized cholesteryl esters during percutaneous coronary and peripheral arterial interventions in humans. Journal of the American College of Cardiology *63*, 1961-1971.

Reddy, S.T., Navab, M., Anantharamaiah, G.M., and Fogelman, A.M. (2014). Searching for a successful HDL-based treatment strategy. Biochimica et Biophysica Acta *1841*, 162-167.

Ruparel, N.B., Patwardhan, A.M., Akopian, A.N., and Hargreaves, K.M. (2008). Homologous and heterologous desensitization of capsaicin and mustard oil responses utilize different cellular pathways in nociceptors. Pain *135*, 271-279.

Schiller, J., Suss, R., Arnhold, J., Fuchs, B., Lessig, J., Muller, M., Petkovic, M., Spalteholz, H., Zschornig, O., and Arnold, K. (2004). Matrix-assisted laser desorption and ionization time-of-flight (MALDI-TOF) mass spectrometry in lipid and phospholipid research. Progress in Lipid Research *43*, 449-488.

Schneider, C.A., Rasband, W.S., and Eliceiri, K.W. (2012). NIH Image to ImageJ: 25 years of image analysis. Nature Methods *9*, 671-675.

Schorpp, M., Jager, R., Schellander, K., Schenkel, J., Wagner, E.F., Weiher, H., and Angel, P. (1996). The human ubiquitin C promoter directs high ubiquitous expression of transgenes in mice. Nucleic Acids Research *24*, 1787-1788.

Segrest, J.P., Garber, D.W., Brouillette, C.G., Harvey, S.C., and Anantharamaiah, G.M. (1994). The amphipathic alpha helix: a multifunctional structural motif in plasma apolipoproteins. Advances in Protein Chemistry *45*, 303-369.

Selvaraj, D., Gangadharan, V., Michalski, C.W., Kurejova, M., Stosser, S., Srivastava, K., Schweizerhof, M., Waltenberger, J., Ferrara, N., Heppenstall, P.*, et al.* (2015). A Functional Role for VEGFR1 Expressed in Peripheral Sensory Neurons in Cancer Pain. Cancer Cell *27*, 780-796.

Shang, S., Zhu, F., Liu, B., Chai, Z., Wu, Q., Hu, M., Wang, Y., Huang, R., Zhang, X., Wu, X.*, et al.* (2016). Intracellular TRPA1 mediates Ca2+ release from lysosomes in dorsal root ganglion neurons. Journal of Cell Biology *215*, 369-381.

Shaw, G., Morse, S., Ararat, M., and Graham, F.L. (2002). Preferential transformation of human neuronal cells by human adenoviruses and the origin of HEK 293 cells. FASEB Journal *16*, 869-871.

Shaw, P.X., Horkko, S., Chang, M.K., Curtiss, L.K., Palinski, W., Silverman, G.J., and Witztum, J.L. (2000). Natural antibodies with the T15 idiotype may act in atherosclerosis, apoptotic clearance, and protective immunity. Journal of Clinical Investigation *105*, 1731-1740.

Silbernagl S. , D.A. (2012). Taschenatlas Physiologie, Vol 8 (Thieme).

Smith M, M.J. (2001). March's Advanced Organic Chemistry: Reactions, Mechanisms, and Structure (New York: Wiley).

Smythies, L.E., White, C.R., Maheshwari, A., Palgunachari, M.N., Anantharamaiah, G.M., Chaddha, M., Kurundkar, A.R., and Datta, G. (2010). Apolipoprotein A-I mimetic 4F alters the function of human monocyte-derived macrophages. American Journal of Physiology: Cell Physiology *298*, C1538-1548.

Spahn, V., Stein, C., and Zollner, C. (2014). Modulation of transient receptor vanilloid 1 activity by transient receptor potential ankyrin 1. Molecular Pharmacology *85*, 335-344.

Springstead, J.R., Gugiu, B.G., Lee, S., Cha, S., Watson, A.D., and Berliner, J.A. (2012). Evidence for the importance of OxPAPC interaction with cysteines in regulating endothelial cell function. Journal of Lipid Research *53*, 1304-1315.

Stemmer, U., Dunai, Z.A., Koller, D., Purstinger, G., Zenzmaier, E., Deigner, H.P., Aflaki, E., Kratky, D., and Hermetter, A. (2012a). Toxicity of oxidized phospholipids in cultured macrophages. Lipids in Health and Disease *11*, 110.

Stemmer, U., and Hermetter, A. (2012). Protein modification by aldehydophospholipids and its functional consequences. Biochimica et Biophysica Acta *1818*, 2436-2445.

Stemmer, U., Ramprecht, C., Zenzmaier, E., Stojcic, B., Rechberger, G., Kollroser, M., and Hermetter, A. (2012b). Uptake and protein targeting of fluorescent oxidized phospholipids in cultured RAW 264.7 macrophages. Biochimica et Biophysica Acta *1821*, 706-718.

Stewart, C.R., Stuart, L.M., Wilkinson, K., van Gils, J.M., Deng, J., Halle, A., Rayner, K.J., Boyer, L., Zhong, R., Frazier, W.A*., et al.* (2010). CD36 ligands promote sterile inflammation through assembly of a Toll-like receptor 4 and 6 heterodimer. Nature Immunology *11*, 155-161.

Story, G.M., Peier, A.M., Reeve, A.J., Eid, S.R., Mosbacher, J., Hricik, T.R., Earley, T.J., Hergarden, A.C., Andersson, D.A., Hwang, S.W*., et al.* (2003). ANKTM1, a TRP-like channel expressed in nociceptive neurons, is activated by cold temperatures. Cell *112*, 819-829.

Sura, L., Zima, V., Marsakova, L., Hynkova, A., Barvik, I., and Vlachova, V. (2012). C-terminal acidic cluster is involved in Ca2+-induced regulation of human transient receptor potential ankyrin 1 channel. Journal of Biological Chemistry *287*, 18067-18077.

Tang, C., Vaughan, A.M., Anantharamaiah, G.M., and Oram, J.F. (2006). Janus kinase 2 modulates the lipid-removing but not protein-stabilizing interactions of amphipathic helices with ABCA1. Journal of Lipid Research *47*, 107-114.

Tardif, J.C., Gregoire, J., L'Allier, P.L., Ibrahim, R., Lesperance, J., Heinonen, T.M., Kouz, S., Berry, C., Basser, R., Lavoie, M.A*., et al.* (2007). Effects of reconstituted high-density lipoprotein infusions on coronary atherosclerosis: a randomized controlled trial. JAMA *297*, 1675-1682.

Tepper, S.J., and Stillman, M.J. (2008). Clinical and preclinical rationale for CGRP-receptor antagonists in the treatment of migraine. Headache *48*, 1259-1268.

Thewalt, J.L., and Bloom, M. (1992). Phosphatidylcholine: cholesterol phase diagrams. Biophysical Journal *63*, 1176-1181.

Usoskin, D., Furlan, A., Islam, S., Abdo, H., Lonnerberg, P., Lou, D., Hjerling-Leffler, J., Haeggstrom, J., Kharchenko, O., Kharchenko, P.V*., et al.* (2015). Unbiased classification of sensory neuron types by large-scale single-cell RNA sequencing. Nature Neuroscience *18*, 145-153.

Ustek, D.D.D.A.E. (2007). Efficient Transfection of 293T Cell Line with Lentiviral Vectors Using FuGENE® HD Transfection Reagent. Biochemical Journal, 28-29.

Van Lenten, B.J., Wagner, A.C., Jung, C.L., Ruchala, P., Waring, A.J., Lehrer, R.I., Watson, A.D., Hama, S., Navab, M., Anantharamaiah, G.M*., et al.* (2008). Anti-inflammatory apoA-I-mimetic peptides bind oxidized lipids with much higher affinity than human apoA-I. Journal of Lipid Research *49*, 2302-2311.

Viana, F. (2016). TRPA1 channels: molecular sentinels of cellular stress and tissue damage. Journal of Physiology *594*, 4151-4169.

Vilceanu, D., and Stucky, C.L. (2010). TRPA1 mediates mechanical currents in the plasma membrane of mouse sensory neurons. PloS One *5*, e12177.

Wang, Y.Y., Chang, R.B., Allgood, S.D., Silver, W.L., and Liman, E.R. (2011). A TRPA1-dependent mechanism for the pungent sensation of weak acids. Journal of General Physiology *137*, 493-505.

Wang, Y.Y., Chang, R.B., Waters, H.N., McKemy, D.D., and Liman, E.R. (2008). The nociceptor ion channel TRPA1 is potentiated and inactivated by permeating calcium ions. Journal of Biological Chemistry *283*, 32691-32703.

Watson, A.D., Leitinger, N., Navab, M., Faull, K.F., Horkko, S., Witztum, J.L., Palinski, W., Schwenke, D., Salomon, R.G., Sha, W.*, et al.* (1997). Structural identification by mass spectrometry of oxidized phospholipids in minimally oxidized low density lipoprotein that induce monocyte/endothelial interactions and evidence for their presence in vivo. Journal of Biological Chemistry *272*, 13597-13607.

Weller, K., Reeh, P.W., and Sauer, S.K. (2011). TRPV1, TRPA1, and CB1 in the isolated vagus nerve--axonal chemosensitivity and control of neuropeptide release. Neuropeptides *45*, 391-400.

Wemmie, J.A., Taugher, R.J., and Kreple, C.J. (2013). Acid-sensing ion channels in pain and disease. Nature Reviews: Neuroscience *14*, 461-471.

White, C.R., Garber, D.W., and Anantharamaiah, G.M. (2014). Anti-inflammatory and cholesterol-reducing properties of apolipoprotein mimetics: a review. Journal of Lipid Research *55*, 2007-2021.

Wongrakpanich, S., Wongrakpanich, A., Melhado, K., and Rangaswami, J. (2018). A Comprehensive Review of Non-Steroidal Anti-Inflammatory Drug Use in The Elderly. Aging and Disease *9*, 143-150.

Woods, N.B., Muessig, A., Schmidt, M., Flygare, J., Olsson, K., Salmon, P., Trono, D., von Kalle, C., and Karlsson, S. (2003). Lentiviral vector transduction of NOD/SCID repopulating cells results in multiple vector integrations per transduced cell: risk of insertional mutagenesis. Blood *101*, 1284-1289.

Wool, G.D., Cabana, V.G., Lukens, J., Shaw, P.X., Binder, C.J., Witztum, J.L., Reardon, C.A., and Getz, G.S. (2011). 4F Peptide reduces nascent atherosclerosis and induces natural antibody production in apolipoprotein E-null mice. FASEB Journal *25*, 290-300.

Wool, G.D., Reardon, C.A., and Getz, G.S. (2008). Apolipoprotein A-I mimetic peptide helix number and helix linker influence potentially anti-atherogenic properties. Journal of Lipid Research *49*, 1268-1283.

Woolf, C.J., and Ma, Q. (2007). Nociceptors--noxious stimulus detectors. Neuron *55*, 353-364.

Wurm, F.M. (2004). Production of recombinant protein therapeutics in cultivated mammalian cells. Nature Biotechnology *22*, 1393-1398.

Yeang, C., Hung, M.Y., Pattison, J., Bowden, K., Dalton, N., Peterson, K.L., Witztum, J.L., Tsimikas, S., and Que, X. (2016). Expression of E06, a natural monoclonal antibody targeted to oxidized phospholipids (OXPL), attenuates the progression of aortic sclerosis in aged hyperlipidemic mice. Atherosclerosis *252*, e229.

Zagranichnaya, T.K., Wu, X., and Villereal, M.L. (2005). Endogenous TRPC1, TRPC3, and TRPC7 proteins combine to form native store-operated channels in HEK-293 cells. Journal of Biological Chemistry *280*, 29559-29569.

Zhang, X., Shi, T., Holmberg, K., Landry, M., Huang, W., Xiao, H., Ju, G., and Hokfelt, T. (1997). Expression and regulation of the neuropeptide Y Y2 receptor in sensory and autonomic ganglia. Proceedings of the National Academy of Sciences of the United States of America *94*, 729-734.

Zheng, J., and Zagotta, W.N. (2000). Gating rearrangements in cyclic nucleotide-gated channels revealed by patch-clamp fluorometry. Neuron *28*, 369-374.

Zimmermann, K., Lennerz, J.K., Hein, A., Link, A.S., Kaczmarek, J.S., Delling, M., Uysal, S., Pfeifer, J.D., Riccio, A., and Clapham, D.E. (2011). Transient receptor potential cation channel, subfamily C, member 5 (TRPC5) is a cold-transducer in the peripheral nervous system. Proceedings of the National Academy of Sciences of the United States of America *108*, 18114-18119.

Zurborg, S., Yurgionas, B., Jira, J.A., Caspani, O., and Heppenstall, P.A. (2007). Direct activation of the ion channel TRPA1 by Ca2+. Nature Neuroscience *10*, 277-279.

7 Directory

7.1 Figures

7.2 Tables

Table 5: Abbreviations

15d-PG	15-deoxy-$\Delta^{12,14}$-prostaglandin
2-APB	2-aminoethoxydiphenyl borate
4-HHE	4-hydroxy-2-hexenal
4-HNE	4-hydroxy-2-nonenal
4-ONE	4-oxo-2-nonenal
AC	Adenylate cyclase
AITC	Ally lisothiocyanate
AM	Acetoxymethyl ester
ANOVA	Analysis of variance
ARD	Ankyrin repeat domain
ASIC	Acid-sensing ion channel
AUC	Area under the curve
BDNF	Brain-derived neurotrophic factor
BSA	Bovine serum albumine
cAMP	Cyclic adenosine monophosphate
cDNA	Complementary deoxyribonucleic acid

CFA	Complete Freund's adjuvans
CGRP	Calcitonin gene-related peptide
CNS	Central nervous system
CREB	cAMP response element-binding protein
CREB	cAMP response element-binding protein
DAG	Diacyl glycerol
DMSO	Dimethyl sulfoxide
DPBS	Dulbecco's Phosphate Buffered Saline
DRG	Dorsal root ganglion/ganglia
EP2-R	E-type prostaglandin receptor
ER	Endoplasmic reticulum
FCS	Fetal calf serum
FLIPR	Fluorescence imaging plate reader
GFP	Green fluorescent protein
H_2O_2	Hydrogen peroxide
HDL	High-density lipoprotein
HEK-293 cells	Human embryonic kidney cells-293
hTRPA1	Human TRPA1
IB4	Isolectin B4
IgM/G	Immunoglobulin M/G
IL-8	Interleukin 8
IP_3	Inositol 1,4,5-trisphosphate

IRES	Internal ribosome entry site
Iso-PGs	Isoprostanes
LDL	Low-density lipoprotein
LOOH	Lipid hydroperoxides
LPC	Lysophosphatidylcholine
LPS	Lipopolysaccharide
LTR	Long Terminal Repeats
mAb	Monoclonal antibody
MALDI-TOF MS	Matrix-assisted laser desorption and ionization time-of-flight mass spectrometry
MAPK	Mitogen-activated protein kinase
MAPK	Mitogen-activated protein kinase
MRGPCR	MAS-related G-protein-coupled receptors
mRNA	Messenger ribonucleic acid
NaCl	Sodium chloride
NADPH	Nicotinamide adenide dinucleotide phosphate
NFκB	Nuclear factor kappa-light-chain-enhancer of activated B cells
NGF	Nerve-growth factor
NO	Nitric oxide
NPY	Neuropeptide Y
Nrf2	Nuclear factor E-2 related factor

NSAID	Non-steroidal anti-inflammatory drug
OH^-	Hydroxyl radicals
$ONOO^-$	Peroxynitrite
OxPAPC	Oxidized 1-palmitoyl-2-arachidonoyl-*sn*-glycero-3-PC
OxPC	Oxidized phosphatidylcholine
PAF	Platelet-activating factor
PC	phosphatidylcholine
PCR	Polymerase chain reaction
PEIPC	1-palmitoyl-2-epoxyisoprostane-sn-glycero-3-PC
PG	Prostaglandin
PGPC	1-palmitoyl-2-glutaryl-sn-glycero-3-PC
PIP_2	Phosphatidylinositol 4,5-bisphosphate
PKA/PKC	Protein kinase A/C
PI	Phospholipid
PLC	Phospholipase C
PLL	Poly-L-lysine
POVPC	1-palmitoyl-2-(5'-oxo-valeroyl)-sn-glycero-3-PC
PPAR	Peroxisome proliferator-activated receptor
PRR	Pattern recognition receptor
RNA	Ribonucleic acid
RO^-	Alkoxy radicals

ROI	Region of interest
ROS	Reactive oxygen species
Rpm	Rotations per minute
SD	Standard deviation
SEM	Standard error of the mean
SRB1	Scavenger receptor B1
TLR	Toll-like receptor
TRPA1	Transient Receptor Potential Ankyrin repeat 1
TRPC5	Transient receptor potential Canonical 5
TRPM	Transient receptor potential Melastatin
TRPML	Transient receptor potential Mucolipin
TRPN	Transient receptor potential NOMPC-like
TRPP	Transient receptor potential Polycystin
TRPV1-4	Transient Receptor Potential Vanilloid
TX	Thromboxane
UV	Ultraviolet
VEGFR	Vascular endothelial growth factor receptor
VGSC	Voltage-gated Na^+ channels
YFP	Yellow fluorescent protein

8 Attachments

8.1 Danksagung

Zwei Dinge sind zu unserer Arbeit nötig. Unermüdliche Ausdauer und die Bereitschaft etwas, in das man viel Zeit und Arbeit gesteckt hat, wieder wegzuwerfen.

Albert Einstein

Mein besonderer Dank gilt meiner Doktormutter Prof. Dr. Heike Rittner, sowie meinen Betreuern Dr. Beatrice Oehler und PD Dr. Robert Blum für ihre Unterstützung. Sie standen mir stets mit Rat und Tat zur Seite und trugen wesentlichen zu allem bei, was ich im Rahmen meiner Promotionsarbeit erreicht habe.

Außerdem danke ich Prof. Dr. Alexander Brack, der AG „Molekulare Schmerzforschung“ und der AG Blum, die mich mit Expertise und Geduld an die Forschungsarbeit heranführten.

Forschung kann nervenaufreibend sein. Zeitweise wird die eigene Frustrationstoleranz auf die Probe gestellt. Besonders wenn man Ergebnisse ganzer Wochen verwerfen muss, ist es wichtig Freunde zu haben, die einen abends auf andere Gedanken bringen.

Herzlich danke ich auch der GSLS Würzburg, sowie der Konrad-Adenauer-Stiftung für deren ideelle und finanzielle Unterstützung.

Nicht zuletzt bedanke ich mich bei meinen Eltern, mit deren voller Unterstützung ich stets rechnen konnte und die mir so die Freiheit einräumten, ein komplettes Semester der Doktorarbeit zu widmen.

8.2 Declarations and study approval

The results of this thesis were published in July 2017 in the journal 'Scientific Reports':

Oehler, B., Kistner, K., Martin, C., Schiller, J., Mayer, R., Mohammadi, M., Sauer, R.S., Filipovic, M.R., Nieto, F.R., Kloka, J.*, et al.* (2017). Inflammatory pain control by blocking oxidized phospholipid-mediated TRP channel activation. Scientific reports *7*, 5447.

Therefore, the figures depicted in section **3** (Results) are also part of this publication.

Figures **1**, **2**, **6** and **16** were created with Servier Medical Art: https://smart.servier.com. They are licensed under a Creative Commons Attribution 3.0, Unported License. https://creativecommons.org/licenses/by/4.0/

Study approval All experiments and study protocols were performed in accordance with the European Union guidelines, and were approved by our institutional Animal Care and Utilization Committee (Regierung von Unterfranken, Wuerzburg, Germany) and by the Home Office, London, UK, and in accordance with the International Association for the Study of Pain.

8.3 Curriculum vitae

Affidavit

I hereby confirm that my thesis entitled "*OxPAPC as an endogenous agonist of TRPA1 channels on nociceptors"* is the result of my own work. I did not receive any help or support from commercial consultants. All sources and/or materials applied are listed and specified in the thesis.

Furthermore, I confirm that this thesis has not yet been submitted as part of another examination process neither in identical not in similar form.

Würzburg, 18.09.2018

Place, Date Signature

Eidesstattliche Erklärung

Hiermit erkläre ich an Eides statt, die Dissertation „*OxPAPC als endogener Agonist von TRPA1 Kanälen auf Nozizeptoren"* eigenständig, d.h. insbesondere selbstständig und ohne Hilfe eines kommerziellen Promotionsberaters, angefertigt und keine andere als die von mir angegebenen Quellen und Hilfsmittel verwendet zu haben.

Ich erkläre außerdem, dass die Dissertation weder in gleicher noch in ähnlicher Form bereits in einem anderen Prüfungsverfahren vorgelegen hat.

Würzburg, 18.09.2018

Ort, Datum Unterschrift